

MECHANISMS OF KAPOSI SARCOMA-ASSOCIATED HERPESVIRUS INDUCED
TUMORIGENESIS

by

Patrick P. Rose

A DISSERTATION

Presented to the Department of Molecular Microbiology and Immunology

and the Oregon Health & Science University

School of Medicine

in partial fulfillment of

the requirements for the degree of

Doctor of Philosophy

January 2007

School of Medicine
Oregon Health & Science University

CERTIFICATE OF APPROVAL

This is to certify that Ph.D. dissertation of
Patrick P. Rose
has been approved

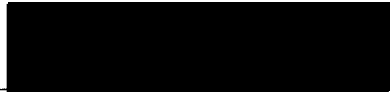
Mentor/Advisor


Klaus Friih, Ph.D.

Committee Member


Ashlee V. Moses, Ph.D.

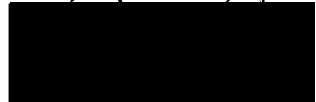
Committee Member


Mary P. Stenzel-Foore, Ph.D.

Committee Member


Charles T. Roberts Jr. Ph.D.

Committee Member


Peter S. Rotwein, M.D.

Committee Member


Jorge H. Crosa, Ph.D.

TABLE OF CONTENTS

Acknowledgements	ii
Abstract	iii
Chapter 1: Introduction	
I. Kaposi Sarcoma-associated Herpesvirus (KSHV).	1
A. A History of Kaposi Sarcoma.	2
B. Epidemiology of Kaposi Sarcoma.	5
C. Pathology of Kaposi Sarcoma.	7
D. Virology of Kaposi Sarcoma-associated Herpesvirus.	8
E. Tools for studying Kaposi Sarcoma-associated Herpesvirus.	12
i. Tissue culture models.	13
ii. Animal Models.	19
II. Tumorigenesis.	21
III. KSHV-induced Tumorigenesis.	25
IV. The Insulin-like Growth Factor System in Cancer.	30
V. Cysteine Protease Involvement in Tumorigenesis.	36
VI. Summary.	40
Chapter 2: Manuscript #1	43
Chapter 3: Manuscript #2	79
Chapter 4: Discussion	129

References	154
Appendix I	185
Appendix II	199
Appendix III	204
Appendix IV	209

Acknowledgements

I would like to thank my mentor and friend Dr. Klaus Früh for everything that he has done to make me a more successful scientist. His experience as a scientist and his patience has greatly contributed to my approach to science. It has been a pleasure working with him. My sincerest appreciation also goes to Dr. Ashlee V. Moses with whom I worked very closely during my graduate studies, benefiting from her ideas and critical suggestions of my own work.

Finally, this dissertation represents the culmination of a very difficult struggle during this chapter in my life. My graduate studies have been at the epicenter of a struggle that has questioned every last fabric of my existence as a scientist but foremost as a human being. This accomplishment, of which I am extremely proud of, could not have been completed without my partner at my side, Kristine M. Rose. She has been my rock to rest on when I was weary. Her strength and love are the essence of my success, and I look forward to taking on many more adventures together with her. My gratitude also goes to my parents, John P. Rose and Barbara U. Rose, for giving me a chance to challenge my limits and not limit my challenges.

Abstract

This dissertation discusses novel findings of the insulin-like growth factor system and cathepsin B in the context of Kaposi sarcoma-associated herpesvirus (KSHV)-induced tumorigenesis. To study KSHV-induced tumorigenesis, a tissue culture model system developed by Ashlee Moses was used, which best resembles *in vivo* conditions. Using a global approach of transcription profiling, KSHV-infected and uninfected E6/E7-immortalized dermal microvascular endothelial cells were compared by microarray to discern what cellular genes are involved in KSHV-mediated tumorigenesis. Within the insulin-like growth factor system, IGFBP-1, -2, -6, the insulin receptor and the insulin-like growth factor II receptor were identified as having important functions in Kaposi sarcoma. In addition, studies described in this dissertation reveal that the cysteine protease cathepsin B intracellularly regulates tumor invasion. Furthermore, a causal link between the insulin-like growth factor II receptor and cathepsin B was discovered, which proves to be necessary for KSHV-mediated tumorigenesis. These discoveries are the first to be documented for Kaposi sarcoma and present potential new targets for designing anti-cancer therapies.

CHAPTER 1

Introduction

I. Kaposi Sarcoma-associated Herpesvirus (KSHV)

The awareness that viruses play a prominent role in cancer has significantly improved over the last decade. In a 2002 census on cancers caused by infectious diseases, it was calculated that on average 1.5 million cases of cancer in developing countries and 390,000 cases of cancer in industrialized nations are attributed to infectious agents each year. Less than 0.1 percent of these recorded cases are caused by infectious agents other than viruses. In addition to the association of viruses with various cancers, some viruses are directly responsible for the cancer. For example, one hundred percent of all cervical cancers are ascribed to human papilloma virus infections (137). These examples make it evident that there is a need to understand virus-driven tumorigenesis. The benefit of studying cancers caused by viruses is that the driving forces behind virus-induced tumorigenesis are viral proteins. We can, therefore, begin to understand the roles of deregulation of developmental and angiogenic pathways in carcinogenesis. Especially since many cancers caused by infectious agents bear the same hallmarks as other non-infectious driven cancers.

With *classic* Kaposi Sarcoma (KS) considered to be an indolent cancer and AIDS or *endemic* KS found to be a more aggressive form, KS is marked with elements of many different cancers. It is expected that deciphering the virus-driven mechanisms of tumorigenesis in Kaposi sarcoma will improve the overall appreciation of how cancers

develop. Ultimately, the hope is to be able to develop novel anti-cancer therapies that have broad applications for non-infectious cancers as well as KS.

A. A History of Kaposi Sarcoma

KS was originally described in 1872 by the dermatologist Moritz Kaposi. Although the first cases described by Dr. Kaposi were of poor prognosis, the sarcoma is categorized as an indolent disease most prominent in the elderly of eastern European, Mediterranean, and Middle Eastern populations (*classical KS*). With some exceptions, it was generally expected that individuals with KS would die of other illnesses or of old age before dying from KS. Observations made in 1962 identified a high prevalence of the typical cutaneous nodules of KS in sub-Saharan Africa. It was noted that mostly young men and children presented with a more aggressive form of the disease (*endemic KS*). Later the AIDS epidemic would have a dramatic impact on KS prevalence in Africa, and still does today, where both endemic and AIDS-KS account for over 10% of all cancers. In 1979, as organ transplants were beginning to be performed on a regular basis, a surge in the cases of post-transplant patients, mainly renal transplants, afflicted with KS was noted (*iatrogenic KS*). The high frequency of iatrogenic KS suggested that immunosuppression may play a key role in the aggressiveness of the disease. This observation concurred with Moritz Kaposi's description, since he noted that a primary illness may have contributed to immunosuppression of the original patients with KS, which had led to their poor prognosis (10).

It was not until the onset of the AIDS epidemic that the pathogenesis of KS became a serious health concern in the United States. The first U.S. cases of AIDS were

reported in 1981, when homosexual men presented with aggressive cases of a vascular neoplasm, *AIDS-KS*. It was estimated that roughly 30-40% of homosexual men with AIDS had KS before effective antiviral drug treatments were available. KS became an indisputable hallmark of AIDS and still is the most common cancer in AIDS patients.

Despite early observations that immunosuppression factored into the aggressiveness of KS, it remained unclear for some time what the source of KS was and why the sarcoma was so prevalent in HIV-positive individuals. Not until 1990 was there any suggestion that an infectious agent other than HIV may be responsible for causing the sarcoma. In 1994 a herpesvirus, KS-associated herpesvirus (KSHV or HHV-8) was identified as the pathological agent of KS (19). Researchers Dr. Yuan Chang and Dr. Patrick Moore employed representational difference analysis to classify KS-associated genetic sequences as part of a new DNA tumor virus. For the first time a causative agent was identified and seroprevalence of KSHV could be directly associated with cases of KS. Since then, KSHV has been linked to three types of cancers: lymphoproliferative disorders of B cells, which include primary effusion lymphoma

Table 1. HHV-8-associated Disease

	Primary Effusion Lymphoma	Multicentric Castleman's disease	Kaposi Sarcoma
Cellular Origin	germinal center B-cells	naive B-cell	endothelial-like spindle cells
Tissue	body cavity	lymph nodes	skin, visceral organs
HHV-8 associated	100% positive for virus	few positive cells	100% positive for virus
Expression Phase	latent	lytic	latent
Tumor microenvironment	monoclonal	polyclonal	polyclonal

[adapted from Hengge et al. (66)]

(PEL) and multicentric Castleman's disease (MCD), and KS, an endothelial cell-derived tumor (Table 1). While these three types of cancers are still considered low risk, the combination of KS and HIV has been significantly reducing population numbers in developing countries. Africa has been especially devastated by KS due to a lack of available antiretroviral treatments against HIV and the high frequency of KSHV. In AIDS patients, the seroprevalence of KSHV changed only slightly with the introduction of antiretroviral inhibitor cocktails, while the occurrence of KS disease was dramatically reduced. The response to antiretroviral inhibitors implicates that the cellular immune surveillance has a good control over the spread of KS by controlling KSHV expression. In fact the restricted gene expression pattern during latency is a mechanism of immune evasion. While antiretroviral inhibitors do not target KSHV, they do improve immune surveillance and thereby limit viral spread and disease progression.

Evidence presented in KS studies suggests that KSHV is not the sole causative agent responsible for disease progression. This supports earlier suggestions that immunosuppression is a key factor in KS development. In the late 80's, Dr. Robert Gallo's group introduced another potential factor in KS tumor development: autocrine and paracrine viral and cellular cytokine stimulation. Today, additional factors have been suggested based on studies in geographic areas with a high prevalence of KS, which also include environmental factors such as soil composition (38, 39, 45), e.g. volcanic soil or high iron content of the soil (118, 213). Today, KSHV-induced tumorigenesis is recognized as a metastatic neoplasm of multifactorial origin. Serological studies have established a direct link between KSHV and disease, and the virus has been shown to be

present in most tumor cells in KS lesions. While KSHV is necessary to establish tumor development, it is not sufficient, leaving many avenues of research still open for study.

B. Epidemiology of KS

KS is found worldwide, although geographic hotspots exist independent of highly susceptible groups (187). Males are more susceptible to developing KS compared to females, the reasons for which are unclear. The mode of transmission remains somewhat unresolved as well. Sexual transmission is considered the major route in most cases. Another route of horizontal transmission is thought to be via saliva. The oral mucosa in conjunction with inflammation has been suggested to be a source of transmission, since KSHV DNA has been found to be more abundant in the saliva than elsewhere (16). Vertical transmission has also been recorded, e.g. saliva and breastfeeding, to explain mother-to-infant and child-to-child infection (165).

While the actual frequency of KS in the global population may vary, studies on the prevalence of the disease suggest the following: Classic KS can be found predominantly in men of Mediterranean or Jewish lineage; however, an increased frequency has also been more recently reported in men of eastern European and Arabian descent. The rate of classic KS generally increases with the onset of old age. A high rate of classic KS can be found in southern Italy and Greece. It is estimated that the occurrence of classic KS is between 0.02-0.06 percent in Western Countries. Meanwhile, in Africa, KS accounts for 10% of all cancers, with a high rate of incidence found in Uganda, Zambia and the Congo Republic. Most affected in Africa are children, for

example in Zambia, KS represents almost 25% of all childhood cancers (63, 137, 165, 2006 #480).

With the spread of HIV, the epidemiological landscape of KS dramatically changed (18, 110, 132, 136, 174, 206). In Italy a doubling of KS occurrence was registered, while in some African nations, KS now accounts for almost half of all cases of cancer (110). In AIDS patients in the U.S., AIDS-KS accounted for up to 40% of all patients presenting the sarcoma before Highly Active Antiretroviral Therapy (HAART) treatment was introduced (31, 149). Now, roughly 15% of all KS patients present with AIDS-KS (10, 33, 65, 66, 137, 165).

The fourth group predisposed to developing KS is comprised of organ-transplant patients, more specifically organ recipients who are iatrogenically immunosuppressed. Due to improved organ transplant procedures, and the need for increased organ replacement, iatrogenic KS has increased over 400 percent. In Africa 3.5% of renal transplant recipients will develop KS, while the rate in the United States and Europe lies significantly lower at 0.6 percent. Interestingly, iatrogenic KS may spontaneously go into remission after discontinuation of immunosuppressive therapy. It appears that the viral load may be lower in iatrogenic cases, despite a similar tumor burden compared to endemic or classic KS (10, 33, 65, 66, 140, 165).

There is currently no consensus on effective treatments for patients presenting with KS; however, presently there are traditional cancer treatments (e.g. chemotherapy, radiation) and a number of antiviral treatments (e.g. ganciclovir) available, in addition to some promising drug candidates in clinical trials (22, 94, 125, 136). Treatment regimens depend on the type of KS, the extent of tumor invasion and organs affected. This is

independent of antiviral therapy against KSHV, for which there are currently no effective treatments available. The rate of survival in AIDS-KS is around 24 months, although in industrialized nations, the availability of HAART treatment has significantly extended survival expectations. Most commonly, patients who are seropositive for KSHV and display KS disease tend to die of old age or other opportunistic infections because of the generally non-invasive pathology of KS (65).

C. Pathology of KS

KS is a multifocal neoplasm typically visible as multiple reddish –brown vascular nodules in the skin. The cancer is not limited to the skin, but can appear in the oral mucosa, in lymph nodes, and with extensive soft-tissue involvement, e.g. lungs, liver, and intestine. Cutaneous KS lesions tend to appear on the extremities first as macular and papular patches. These lesions evolve into plaque-like or nodular tumors that become elevated and are spongy to the touch. The macular and papular patches are generally symptomless, while nodular lesions can be painful causing edema, maceration and ulcerations. KS lesions commonly reveal widespread neoangiogenesis and include a heterogeneous combination of infiltrating inflammatory cells, extravasated erythrocytes and endothelial cells (EC). The sarcoma is diagnosed in three stages: 1. Patch stage consists of irregular endothelium expanding around normal dermal vessels. 2. Plaque stage defines small lesions of spindle cells involved in neoangiogenesis that begin to form distinct vascular channels. 3. Nodular stage describes invading sheets of spindle cells that create extensive networks of vascular spaces. All of these stages are accompanied by infiltrating inflammatory cells. Spread of KS to visceral organs is more

life threatening than cutaneous forms because it can quickly lead to organ dysfunction and lymphatic obstruction (10, 65, 165, 188).

D. Virology of KSHV

KSHV (HHV-8) belongs to the superfamily of herpesviridae. Herpesviruses are large DNA tumor viruses that are subdivided into three subfamilies, the *alpha-*, *beta-*, and *gamma-herpesviridae*. A distinct characteristic of *gamma-herpesviridae* lies in their ability to latently infect B or T-cells. The γ -herpesvirus subfamily is further subdivided into the *Lymphocryptoviridae* (*gamma-1 herpesviridae*) and the *Rhadinoviridae* (*gamma-2 herpesviridae*) family. KSHV is unique among *Rhadinoviridae* because it is currently the only identified human *gamma-2* herpesvirus.

The KSHV genome consists of a large linear, double-stranded DNA, which upon infection circularizes and remains as a double-stranded episome in the nucleus of the target cell. KSHV has incorporated homologs to many cellular growth and signaling molecules as it evolved. In addition, KSHV contains many unique genes that are involved in regulating cell survival and proliferation pathways. The viral genome consists of a 145 kilobase gene coding region, flanked by multiple GC-rich terminal repeat units. The coding region contains about 87 open reading frames (ORFs), although some coding regions remain to be identified (83). With the large number of genes encoded in its repertoire, KSHV is very efficient at interfering with cellular signaling cascades, evading cellular immunity, and inducing angiogenesis. This gives the gamma-2 herpesvirus a

substantial advantage over its host, and provides for a productive viral life-cycle (10, 26, 33, 83).

A feature of the herpesvirus life-cycle is the ability to switch between two different gene-expression programs, a latent and lytic phase (10, 121, 200). As a result of differential expression patterns, many herpesviruses have acquired multiple origins of replication; KSHV contains two origins of lytic replication (33). While lytic genes are highly conserved across herpesvirus families, latently expressed viral genes are very distinct for each virus, as these genes have evolved to manage their tissue-specific tropism (121). During the latent gene-expression program, a minimal gene-expression pattern is observed and no virions are produced. In this nonproductive stage, viral genes are involved in promoting cellular proliferation and maintaining the viral episome, thereby ensuring replication and equal distribution of the viral genome to dividing daughter cells. Four genes have been associated with the latent gene expression pattern. The most prominent genes expressed during latency, as summarized in Table 2, are ORF73 (latency-associated nuclear antigen-1, LANA-1), ORF72 (viral Cyclin D, vCyc), K13 (the viral FLICE protein, vFLIP), and K12 (Kaposin) (10, 26, 33, 84, 121, 200).

LANA-1 fulfills multiple prominent roles that coincide with maintaining a latent phase, viral persistence, and cellular transformation. LANA-1 can activate cellular and viral replication by interacting with transcription factors such as Sp1 and NF- κ B, or it can repress transcription of lytic genes by directly binding the origins of lytic replication. To prevent cells from activating programmed cell death, LANA-1 neutralizes p53 by downregulating expression of p53 mRNA and degrading existing p53 protein. The interaction with p53 can also lead to chromosomal instability, which may be a stimulus

for transformation. Along the same lines, LANA-1 can bind and inactivate the Retinoblastoma protein (pRB), which also leads to initiation of E2F-dependent transcription. pRB disruption provides cells the unlimited capacity to proliferate, and cells are therefore more likely to become tumorigenic. There have been other binding partners described for LANA-1, which include transcription factors such as the acetyl

Table 2. KSHV Latent Genes.

HHV8 gene	HHV8 protein	Predicted Functions
ORF73	LANA-1	neutralizes p53; episomal maintenance; inactivates Retinoblastoma protein (pRB); manipulates transcription factors such as the acetyl transferase pCBP, p300, and MND A
ORF72	vCyclin	stimulates G ₁ -to-S transition during the cell cycle; disrupts the pRB G1/S tumor suppressor checkpoint
ORF73	vFLIP	inhibits cell death by blocking caspase activity; constitutively induces NF-kB pathways
ORF K12	Kaposin	transformation; activates serine/threonine kinase pathways; reorganizes F-actin

transferase CBP, p300, and MND A. Most importantly, LANA-1 tethers the viral genome to the cellular chromatin, ensuring efficient maintenance of the viral episome during cellular division (33, 34, 84, 121, 147, 199, 200, 212).

vCyc is the viral homolog to the cellular cyclin D2, which stimulates G₁-to-S transition during the cell cycle. Expression of vCyc ensures active cell cycling by disrupting the pRB G1/S tumor suppressor checkpoint and by forming a complex with cdk6 that is resistant to cellular degradation. Cell cycle inhibitors are unable to block this complex, and cdk6/vCyc phosphorylates RB1 and histone H1 to stimulate cell cycle progression. As a consequence of active cell cycling both cellular and viral replication are assured. This guarantees that quiescent cells infected with KSHV begin cell division allowing the number of KSHV-positive cells to increase (10, 33, 119, 120, 200).

vFLIP has essentially been found to be a strong inducer of transformation by interfering with a number of programmed cell death and proliferation pathways. vFLIP

inhibits virally-induced FAS receptor signaling and the downstream induction of FADD-mediated apoptosis. Similarly, vFLIP can inhibit cell death by blocking caspase activity. A focus of recent studies is the ability of vFLIP to constitutively induce NF- κ B pathways. Although the actual mechanism remains to be resolved, activation of NF- κ B pathways has been suggested to stimulate pro-survival molecules and desensitize the host cell to external apoptosis stimuli. The same pathway has also been implicated in autocrine/paracrine expression of cytokines and growth factors, which enriches the environment for tumor development (10, 21, 56, 183).

Finally, Kaposin is a unique viral gene with no cellular homology, and it is the most abundant of all latently expressed viral genes. Understanding Kaposin function is a challenge because it is highly polymorphic. There are three transcripts, Kaposin A, B, or C, generated from the K12 locus, which consists of the open reading frame and upstream direct repeats. The product is a very hydrophobic protein that transforms cultured cells, which can then form tumors when injected into mice. Studies have also shown that Kaposin can activate serine/threonine kinase pathways and reorganizes F-actin (33, 113, 159). More recently, it has been shown that Kaposin B can stabilize cytokine mRNAs thereby increasing cytokine stimulation.

In concert these latent viral genes modulate cellular growth, maintain viral persistence and are responsible for KSHV-induced tumorigenesis, along with paracrine effects of lytic genes. During latency, on average about 5% of cells infected with KSHV may auto-reactivate and switch to the lytic replication phase (23, 33, 55). Auto-reactivation may play a key role in establishing an environment for the latent virus to thrive in. Transformation of the cell by latent genes contributes to tumorigenesis, while

the release of viral and cellular cytokines by newly infected cells may enhance the environment for tumor development (45).

The delicate balance between latent and lytic phase is controlled by LANA-1 and RTA (replication and transcription activator) along with other still unknown cellular and viral factors. LANA-1 represses RTA expression as well as inhibits RTA-dependent transactivation, therefore the virus moves to the latent phase of its life cycle (100, 199). If there is cellular distress, the viral gene expression program changes very quickly to a productive replication phase. The lytic phase entails sequential expression of the complete viral genome, which is driven by the lytic promoter, RTA. During the lytic phase, viral genes are separated into three sequential viral gene expression patterns, immediate-early, early, and late. Immediate early genes include viral regulators of transcription and effectors of cell dissemination. Early genes represent viral DNA replication machinery and late genes are required for virus assembly. During the lytic phase, viral transcription becomes fully active and newly synthesized infectious particles are released from the cell. This completes the viral life-cycle as new progeny then infect additional targets and begin the cycle again (26, 179).

E. Tools for studying KSHV

The discovery that KSHV is the major pathological agent of KS was only made in 1994, while the disease had been described over one hundred years earlier in 1872. In light of the more recent discovery, effective model systems and tools for studying the virus are still being improved (112). KSHV has not only been implicated in KS, an endothelial-based disease, KSHV is also associated with B cell disorders (PEL and

MCD) (33, 121). KS lesions contain a heterogeneous population of cells, which include infiltrating populations of inflammatory cells. KS spindle cells express markers of a variety of cell lineages, which include smooth muscle cells, macrophages, fibroblasts, dendritic cells, as well as endothelial cells (11, 18, 33, 206). For that reason, much attention has been put towards better defining what type of cell the spindle cells, the apparent target cell of KSHV in KS, actually represent (35, 140). It appears that KSHV-infected blood or lymphatic endothelial cells best represent the lineage described *in vivo*. Gene expression profiling studies have focused on KSHV infection of different endothelial cell lineages. The data points towards KSHV inducing dedifferentiation of various endothelial cell lineages and driving expression of different cell lineage markers for the benefit of tumor development (15, 76, 112, 178, 204). *In vitro*, infection of blood or lymphatic EC with KSHV leads to a more de-differentiated state. Cellular markers that indicate a reprogramming of the cell takes place include KSHV induced PROX1, which is essential for embryonic development of the lymphatic system and VEGFR-3, which stimulates lymphatic angiogenesis (45, 76, 204). These markers further suggest that a lymphatic-like phenotype rather than a blood EC phenotype exists in KSHV-infected EC.

To better understand KSHV pathogenesis, different approaches have been employed to develop a model system. This section discusses the various model systems currently in use and highlights their strengths and limitations.

i. Tissue culture models

First attempts to culture KSHV were done using primary effusion lymphoma (PEL)-derived cell lines. Explanted PEL cell lines are easily cultured and efficiently maintain 100 % of the virus latent, even after long-term passage. The viral gene expression pattern of KSHV is analogous to that of KS. PEL cells harbor almost 10 times as many viral genome copies compared to endothelial cells. While cultures of KSHV-infected cells remains primarily latent, the lytic replication phase can easily be induced in these cell lines. Interestingly, *de novo* infection of B cells is not as good at maintaining the infection after serial propagation (33, 66, 84, 112). PEL lines are suspension cells and present different disease pathology than Kaposi sarcoma. KSHV-associated lymphoproliferative disorders maintain some similarities to KS; however, the lymphoproliferative disorders are generally not invasive and do not present similar characteristics of transformation as do KS spindle cells. It therefore remains to be seen how valuable PEL cell lines will be to understanding KS pathogenesis.

Later attempts to recapitulate KS pathogenesis began with trying to culture explanted KS spindle cells, since these are the cells in a KS lesion that consistently contain KSHV. Three explanted cell lines, KSSKL, KS IMM and KSY-1, were the first to culture explanted KS spindle cells (2, 67, 108, 148, 173). This approach had some unexpected problems because explanted cells quickly lost the viral genome under proliferating conditions. In addition, these cells were not able to form foci, grow in soft agar, or even form tumors when implanted into mice, therefore they lack the transformed phenotype of KS (2, 108). The observations suggest that other factors are required to preserve an amenable tumor microenvironment for virus-harboring spindle cells, and this combination of virus and other stimulatory factors enables tumor development. The

additional factors have been suggested to be exogenous growth factors secreted from surrounding non-infected cells, as well as a cytokine-conditioned environment provided by activated T-cells. The hypothesis is that reciprocal signaling events occur between non-infected surrounding tissue, KS spindle cells and the infiltrating inflammatory cells to create the tumor microenvironment (45, 55). Furthermore, the inability of KSHV to persist in explanted cells, suggests that KSHV latency alone is not sufficient to cause KS. In addition, epigenetic events may also be required, such as changes in chromatin structure, DNA methylation or histone modification (33, 55, 84).

A different approach for a model system started with *de novo* infections of primary endothelial cells to reconstitute the KS spindle cells. Primary cells are only limited by senescence, and if KSHV could overcome cellular checkpoints for senescence, these cells would be very useful to study KS. KSHV infection of primary endothelial cells appears to be very similar to cultures of explanted KS spindle cells in many aspects. While *de novo* KSHV infections of primary endothelial cells have provided much insight into the initial stages of infection, this approach has proven to be limited in understanding the effects of long-term latency.

Primary endothelial cells infected with KSHV can only be propagated for a couple of weeks longer than passage-matched uninfected cultures. Furthermore, only small subsets of infected cells survive long term (1-6%) and viral spread is minimal. To maintain a culture of KSHV-infected cells, they need to be constantly replenished with fresh uninfected cells. The constant feeding of KSHV-infected cultures with fresh uninfected cells underscores the potential for a paracrine mechanism in KS. Not all freshly added uninfected cells become infected, so they may contribute to the culture

environment by responding to viral cytokine exposure. In addition, KSHV infected primary endothelial cells need excessive amounts of VEGF to prevent them from undergoing apoptosis. Despite these requirements to maintain the culture, KSHV can induce transformation in primary endothelial cells. The virus appears to extend cell survival because the cells acquire telomerase activity and are capable of anchorage-independent growth, although less than 1% of cells generally produce small colonies (23, 33, 45, 55). Some groups have suggested that primary cells cannot establish long-term latency because they are more sensitive to induction of the lytic cycle (52); however, the determinants for creating long-term infected primary endothelial cultures need to be further elucidated.

The two approaches described so far have provided valuable information about potential co-factors required for the tumor microenvironment. Furthermore these efforts have shown that KSHV latency alone is not sufficient to recapitulate KS in explanted or newly infected primary cell cultures. A major limitation of these methods has been the inability to match age and passage between uninfected and KSHV-infected cultures to discern true KSHV-induced changes. With that understanding, a different approach was taken, whereby primary endothelial cells were first immortalized with telomerase or human papilloma virus genes E6 and E7 (3, 15, 97, 123, 127, 198). By transforming the cells, they appear to be primed to better maintain a latent KSHV infection and mimic the proper environment for KS spindle cell formation. Telomerase-induced endothelial cells, which have been transduced with hTERT for life extension, have been a more popular approach. There is some concern that using human papilloma genes E6 and E7 to

immortalize EC (discussed below) interferes with KSHV biology and may cause KS-unrelated events in endothelial cells.

Telomeres protect the cells' genomic DNA from irreparable damage. Shortening of the telomeres maximizes the number of cellular divisions possible, while limiting the rate of mutation and thereby the probability of tumor formation (discussed in more detail in Section II) (170, 171). Consequently, by reactivating telomerase activity, the number of cell divisions can be extended in as far as the mutation rate does not severely impede normal cell functions. There have been a number of groups who have created different telomerase-transformed endothelial lineages under the assumption that a particular primary endothelial cell lineage employed, e.g. blood versus lymphatic endothelial cells, is more likely to be the KSHV target cell (3, 97, 127, 198). Results have been mixed and researchers are presented with concerns similar to those using non-immortalized cells. Telomerase-induced endothelial cell lines lose KSHV after longer passage of the cells. They do not lose contact inhibition and are not able to form foci. These cells cannot grow colonies in soft agar or form tumors in mice. Interestingly, uninfected telomerase-induced endothelial cells already display spindle cell morphology contributing some ambiguity to the system (112).

E6/E7-transduced dermal microvascular endothelial cells (E-DMVEC) were the first attempt to immortalize primary endothelial cells in order to establish long-term latency of KSHV-infected cells. E6 and E7 overlap in some functions with two of the latency genes of KSHV, LANA-1 and vCyc. Although E6 and E7 are able to immortalize cells, E-DMVEC do not show any abnormal transformation besides the extended lifespan over primary or explanted cells. E-DMVEC are cobblestone in

morphology and become quiescent upon reaching confluency. Furthermore, uninfected E-DMVEC are unable to grow colonies in soft agar or form tumors in mice. When E-DMVEC are infected with KSHV, the cells begin to show phenotypical traits of KS. KSHV-infected E-DMVEC develop spindle cell morphology and begin to form foci post-confluency. Equally as successful is the ability of KSHV-infected E-DMVEC to grow colonies in soft agar and develop tumors in mice. Over 90% of E-DMVEC harbor KSHV and continue to do so over long-term passage. In contrast, only a minute percentage of explanted, primary, or telomerase-immortalized endothelial cells maintain the viral episome over a few passages. Human papilloma virus genes E6 and E7 subsequently seem to assist in stable episomal maintenance of the viral genome (112, 123-125). Consistent with other studies, a small percentage of latently infected E-DMVEC autoreactivate into the lytic cycle; however, it is very difficult to induce lytic replication of all infected E-DMVEC.

It is apparent from the various systems employed to study KS pathogenesis that there still remains much to be clarified about the disease. Although there are considerable differences between model systems, there have been some concurrent findings across all model systems, which have aided in advancing the understanding of KS. Furthermore, McAllister et al. propose, in a recent review of the *in vitro* model systems, that the variability of the systems may benefit the field of KSHV because each system can provide a different perspective on aspects of KS development and viral responses that are dependent on the microenvironment of the culture (112). The danger is that the majority of the discoveries may be found to be unique to the model system

studied. Consequently, it will be very important to validate *in vitro* findings either in an animal model system or *in vivo*.

ii. Animal Models

There is much effort being put forth to develop amenable *in vitro* culture model systems, as there currently is no good *in vivo* model to facilitate KSHV studies. Mice and primates are resistant to long-term KSHV infections making it difficult to study in animals. Primates do carry gamma-2 herpesviruses that are closely related to KSHV, which currently provide the best tool for studying KSHV *in vivo*. Rhesus monkey rhadinovirus (RRV) is one of two gamma-2 herpesviruses that are most closely related to KSHV. Similarities to KSHV exist both in the genomic organization as well as the disease the animals present with. RRV infects B cells and causes a lymphoproliferative disorder that is most analogous to Multicentric Castleman's disease, which is caused by KSHV. Reminiscent of KS, an underlying population of healthy animals infected with RRV do not present with disease. Instead, a combination of RRV and simian immunodeficiency virus is able to induce disease progression, which is not unlike KSHV in HIV-positive individuals. A *de novo* infection of RRV has been successfully cultured in BJAB and 293-HEK cells, where a latent expression pattern dominates the infection. In contrast in the natural target cells of rhesus monkeys, B-cells, RRV displays a robust lytic expression cycle (168, 208).

A second gamma-herpesvirus was also discovered, retroperitoneal fibromatosis herpesvirus, which has even closer homology in genomic organization to KSHV than RRV does. The disease is also more similar to KS compared to the B cell

lymphoproliferative disorder caused by RRV. It has been shown that this virus can cause KS-like vascular tumors, although the incidence of occurrence is rare. Unfortunately there has been little progress made with retroperitoneal fibromatosis herpesvirus because it has not been isolated and cultured for *in vivo* pathogenesis studies (156, 157). Consequently, RRV remains a more relevant model system to study the viral life cycle of KSHV but not Kaposi sarcoma.

While the rhesus rhadinovirus model makes strides towards providing a good model system to study KSHV, the convenience of having a small-animal model has not been ignored. There have been some attempts to use small-animal models to study KSHV pathogenesis *in vivo*. The success has been somewhat limited and none have been able to recapitulate precisely KS tumorigenesis. In mouse models used, the target cell of KSHV was lymphocytes and not endothelial cells (32, 47, 139, 144). KSHV cannot be propagated in severe combined immunodeficiency (SCID) mice, even when the mice are reconstituted with human peripheral blood cells. One approach has been to graft human thymus and liver tissue into SCID mice, which can be infected with KSHV. Latent and lytic transcripts are detected by PCR in lymphocytes, which are mainly found in the implanted tissues. The viral infection can persist in implanted tissue but does not spread, and the tissue shows no signs of any cytopathic effect. In addition, coinfection with HIV does not alter KSHV pathogenesis of infected SCID mice. Finally, there is no histological phenotype in KSHV-infected mice that is similar to any of the KSHV diseases (32).

A more recent approach used NOD/SCID mice that were directly injected with KSHV or first implanted with human hematopoietic tissue grafts. The graft was

implanted to measure the humanized humoral response against KSHV infection. The virus was able to persist long-term in these mice, and the virus was mainly found in B-cells. Latency did not establish itself until 1 month after infection, which was followed by a steady rise of lytic reactivation. In these KSHV infected mice only 6% developed splenic enlargement (139).

The mouse models so far have shown promise to enhance KSHV replication and infection studies. In light of the fact that the predominant target cells in these mice are lymphocytes, the ability to study KS in the context of these small-animal models remains limited.

II. Tumorigenesis

“If a single mutation can cause a cell to become malignant, we can explain all the cancers we wish” (172). This statement best expresses the appreciation for the complexity of tumors and the frustration for a lack of scientific accord about which changes, and how many of them, are required to cause cancer. Tumors develop because of a replicative advantage over normal cells as well as a failure to die, and there are many factors that determine this advantage. Such factors include cell growth, cell turnover, mutation rates, and extrinsic factors (such as viruses). The pathogenesis of cancer is dependent on tumor agents in order to overcome the various cellular safety mechanisms, which otherwise would limit the possibility of tumor growth by inducing programmed cell death. Oncogenes are the most recognized contributors to cancer, as they represent dominant changes in normal cell development that stimulate loss-of-contact inhibition, invasion, and an unlimited proliferative capacity. As antagonists, tumor suppressors can

react to such unwanted changes; however, dominant-negative changes in tumor suppressor function can also facilitate tumor development. An inactive tumor suppressor facilitates extended cell growth, increasing genomic instability and inactivating programmed cell death (171, 172).

It is estimated that cells accumulate a mutation every 20-30 cell divisions. Generally, this mutation is recessive, and many more mutations are necessary before the cell acquires oncogenes or inactive tumor suppressors. Consequently, for a cell to become tumorigenic, it must overcome tremendous odds. Tumor suppressor mechanisms further limit the number of divisions a cell completes in order to prevent mutations from arising via DNA damage. This also includes telomere shortening. Telomeres protect genomic DNA and simultaneously act as a molecular clock by counting the number of cell divisions. Once any of these events of DNA damage or telomere shortening occurs, cell division is inhibited, and the cell generally enters senescence (171, 172). Senescence can also act as a tumor suppressor mechanism by responding to changes in abnormal protein expression patterns or signal transduction pathways. Therefore, senescence becomes a vital checkpoint in normal cell progression. Overcoming senescence is a major step in the evolution of most malignancies. Damage to cell cycle regulation, reactivated telomere maintenance, or loss of important apoptosis-inducing proteins p53 and pRb, are some examples of the critical hurdles that need to be conquered to surmount senescence. Yet, stopping cell division may not be sufficient to prevent mutations from leading to tumor development, as senescent cells remain metabolically active and secrete factors that can stimulate the tumor microenvironment (171).

An increase in the number of tumor cells effectively improves the probability that mutations will overcome the aforementioned checkpoint. Once senescence has been passed and a tumor cell acquires an unlimited capacity to proliferate, tumorigenic cells face certain genomic instability. Next, the cell reaches the second major checkpoint, termed crisis. Crisis prevents severely malfunctioning cells from uncontrollably proliferating. This cellular checkpoint can be overcome with greater ease than senescence because genomic instability favors tumorigenesis. Studies have shown that people with defects in mechanisms to minimize genomic instability have a very high likelihood of developing cancer (172). Once a cell overcomes this second tumor suppressor mechanism, the tumor cell is immortalized and has an unlimited capacity to accumulate further mutations while expanding a clonal population of tumorigenic cells.

As a tumor begins to develop, normal cellular processes necessary in early developmental stages are pirated and reactivated for the benefit of the growing tumor. Tumor growth begins with procuring blood vessels from the surrounding tissue. Depletion of the blood supply to the surrounding tissue induces hypoxia. With the onset of hypoxia, survival programs are activated that lead to secretion of the vascular endothelial growth factor (VEGF) among other factors and consequent remodeling of established networks of blood vessels, defined as angiogenesis, begins. VEGF and other factors stimulate endothelial cells lining the blood vessel thereby enabling sprouting angiogenesis. Activated endothelial cells stimulate degradation of the extracellular matrix by activating proteolytic pathways. Furthermore, endothelial cells promote proliferation by reactivating signal transduction pathways normally required for neonatal development. The event of neovascularization simulates wound healing, and

inflammatory cells, e.g. macrophages and leukocytes, are also attracted to the tumor environment. Activation of macrophages and leukocytes generates secretion of various cytokines, e.g. CCL21, and other stimulatory factors that inadvertently support tumor growth. Hence, wound healing and inflammation become pathological conditions and along with neovascularization are pirated by the tumor to create an environment that is enriched with stimulatory factors promoting tumor growth (160, 186).

Despite the extremely low mutation frequency of cells, the occurrence of cancer is much more prevalent. It is apparent that extrinsic factors significantly increase the probability that tumors will develop by promoting cell division, inhibiting apoptosis and even inducing DNA damage (172). There is considerable evidence for viruses acting as such an extrinsic factor and being the causative agent for different cancers (Table 3). Many DNA and RNA viruses have been documented as being responsible for cancer development because the viral proteins have evolved oncogenic and anti-tumor suppressor-like features (137, 153). Viral genes have adapted cellular functions that induce deregulation of cell cycle controls, inactivation of tumor suppressor proteins, and activation of signal transduction pathways to guarantee a productive viral life cycle. Target cells for viral replication may even involve senescent cells, where the virus has adapted viral proteins to revive cellular replication machinery, and as a consequence, cell division (44).

A retrospective study done in 2002 on the global burden of infection-associated cancers has attributed 1.9 million cases of cancers to infectious agents. This represents 17.8% of all cancers reported worldwide. Twelve percent of these cancers have been shown to be due to a viral infection. The distribution of such cancers follows the pattern

of available antiviral drug treatments, as 26.3% of all virus-attributable cancers were found in developing countries. Vaccines against viral agents have convincingly shown that there is a significant correlation between successfully preventing infections and the occurrence of an associated cancer (137). Clearly extrinsic factors, such as viruses, become a major driving force in cancer development. The effectiveness with which viruses can cause cancer suggests that, while cancers can develop through a stepwise orchestration of complex events at random, tumor progression can also occur in leaps with the help of extrinsic factors.

Table 3. Cancers Attributable to Viral Infections.

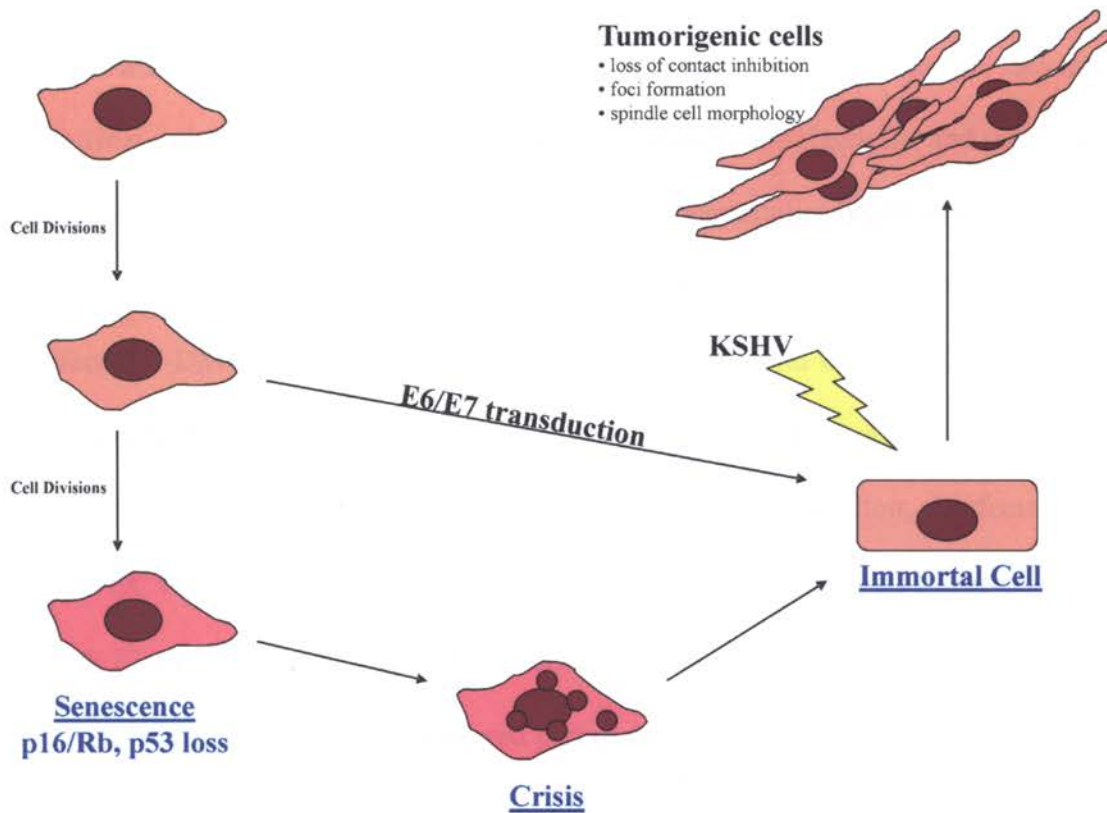
Extrinsic Viral Factor	Associated Cancer
Human papillomavirus	Cervical carcinoma
Hepatitis B virus Hepatitis C virus	Liver carcinoma
Epstein-Bar virus	Nasopharyngeal carcinoma Burkitt lymphoma Hodgkin lymphoma
Human T-cell lymphotropic virus type I	Adult T-cell lymphoma
Kaposi sarcoma-associated herpesvirus	Kaposi sarcoma Non-Hodgkin lymphomas

III. KSHV-induced Tumorigenesis

In KS, KSHV is the extrinsic factor that exerts selective pressures on infected endothelial cells to become tumorigenic. While KSHV has been identified as the causative agent, the virus is not sufficient to cause cancer. Nevertheless, the sarcoma does not develop without KSHV (65, 66, 137). When KS develops, it presents all

previously described characteristics of tumor growth (39), which include neovascularization, a hallmark trait of KS skin lesions typically identifying AIDS-patients, infiltrating inflammatory cells (66), and hypoxia (61) (Camillo Raggio and Klaus Früh, unpublished observations), among others.

KSHV has existed for a long time and has co-evolved with humans, thereby adapting viral proteins to function like their human counterparts. Consequently, viral proteins function as oncogenes disrupting normal cell function to the advantage of viral replication and maintenance of the viral genome (15, 125, 204). KSHV does not seem to be sufficient to overcome the two major checkpoints of tumor suppression, senescence and crisis, because explanted KSHV-infected spindle cells quickly lose the virus *in vitro*. In the system used for this dissertation, developed by Ashlee Moses (123), E6 and E7 establish an immortalized cell line from primary EC that has as a consequence most likely overcome senescence and crisis (Figure 1). This immortalized cell line creates a good environment for the virus to establish itself and promote tumorigenesis. Once the immortalized E-DMVEC are infected with KSHV and remain latently infected long-term, the cells begin to show signs of tumorigenesis.



adapted from Shay J.W. et al. *Carcinogenesis* 26(5):867, 2005

Figure 1. The E-DMVEC Model for KS. A cartoon suggesting how the E-DMVEC infected with KSHV succeed at representing the *in vivo* phenotype of KS spindle cells. Primary dermal microvascular endothelial cells are transduced with a retroviral vector containing E6 and E7 of Human Papilloma virus, which immortalizes the cells by overcoming senescence and crisis. E6/E7 stimulate as yet undetermined events *in vivo* to prime immortalized cells. Predisposed E-DMVEC are then infected with KSHV and over weeks begin to develop tumorigenic traits of spindle cell formation, loss of contact inhibition and foci formation.

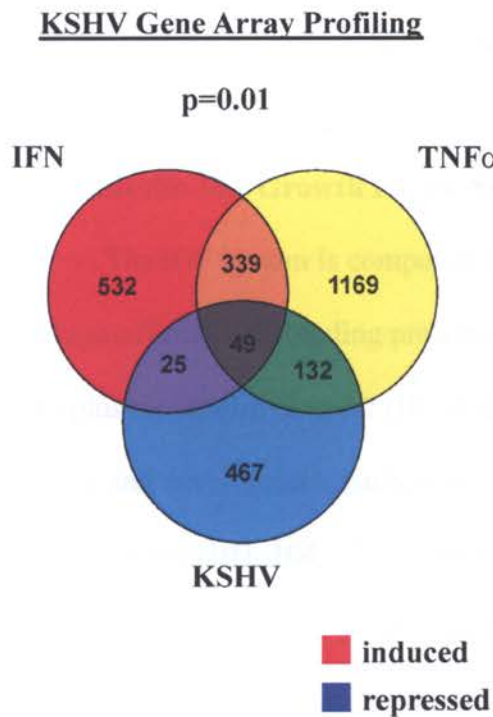
Tumor development is not only driven by latent and lytic viral genes, but also from virus-activated cellular oncogenes and inactivated tumor suppressors. Several of the virus-induced host proteins are required to support tumorigenesis, and the most appropriate way to assess the changes at the time these studies began was to employ microarray gene expression profiling techniques. Passage- and age-matched KSHV infected E-DMVEC and uninfected were grown over several weeks and the gene transcription pattern was compared with Affymetrix microarray gene chips. To dissect KSHV-induced changes from the cellular response to viral infection, uninfected E-DMVEC were also treated with interferon- γ (IFN) or tumor necrosis factor- α (TNF- α) for 6, 12, or 24-hrs and compared to KSHV-infected E-DMVEC.

IFN and TNF- α are considered part of the initial innate immune response to viral infection and will themselves create unique gene expression profiles (Figure 2).

Uninfected E-DMVEC cultures were used as a baseline for gene expression and the various conditions were compared to the uninfected expression pattern. It could easily be determined which changes in gene expression changes were due to viral proteins or a cellular response to the viral infection. A comprehensive list of changes in gene expression can be found in Appendix I. The tables compiled in the appendix represent changes that were identified in all treatments as being repressed or induced. Furthermore genes were sorted based on the unique downregulation or upregulation by KSHV.

In light of the described de-differentiated phenotype of KSHV-infected cells, combined with an unlimited proliferative capacity of KS tumor cells we proposed this underlying hypothesis: KSHV needs to reprogram growth-stimulating pathways, such as the insulin-

A.



B.

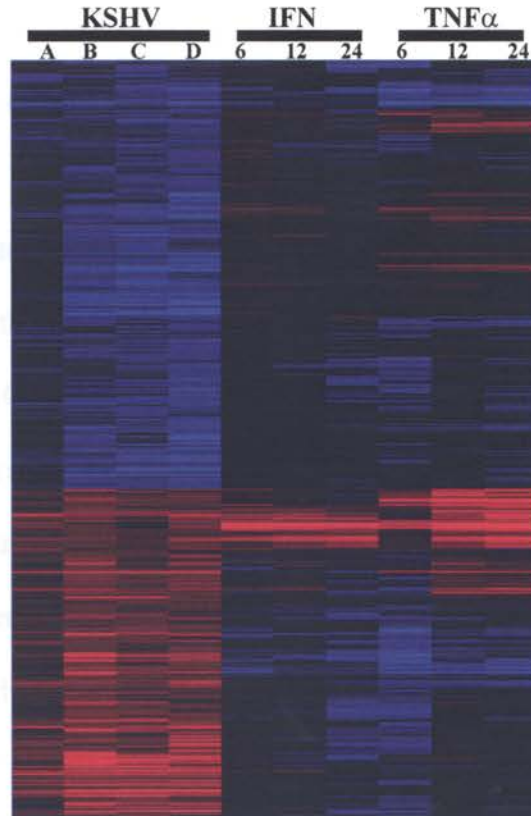


Figure 2. Microarray Gene Expression Profiling. (A) Venn diagram representing similarities and differences between the gene array profiles of KSHV-infected E-DMVEC, IFN- or TNF- α treated E-DMVEC. (B) Microarray heat map of probe sets representing all significant changes ($p=0.01$) in each of the conditions. 4 independent KSHV infections (A-D) were compared to 3 different time-points of IFN- or TNF- α treatment. Red indicates induced gene expression, blue repressed.

like growth factor system and associated house-keeping genes, such as regulatory cysteine proteases, to promote tumorigenesis.

IV. The Insulin-like Growth Factor System in Cancer

The IGF system is composed of three peptide ligands, IGF-I, IGF-II, and insulin, six high-affinity IGF-binding proteins (IGFBP 1-6), and two IGF receptors (IGF-IR, IGF-IIR) plus the insulin receptor (IR) (Figure 3). The insulin-like growth factors regulate growth and development, particularly during embryogenesis, but are also involved in tumorigenesis (103, 104, 122). The secreted ligands (IGF-I and II) are homologous to insulin, but differ in their processing and contain additional unique domains (180). In contrast to insulin, they are produced by almost every cell of the body and circulate in high concentrations. Both IGF-I and IGF-II signal through the IGF-IR, although IGF-II has an approximately 4-fold lower affinity for the IGF-IR compared to IGF-I (122). The IGF-IR is homologous to the IR, and both are members of the receptor tyrosine kinase superfamily. In addition to acting via independent signaling pathways, IGF-IR and IR can also heterodimerize. Most effects of IGF-I arise from its activation of the IGF-IR, although IGF-I/IR heterodimers are also activated by IGF-I, but not insulin (128). IGF-II can activate IGF-IR, IGF-IIR, and IR. The IGF-IIR has a 100-fold higher affinity for IGF-II than for IGF-I or insulin, but does not signal. The IGFII-R functions as a clearance receptor, regulating the levels of IGF-II by internalization and degradation (30). The IGF-IIR is also known as the cation-independent mannose 6-phosphate receptor (M6PR) that plays a role in endocytosis and intracellular trafficking of mannose 6-phosphate-tagged proteins such as lysosomal enzymes (9, 64).

The IR exists as two spliced variants, IR-A and IR-B. The IR-A splice variant lacks a 12-amino acid sequence at the C-terminus of the extracellular α -subunit encoded by exon 11 and binds IGF-II with higher affinity than insulin (28, 29, 49). Normally, IR is a mediator of metabolic effects by insulin on specific tissues such as adipose and skeletal muscle; however, IR also plays an important role in mediating proliferative responses. IR-A is mainly found in hematopoietic cells to mediate predominantly proliferating effects. In contrast, the IR-B splice variant is more prominent in adipose tissue, liver, and muscle, and mediates the metabolic effects of insulin (29, 49, 166).

Binding of ligands to IGF-IR or IR-A triggers a signal cascade that leads to activation of downstream effector molecules which regulate cell growth and survival. Following ligand binding, the receptors undergo autophosphorylation on specific tyrosine residues, which provide attachment sites to facilitate the recruitment and subsequent tyrosine phosphorylation of the insulin receptor substrate (IRS) and src-homology collagen protein (Shc) family members of scaffolding/adaptor proteins. These factors in turn, recruit PI3 kinase and the grb-2/mSOS complex to initiate the activation of the PKB(Akt) and ERK cascades. The endpoint is Forkhead responding to Akt and Ets transcription factor families, which promote growth, survival, adhesion, and motility of cells (129).

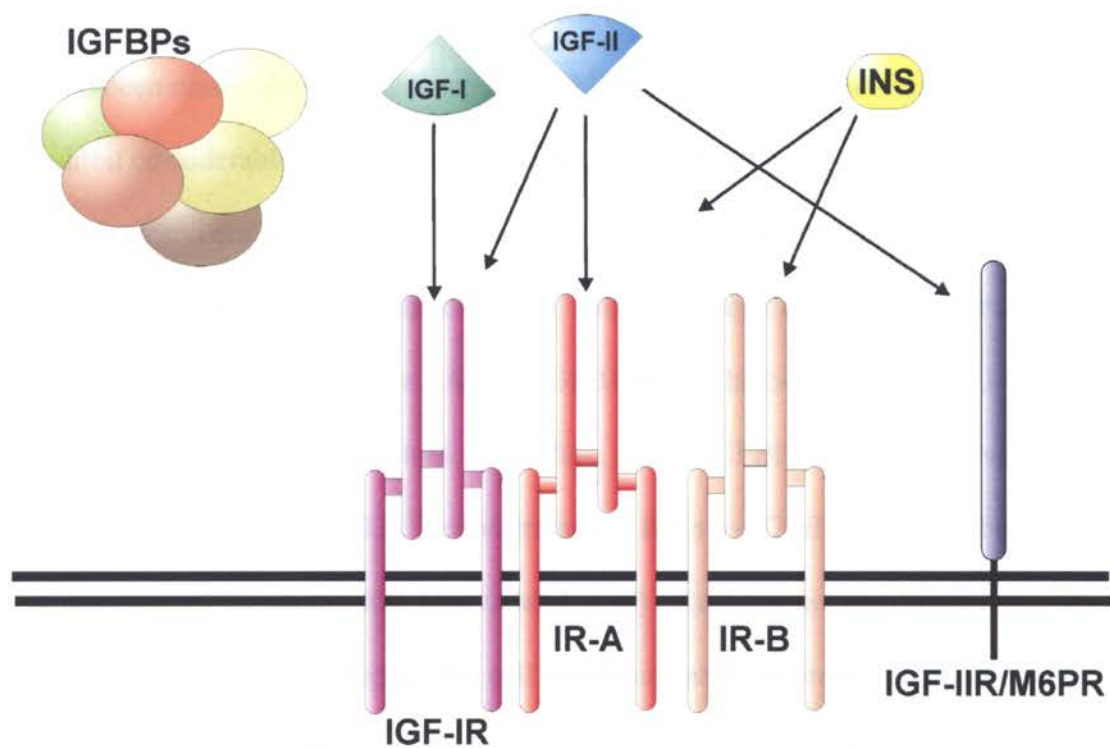


Figure 3. The Insulin-like Growth Factor System. Members of the insulin-like growth factor system consists of three ligands, insulin (INS), and insulin-like growth factors I and II (IGF-I and IGF-II). There are three receptors, the insulin receptor, represented by its two spliced variants, IR-A and IR-B; and the insulin-like growth factor-receptors I and II. In addition, there are six insulin-like growth factor binding proteins. The possible interactions shown between the ligands and receptors are not comprehensive.

The vast majority of IGFs in circulation are complexed with IGF-binding proteins. IGFBP regulate the interaction of IGFs with their receptors; however, they do not bind to insulin. The major IGFBP in the circulation is IGFBP-3, which can bind IGF-I or IGF-II in an equimolar ternary complex (42). Six high-affinity IGFBP, IGFBP 1-6, have been reasonably well characterized at both the structural and functional levels and exhibit considerable similarity at the protein level. IGFBP have multiple conserved cysteines and are presumably similar in secondary structure; however, they vary in their degree of glycosylation, phosphorylation, and presence of binding sites for integrins (RGD sequences) and heparin. All six IGFBP have a higher affinity for IGF ligands than the ligands do for their receptors. Therefore, all six IGFBP are able to prevent binding of IGFs to their receptors (203). Sequestration of IGFs by IGFBP becomes the major mechanism of regulating IGF bioavailability (7). At the same time, IGFBP can also act as transporters of IGFs through the cell membrane and can prolong IGF persistence in the circulation, thus potentiating IGF effects. To balance the system, IGFBP are sensitive to proteolysis by cysteine proteases. Proteolytic cleavage has been implicated as the most likely method of down-regulation of IGFBP activity, with concomitant alteration of IGF bioavailability (42). One of the more prominent insulin-like growth factor binding proteins is IGFBP-2. This protein is neither glycosylated nor phosphorylated, but contains an RGD sequence. IGFBP-2 inhibits IGF actions, in particular those of IGF-II, possibly due to its higher affinity for IGF-II (85). Overexpression of IGFBP-2 in embryonic fibroblasts results in the inhibition of cell proliferation, which can be reversed by addition of IGFs (74). IGFBP-2 has been shown to be mitogenic for uterine endometrial epithelial cells and osteosarcoma cells in the absence of IGFs (4, 177).

Interestingly, IGFBP-2 knockout mice are viable and fertile and show only minor defects in liver and spleen size (209).

In addition, the IGFBP also exhibit IGF-independent activities (7, 203). Of these, the activities of IGFBP-3 have been the most well characterized (131, 151). Mouse embryonic fibroblasts with a targeted disruption of the IGF-IR gene show a 10-fold slower growth rate and undergo apoptosis when transfected with IGFBP-3 (196). IGF-independent activity could be either mediated through cell-surface receptors for IGFBP-3 or through direct import and translocation of IGFBP-3 to the nucleus. Evidence for both mechanisms exists because novel cell-surface binding proteins as well as nuclear import receptors for IGFBP-3 have been identified (203).

IGFBP-5 is similar to IGFBP-3 in its biological activity, and it is thought to also share some of its IGF-independent functions and mechanisms (203). IGF-independent functions for IGFBP-1 have also been demonstrated. IGFBP-1 binds to $\alpha 5 \beta 1$ -integrin, which stimulates cell migration (86). IGFBP-1 contains an integrin-binding sequence motif, RGD, in its C-terminus, and peptides containing this sequence can stimulate focal adhesion kinase (FAK), which influences cell attachment and cell death (142).

The IGFs, their receptors, and IGFBP have all been implicated in carcinogenesis (122). Overexpression of IGF-II has been observed in many cancers, including hepatocarcinoma, adenocarcinoma and colon cancer, consistent with IGF-II-mediated autocrine stimulation of the IGF-IR (25, 48, 163). Highly metastatic cancer cells have been shown to express higher levels of IGF-II and IGF-IR compared to tumor cells that are less prone to metastasize (57). High circulating levels of IGF-I have been associated with an increased risk of breast, prostate and colon cancer, suggesting endocrine

mechanisms of tumorigenesis (146, 207). In experimental models, the growth of many established cancers can be inhibited by pharmacological strategies that reduce IGF-IR signaling.

The IGF-II/M6P-R is generally regarded as a tumor suppressor that acts as an IGF-II sink (130). Consequently, a loss of function for regulating lysosomal trafficking or internalization of IGF-II has also been indicated as part of a multistep process in tumorigenesis (64, 107, 205).

Finally, the IR has also been implicated in cancer. The insulin receptor is differentially expressed, which is dependent on the stage of development (77, 135). A preferential expression of the IR-A isoform in less-differentiated tissue has been shown to be associated with several different cancers, including lung, colon, breast, ovarian, and thyroid cancer (29, 49, 89, 91, 166, 167, 197). Splicing of IR presumably alters the affinity of the receptor for its ligand. While both isoforms have a high affinity for insulin, IR-A has a higher affinity for IGF-II, which is able to activate predominantly mitogenic rather than metabolic signaling pathways (28, 29).

The role of IGFBP in cancer is complex given their stimulatory and inhibitory effects on IGF activity and their additional IGF-independent functions. Altered levels of circulating or tissue-specific IGFBP have been associated with certain cancers, notably in prostate, colon and the central nervous system (122). In particular, IGFBP-2 overexpression is frequently associated with tumor progression in several tissues. DNA microarray analysis revealed a strong correlation between IGFBP-2 over-expression and high grade glioblastomas, compared to lower-grade tumors (51). IGFBP-2 expression has also been associated with poor patient survival in diffuse gliomas (36, 37, 161).

Elevated serum levels of IGFBP-2 have been reported for ovarian, colon, central nervous system and prostate cancers (24, 46, 69, 90, 126). In a mouse model of androgen-independent progression to advanced prostate cancer, IGFBP-2 expression was observed to be elevated in LNCaP tumor cells both *in vitro* and *in vivo* after androgen withdrawal (92). Forced expression of IGFBP-2 via retroviral vectors results in more rapid tumor progression. In contrast, treatment of LNCaP tumor cells with antisense oligonucleotides to IGFBP-2 reduced LNCaP cell growth and increased apoptosis. Overexpression of IGFBP-2 in human epidermoid carcinoma increased tumorigenesis (115), and overexpression of IGFBP-2 in Y-1 adrenocortical cells resulted in enhanced proliferation and increased cloning efficiency independent of IGF-I (70). Based on these and many other examples, the IGF axis is a potent target for cancer therapy (184).

V. Cysteine Protease Involvement in Tumorigenesis

The role of proteases in tumor growth, invasion, migration and metastasis has been studied extensively for many years (20, 87, 88, 93, 194). The highly vascular and invasive nature of tumors requires extensive degradation and remodeling of the extracellular matrix to allow the tumor to invade surrounding tissue, as well as co-opt blood vessels from neighboring tissues. Particular attention has been given to proteases involved in the apoptotic cascade (caspases), remodeling of the extracellular matrix (matrix-metallo proteases) and general protein turnover (proteasome). Inhibitors for each of these classes are undergoing clinical trials in a variety of cancers (1, 109, 143). In addition to these well studied proteases, evidence points to cysteine proteases being involved in carcinogenesis (194).

The cysteine protease family is separated into three families: papains, calpains and interleukin 1 β -converting enzymes. Interleukin 1 β -converting enzymes are regulators of apoptosis. Calpains play a role in regulating membrane signaling and papains are involved in digestion and hormone processing, among others functions. Within the papain superfamily are the lysosomal cysteine proteases, also known as cathepsins (20, 192, 195). Cathepsins are made as preproenzymes, which are targeted to the endosomal/lysosomal compartment by gaining post-translationally a mannose 6-phosphate residue (Figure 4). The recognition pattern of the mannose 6-phosphate residue allows mannose 6-phosphate receptors, e.g. the IGF-IIR, to transport the enzyme from the golgi network to the lysosomes (64, 202).

Currently, the cathepsin family is comprised of 11 members in the human genome (191, 194, 195). Most cathepsins are ubiquitously expressed. Traditionally, cathepsins are known for their role in protein degradation in the endosomal/lysosomal compartment and, as such, are involved in many physiological processes, including protein turnover, protein processing, and antigen processing (191, 195). The importance of other functions besides the expected lysosomal protein degradation for cathepsins is becoming better appreciated. These functions include bone remodeling, MHC Class II processing, epidermal homeostasis, regular hair-follicle morphogenesis, and activation of serine proteases in granules of inflammatory cells (20). Understanding the assorted roles for cathepsins has helped to explain how a functional imbalance of cathepsins play a pivotal role in a wide range of diseases including rheumatoid arthritis, osteoarthritis, neurological

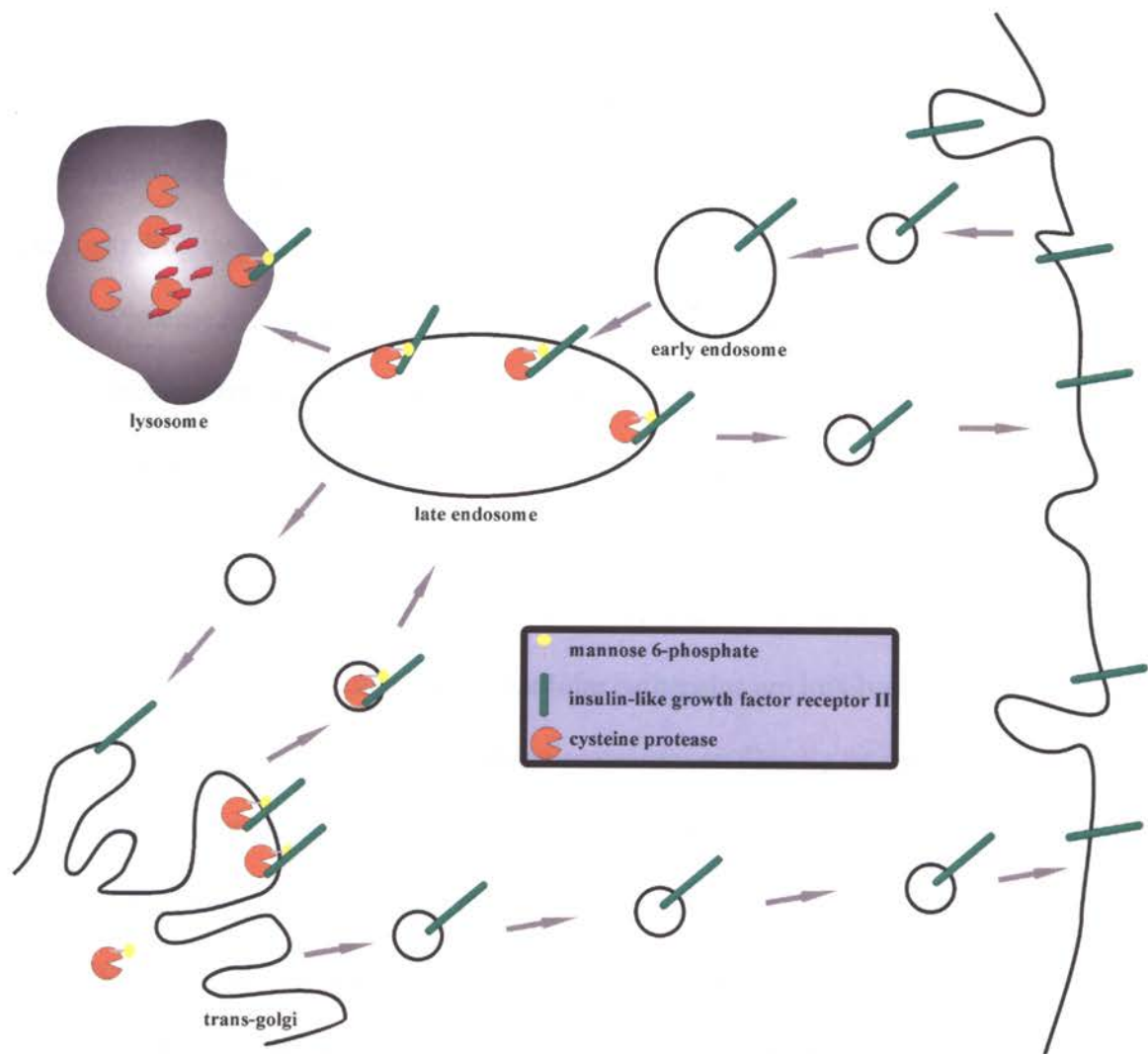


Figure 4. Mannose 6-phosphate-dependent Transport of Cysteine Proteases.

Cysteine proteases are post-translationally tagged with a mannose 6-phosphate, which is recognized by a mannose 6-phosphate receptor (IGF-IIR) in the trans-golgi network. IGF-IIR then transports the cysteine protease to lysosomes or the extracellular space where the protease is released and becomes active. Meanwhile, the mannose 6-phosphate receptor is recycled to the golgi.

disorders, osteoporosis, lysosomal storage diseases, and cancer (87, 88, 191, 193-195). Not surprisingly, 4 of the 11 characterized human cathepsins have been crystallized by pharmaceutical companies, since their implications in various diseases make them excellent drug targets (193).

Protease activity is generally a tightly controlled process and changing this control mechanism during tumor growth may facilitate angiogenesis, invasion, or even loss of contact inhibition (79, 158, 175). The involvement of cathepsins in tumor growth may be due to increased proteolytic activity (87, 88, 176), a change in protease expression levels, which has been correlated to the malignancy grade of tumors, or both (181, 182). Both extracellular and intracellular cathepsins are involved in degradation of extracellular matrix components. Cysteine proteases can directly be responsible for tumor invasion by proteolytically degrading various components of extracellular matrix e.g. collagen, laminin, and fibronectin (98, 176). Cathepsins can also activate other proteolytic pathways for degrading the extracellular matrix, e.g. matrix metallo proteases (87). Alternatively, cathepsins can process components of regulatory networks, i.e. growth factors, signaling molecules or adhesion molecules to stimulate angiogenesis or tumorigenesis. For example, cathepsins control processing and release of VEGF (211) or urokinase plasminogen activator (54, 88).

Cysteine proteases also play a role in the processing of IGFBP (12, 214). *In vitro*, cathepsin D and cathepsin G cleave IGFBP 1-6 (12, 53). Cathepsin L-deficient mouse fibroblasts show a decreased degradation of IGFBP-3 (214). When IGFBP are cleaved, they lose their affinity for IGFs. Proteolytic processing may either enhance or decrease

the IGF-independent function of IGFBP. Therefore, cathepsins could be involved in cancer progression by regulating the IGF signaling axis.

VI. Summary

This dissertation uncovers some important mechanisms of KS tumorigenesis, changed in endothelial cells by KSHV. Latent infection of endothelial cells with KSHV alters cellular differentiation and is accompanied by significant transcriptional changes. In an attempt to survey the changes that occur upon viral infection, we employed the most amenable *in vitro* system to study KS (123) and compared gene expression profiles of passage- and age-matched KSHV-infected and uninfected E-DMVEC. Four different long-term KSHV infected cultures with their passage- and age-matched uninfected counterparts were contrasted.

We have discovered that well-characterized pathways deregulated in many other cancers also play a prominent role in KS, the IGF signaling axis and cathepsin B activity. Consequently, findings presented in the next two chapters have the potential to improve both KS as well as general cancer therapies. KS is becoming a well-defined tumor model and a valuable tool to study general tumorigenesis. The E-DMVEC system has been extremely useful for evaluating changes in the cellular transcriptome and lead to the identification of oncogenes involved in tumorigenesis (111, 124, 125, 150). Some of these previous discoveries already have led to improved treatment possibilities, and the hope is that it will be possible to broaden treatment options with the findings presented in this dissertation.

The action of the IGF system has been implicated in many malignancies and recent data have demonstrated that the IGF-IR is required for *in vitro* growth of the KS-derived cell line KSIMM (17). We examined the expression and function of all IGF ligands, receptors, and binding proteins in KSHV-infected, immortalized dermal microvascular endothelial cells. The expression of the IR was strongly induced in latently infected E-DMVEC, whereas the expression levels of the IGF-IR remained unchanged. Gene knockdown of IR, but not IGF-IR, prevented the characteristic focus-formation seen in KSHV-infected E-DMVEC, which typically exhibit contact independent growth. Focus formation was similarly inhibited by treatment of KSHV-infected E-DMVEC with the IR-specific small-molecule inhibitor HNMPA-(AM₃). These data suggest a role for the IR, but not the IGF-IR, in KSHV-induced transformation of vascular EC.

Since in many cancers tumorigenesis is associated with an increase in the activity of the cathepsin family, we also studied the role of cathepsins in KS. Small-molecule inhibitors and small interfering RNA targeting cathepsin B, but not other cathepsins, inhibited KSHV-induced post-confluent proliferation and spindle cell and foci formation of dermal microvascular EC. Interestingly, neither cathepsin B mRNA nor protein levels were induced in EC latently infected with KSHV; however, secretion of cathepsin B was strongly diminished upon KSHV infection. Increased targeting of cathepsin B to endosomes was caused by KSHV-induced expression of the IGF-IIR, a mannose 6-phosphate receptor, which facilitates cathepsin transport from the trans-golgi network. Inhibiting IGF-IIR expression by siRNA released cathepsin B for secretion. In contrast to the increased secretion observed in most other tumors, we reveal that viral inhibition of

cathepsins B secretion via induction of a mannose 6-phosphate receptor is crucial for transformation of endothelial cells.

These results are a cumulative effort to describe how KSHV deregulates the IGF system. While deregulation of the IGF system was identified by changes in expression levels, this was not the case for CTSB. In fact, CTSB involvement in KSHV-induced tumorigenesis appears to be a responsive downstream element of the deregulated IGF system, instead of an independently targeted deregulation by KSHV. This is described in more details in the following chapters.

CHAPTER 2

The Insulin Receptor is Essential for Virus-induced Tumorigenesis of Kaposi's sarcoma

Patrick P. Rose¹, Julie M. Carroll², Patrick A. Carroll³, Victor R. DeFilippis¹, Michael Lagunoff³, Ashlee V. Moses¹, Charles T. Roberts, Jr.², and Klaus Früh^{1,4}.

¹Vaccine and Gene Therapy Institute, Oregon Health and Science University, Portland, Oregon, United States, 97239.

²Pediatrics, Oregon Health and Science University, Portland, Oregon, United States, 97239.

³University of Washington School of Medicine, Seattle, Washington, United States, 98195.

⁴To whom requests for reprints should be directed at the Vaccine and Gene Therapy Institute, Oregon Health and Science University, 505 NW 185th Ave, Beaverton, OR, 97006. Phone: 503 418 2735 (KF), 503 417 2712 (AM), Fax: 503 418 2701; email: fruehk@ohsu.edu

PP Rose, JM Carroll, PA Carroll, VR DeFilippis, M Lagunoff, AV Moses, CT Roberts Jr and K Früh. *Oncogene*, **advanced online publication**, 25 September 2006

ABSTRACT

Kaposi sarcoma (KS), a multifocal neoplasm of the skin that can spread to visceral organs, is the most prevalent malignant tumor in AIDS patients. KS-associated herpesvirus (KSHV or HHV8) is considered the primary etiological factor of this malignancy, as well as of primary effusion lymphoma and multicentric Castleman's disease. KS lesions are characterized by proliferating spindle cells of endothelial cell (EC) origin. The action of the insulin-like growth factor (IGF) system has been implicated in many malignancies, and recent data have demonstrated that the IGF-I receptor (IGF-IR) is required for *in vitro* growth of the KS-derived KSIMM cell line. To examine whether the IGF pathway is also involved in KSHV-mediated transformation of ECs, we examined the expression and function of the IGF system in KSHV-infected, immortalized dermal microvascular EC (E-DMVEC). The expression of the insulin receptor (IR) was strongly induced in latently infected E-DMVEC, whereas the expression levels of the IGF-IR remained unchanged. Gene knockdown of IR, but not IGF-IR, prevented the characteristic focus formation seen in KSHV-infected E-DMVEC. Similarly, treatment with the IR-specific small-molecule inhibitor HNMPA-(AM₃) inhibited post-confluent growth. These data suggest a role for the IR, but not the IGF-IR, in KSHV-induced transformation of vascular ECs.

INTRODUCTION

Kaposi sarcoma (KS) is the most prevalent malignant tumor in AIDS patients, particularly in sub-Saharan Africa (132). The γ 2-herpesvirus KS-associated herpesvirus (KSHV or HHV8) is the pathological agent of KS and of lymphoproliferative disorders in B cells (84). KSHV establishes persistent infection for the duration of the host's existence, with the virus exhibiting a restricted gene expression program that maintains the circularized viral DNA genome during cellular replication (138). KS lesions are mainly composed of interweaving bands of vascularizing spindle cells that are of endothelial origin and frequently associated with infiltrating inflammatory cells (11). Although most spindle cells harbor latent virus (178), KS-derived spindle cells rapidly undergo senescence in cell culture, and the few KS-derived cell lines, such as KSY1 or KSIMM, are highly altered in their karyotypes and do not contain virus (2, 43, 108). KSHV is unable to immortalize endothelial cells *in vitro*. However, long-term latent infection of KSHV was observed after immortalization of dermal microvascular endothelial cells with human papillomavirus E6/E7 proteins (E-DMVECs) (123). Uninfected E-DMVECs grow as discrete monolayers of cobblestone phenotype, are contact-inhibited, and enter senescence if not passaged after attaining confluence. Upon infection with KSHV, E-DMVECs develop a spindle cell phenotype, lose contact inhibition, form foci when cultured post-confluence, and acquire the ability to form colonies in soft agar. The E-DMVEC system has thus been extremely useful for evaluating changes in the cellular transcriptome and proteome, ultimately leading to the identification of both known as well as novel oncogenes that are likely to be involved in KS tumorigenesis (111, 125, 150).

A recent report showed that autocrine stimulation of the IGF-IR by IGF-II is required for continued growth and protection against apoptosis of KS-derived KSIMM cells (17). IGFs are part of a complex system of growth factors, growth factor receptors, and IGF-binding proteins and deregulation of IGF action has been implicated in tumorigenesis in many cancers (104). Since KSIMM cells lack viral genomes, we were interested to determine whether the IGF system is involved in maintaining the transformed phenotype of endothelial cells latently infected with KSHV. Here we demonstrate that the insulin receptor (IR), but not IGF-IR is strongly induced by KSHV infection. Moreover, gene knockdown or pharmacological inhibition of IR prevented KSHV-mediated tumorigenesis whereas expression of IGF-IR was not required. The IR is homologous to the IGF-IR, both are members of the receptor tyrosine kinase (RTK) superfamily, and both can be activated by IGF-II (166). Binding of ligands to the IGF-IR or the IR triggers a signal cascade that leads to a similar activation of downstream effector molecules that regulate cell growth and survival (133). Our data suggest that latently infected KS cells can grow independent of the IGF-IR, but require IR-dependent signaling for continued growth.

METHODS AND MATERIALS

Viruses, cell culture, and reagents. KSHV-infected E-DMVEC were established and maintained as previously described (123). KSHV-infected DMVEC were used in experiments when >90% of the cells expressed LANA-1. The infection rate was approximately 70% for the TIME cells and primary DMVEC (97). HNMPA-(AM₃) was obtained from EMD Biosciences (San Diego, CA). Antibody α IGF-IR mAb 33255 (Cat# MAb 391) was purchased from R&D Systems (Minneapolis, MN). Polyclonal antibodies [IGF-IR β (C-20), IGF-IIR (H-20), and IR β C-19)] and monoclonal antibody anti-phosphotyrosine (PY20) were obtained from Santa Cruz Biotechnology (Santa Cruz, CA). Mouse monoclonal anti-calreticulin (SPA-601) was purchased from Stressgen, (Victoria, BC, Canada). Antibodies for phospho-Erk (#9101), Erk (#9102), phospho-Akt (#4058) and Akt (#9272) were obtained from Cell Signaling Technologies (Danvers, MA).

Microarray experiments and analysis. cDNA synthesis, hybridization to HG_U133A and B (Affymetrix) and signal intensity normalization were performed at the OHSU microarray core facility (www.ohsu.edu/gmsr/amc). GeneChip data were analyzed with Arrayassist (Stratagene). Comparisons were made between passage-matched KSHV-infected E-DMVEC and mock-infected E-DMVEC in 4 separate experiments. A master data table consisting of expression values extracted from all CEL files was created with the Probe Logarithmic Error Intensity Estimate (PLIER) method. To define the baseline from which changes in gene expression data was determined in KSHV-infected samples, a virtual chip comprising all mock-infected control expression data was used. Significant

changes with a p-value of $p=0.01$ was determined by ANOVA with variance stabilization and no p-value correction.

RT-PCR. qPCR was performed on an ABI7700 sequence detection system (Applied Biosystems, Foster City, CA). Target gene expression was compared to the housekeeping gene GAPDH. Total RNA was purified from E-DMVEC, primary DMVEC, and TIME cells using RNeasy spin columns (Qiagen Inc, Valencia, CA). Human tissue was a generous gift from H. Koon and B. J. Dezube and prepared as previously described (150). Total RNA was treated with DNase I (DNase Free: Ambion, Austin, TX) before synthesis of cDNA by random hexamers and Superscript III (Invitrogen, Carlsbad, CA). The following primers were selected by using the software Primer Express (Applied Biosystems): IGF-II 854F: TTCCGGACAACCTCCCCAG, 919R: 5'TGGACTGCTTCCAGGTGTCA; IGF-I 318F: TTTCAACAAGCCCACAGGGT, 379R: 5'CCACGATGCCTGTCTGAGG; IGF-IIR 6333F: GCAGAAGCTGGGTGTCATAGG, 6420R: 5'CACGGAGGATGCGGTCTTAT; IGF-IR 2184F: GGAGGAGGCTGAATACCGC, 2252R: 5'TCAGGTCTGGGCACGAAGAT, IR 1103F: GGTCCCTGTCCCAAGGTGT, 1161R: 5'GTCACCGAGTCGATGGTCTTC. Reactions were performed using SYBR green PCR core reagents. Relative expression values between mock and uninfected, normal skin, and KS tissue were calculated by the comparative C_t method (106). Dissociation curves were performed on human reference RNA after each amplification run to control for primer-dimers.

RT-PCR to determine IR isoforms was performed by standard approaches using the following primers: 2229F: 5'AACCAGAGTGAGTATGAGGAT; 2844R: 5'CCGTTCCAGAGCGAAGTGCTT.

Western Blot analyses and immunoprecipitations. For immunoprecipitation, cells were washed twice with ice-cold PBS, lysed in NP-40 buffer [1% NP-40, 150 mM NaCl, 10% glycerol, 20 mM Tris-HCl (pH 8.0), 1 mM EDTA (pH 8.0), 0.2% SDS], containing protease inhibitors (Roche Diagnostics; Indianapolis, IN), 1 mM NaVO₄, and 1 mg/ml pepstatin. Lysates were cleared and protein concentration was determined as above. For IGF-IR and IR, 500 µg of whole-cell lysate protein was immunoprecipitated with 10 µg of anti-IGF-IR or anti-IR antibody and incubated overnight at 4°C while rocking. 100 µl of protein A-agarose bead slurry (Upstate) was added for 2 hours rocking at 4°C. Three washes were performed and the pellet was boiled in 2x SDS sample buffer. The beads were spun down and the supernatant was separated by a 7% SDS-PAGE followed by transfer to nylon membranes. Blots were probed with anti-phosphotyrosine, stripped in 5x stripping buffer [1M Tris-Cl, pH 6.8; 10% SDS; 0.7% (v/v) β-mercaptoethanol], and reprobed with their respective antibodies. Bound antibodies were detected by enhanced chemiluminescence (Amersham), and film exposures were quantitated using a scanning densitometer (Bio-Rad).

siRNA treatments. KSHV-infected E-DMVEC were seeded the day prior to siRNA treatment at 30% confluency in 35-mm polystyrene dishes (Corning). On the day of treatment, for each sample, 3 µl Oligofectamine (Invitrogen) was mixed with 12 µl

OptiMEM (GIBCO-Invitrogen) for 5 minutes at room temperature. A mix of 200nM siRNA and 180 μ l OptiMEM were added to Oligofectamine mix and incubated 20 minutes at room temperature. Cells were washed once in OptiMEM and 800 μ l OptiMEM was added to dish prior to adding 200 μ l siRNA mix. Cells were incubated 6 hrs before receiving a second treatment of siRNA as before. Cells were incubated overnight and siRNA mix was removed and replenished with 2 ml complete media. siRNA-treated cells were incubated 4-6 days to determine peak of downmodulation at which point protein levels were assayed by Western Blot or mRNA expression by qRT-PCR. Dishes used for microscopy were washed twice in PBS and fixed in 3.7% paraformaldehyde for 20 minutes before washing again and adding a coverslip over 80 μ l glycerol.

Focus inhibition assay. KSHV-infected E-DMVEC were seeded 30-50% confluency on 35-mm dishes (Corning) and treated either with siRNA or the IR small-molecule inhibitor, HNMPA-(AM₃) for a two week period. Inhibitor was added during change of medium (every 3 days) whereas a second round of siRNA treatment was performed 7 days after the first treatment to maintain knockdown of specified genes. Cells were examined for spindle-cell formation, loss of contact inhibition a result of adherent foci in the monolayer, or virus-induced cytopathic effect by microscopy.

Immunofluorescence microscopy. Cells were washed twice with 1X PBS, and fixed with 3.7% formaldehyde (in PBS) for 20 minutes at room temp. Cells were washed twice with 1X PBS and permeabilized with 0.1% Triton X-100 (in PBS), for 5 min.

Afterwards, cells were washed three times with 2% PBA (BSA in PBS). Primary rabbit polyclonal anti-LANA-1 (ORF73) (a gift from Dr Bala Chandran; Rosalind Franklin University, Chicago, IL) was added at 1:500 for 2 hrs at 37°C. Cells were washed three times with 2% PBA (BSA in PBS) and incubated with goat anti-rabbit 594 Alexa Fluor secondary (Molecular Probes, Eugene, OR), 1:500 for 45 min at 37°C. Images were analyzed with a Nikon fluorescence microscope.

Cell viability assay. Cell viability was measured as protocol suggested in the ATP Determination Kit (Molecular Probes, Cat #A-22066). KSHV-infected E-DMVEC treated with HNMPA-(AM₃) for 14 days in a 96-well plate were lysed in 1% Triton X-100 for 10 minutes. 5µl of D-luciferin/luciferase mix was added per sample and immediately read in a luminometer.

Soft agar assay. Forty thousand KSHV-infected E-DMVEC treated with HNMPA-(AM₃) or left untreated for 14 days were plated in 1.5 ml endothelial-SFM growth medium supplemented with 10% human AB serum, 25 µg/ml endothelial cell growth supplement, and 0.4% melted agarose onto a 3-ml bottom layer of 0.5% agarose medium per well of a 6-well dish. The cells were fed several drops of medium every 3 days, and colonies were photographed after 2-3 weeks.

Annexin V-FITC apoptosis detection assay. Apoptosis in KSHV-infected E-DMVEC was analyzed with the R&D System Annexin V-FITC Apoptosis Detection kit (Cat # TA4638). Cells were washed once in PBS and resuspended in serum-free medium,

followed by treatment with Staurosporine (1 μ M), HNMPA-(AM₃) (50 μ M), or left untreated overnight. Cells were trypsinized and washed in 2% BSA in PBS before each sample was resuspended in 100 μ l Annexin Reagent (10 μ l 10X Binding Buffer, 10 μ l Propidium Iodide, 1 μ l Annexin V-FITC, and 79 μ l ddH₂O) for 15 minutes at room temperature. 400 μ l 1x Binding Buffer was added before samples were analyzed by flow cytometry.

RESULTS

Deregulation of the IGF pathway in latently infected E-DMVEC.

To examine whether latent infection by KSHV modulates the IGF-pathway, we extracted the expression profiles for the transcripts encoding insulin, IGF-I, and IGF-II, their respective receptors (IR, IGF-IR, and IGF-IIR), and the six insulin-like growth factor binding proteins (IGFBPs) from whole genome expression arrays (Affymetrix U133A and B). Four independently KSHV-infected E-DMVEC cultures were compared to their respective age- and passage-matched uninfected controls. IGF-IR was present but remained unchanged, whereas the two Affymetrix probe sets for the IGF-IIR were induced in two of the four comparisons. Of the two probe sets representing the IR, one was induced in two, while the other one was induced in all four comparisons (Figure 1a).

To confirm the gene array results, we performed quantitative real-time RT-PCR (qPCR). There was no significant change in IGF-IR mRNA expression levels, while IR and IGF-IIR transcripts were strongly induced (Figure 1b). IGF-I and IGF-II mRNA expression was barely measurable by qPCR, while insulin mRNA was undetectable; neither transcript changed upon KSHV infection. Protein levels for all three receptors in infected and uninfected E-DMVEC lysates, measured by Western Blot analysis was consistent with mRNA expression levels (Figure 1c).

To confirm our observations in endothelial cell-based culture systems that permit transient infection with KSHV, we examined IR expression in DMVEC immortalized with telomerase (TIME cells) (97) and primary DMVEC (23). IR-induction was observed in either cell system (Figure 1d). Moreover, RNA extracted from a dermal KS tissue biopsy showed a significant increase in IR gene expression when compared to

normal skin tissue (Figure 1d). The consistent induction of IR mRNA in KSHV-infected primary DMVEC and TIME cells, as well as in KS tissue, underscores that our findings in E-DMVEC reflect a true feature of KS tumorigenesis.

IGF-IR is not a transforming factor in KSHV-induced tumorigenesis of E-DMVEC.

Although expression levels of the IGF-IR did not change upon KSHV-infection, it was still possible that the IGF-IR contributes to KSHV-driven tumorigenesis. To examine this possibility, we used small interfering RNA (siRNA) to knock down IGF-IR mRNA and protein expression. Upon siRNA-treatment mRNA levels were reduced by 80% and protein levels were also dramatically reduced (Figure 2); however, IGF-IR siRNA treatment did not affect KSHV-mediated tumorigenesis as measured by post-confluent growth, formation of spindle cells, and foci formation (Figure 2c). Similar results were obtained with IGF-IR-specific polymorpholino antisense oligomers (Supplemental Figure1).

In an independent approach we used the blocking antibody MAb 391 to inhibit IGF-IR function (184), which has been shown to downregulate IGF-IR during chronic treatment (59). Inhibition of IGF-IR activation by MAb 391 was confirmed in IGF-IR-transfected NIH-3T3 cells (Figure 2d, e). Treatment of KSHV-infected E-DMVEC for 14 days with MAb 391 did not prevent post-confluent growth and the development of spindle cell-containing foci (Figure 2f). Taken together with the siRNA data, these data rule out the IGF-IR for post-confluent growth of KSHV-infected E-DMVEC.

The IR is necessary for KSHV-induced tumorigenesis.

The IR is encoded by two splice variants that differ by 12 amino acids in the cytoplasmic C-terminus: IR-A, which lacks exon 11, and a full-length IR-B (28). To determine if these isoforms are differentially induced by KSHV, we performed RT-PCR on two independently derived lines of E-DMVEC, either uninfected or latently infected with KSHV. IR-A and IR-B were expressed in both KSHV-infected and uninfected E-DMVEC; however, IR-A was more abundant (Figure 3a). While increased levels of both isoforms were seen following KSHV infection, their ratio did not change. Thus, IR-A is the predominantly expressed isoform in KSHV-infected E-DMVEC as has been observed in other cancers (28).

To examine whether IR is involved in KSHV-induced transformation of E-DMVEC, we employed a pool of siRNA molecules targeted against both isoforms of IR to reduce IR mRNA levels. Transfection of this pool into KSHV-infected E-DMVEC resulted in an approximately 85% reduction in mRNA levels as determined by qRT-PCR (Figure 3b). Protein levels were also reduced significantly, as shown by Western Blot (Figure 3c). To determine the effect of inhibiting IR protein expression on KSHV-mediated tumorigenesis, we performed gene silencing experiments as above. As shown in Figure 3d, spindle cell formation, post-confluent growth and foci formation was dramatically reduced in IR-siRNA treated cells compared to untreated cells. In contrast, control siRNA-treated cells were indistinguishable from untreated cells (not shown). Similar results were obtained when translation of IR-mRNA was blocked with PMO-AS (Supplemental Figure 1). We conclude that expression of the IR is important for the post-confluent growth of KSHV-infected E-DMVEC.

Inhibiting IR signaling impedes KSHV-mediated spindle cell foci formation.

Upon ligand binding, RTKs autophosphorylate and activate pro-survival signaling cascades. To determine whether increased expression of IR correlated with increased activation we analyzed IR autophosphorylation. As shown in Figure 3e, KSHV-induced IR-expression correlated with increased phosphorylation. In contrast, IGF-IR phosphorylation remained below detection in both infected and uninfected E-DMVEC.

To examine whether signaling by the IR is required for KSHV-mediated post-confluent growth, we used the IR-specific inhibitor HNMPA-(AM₃) [hydroxy-2-naphthalenyl-methyl phosphonic Acid Trisacetoxymethyl Ester] (6, 162). Treatment with 25 μ M, 50 μ M, and 100 μ M HNMPA-(AM₃) inhibited the development of spindle cell-containing foci (Figure 4a) over a period of 14 days. This seemed to be due to the specific elimination of KSHV-infected cells and outgrowth of uninfected cells since the major latency associated protein LANA-1 was expressed in approximately 70% of untreated cells, whereas only 8% of cell expressed LANA-1 in cells treated with 50 μ M HNMPA-(AM₃) for 14 days (Figure 4b). Alternatively, it is also conceivable that KSHV-genomes were lost from HNMPA-treated cultures as described for other endothelial cell lines (55).

At 50 μ M, the inhibition of post-confluent growth was not due to a general effect on cell viability as shown by measuring ATP availability upon treatment for two weeks (Figure 5a). Furthermore, HNMPA-(AM₃) did not alter normal cell proliferation of KSHV-infected E-DMVEC prior to reaching confluency (Figure 5b). In contrast, post-confluent cell proliferation was reduced by HNMPA-(AM₃) (Figure 5c).

One of the characteristics of latently infected E-DMVEC is their ability to form colonies in soft agar (123). Untreated KSHV-infected E-DMVEC formed colonies as expected, while inhibition by HNMPA-(AM₃) reduced colonies in a concentration-dependent manner (Figure 6a). Taken together, these results suggest that IR-dependent signaling is not required for KSHV-independent cell proliferation prior to reaching confluency, but is essential for the KSHV-driven post-confluent growth. The IR could thereby be required either for maintaining the infection or as part of the KSHV-mediated cellular changes required for contact-independent growth.

Signaling by the IR promotes survival (133, 167), which, when inhibited by HNMPA-(AM₃), could trigger apoptosis. Accordingly, HNMPA-(AM₃)-treated cells were assayed for apoptosis using Annexin V-FITC staining. Both treated and untreated E-DMVEC showed no difference in apoptosis sensitivity (Figure 6b) compared to the apoptosis-inducing compound Staurosporine. This suggests that IR is not involved in preventing apoptosis of KSHV-infected E-DMVEC during foci formation.

IR signaling mediated by mitogen-activated protein kinases.

IR activation leads to activation of the Erk mitogen-activated protein kinase (MAPK) and phosphoinositol-3 kinase (PI3K) pathways (101). We assessed the effect of KSHV infection on the activation of these pathways by determining the levels of phosphorylated Erk and Akt. As shown in Figure 7a, only Erk phosphorylation is significantly increased in KSHV-infected E-DMVEC. We then inhibited IR activation in KSHV infected E-DMVEC with HNMPA-(AM₃) to verify a potential link between Erk phosphorylation and IR activation. Treatment with HNMPA-(AM₃) was able to reduce

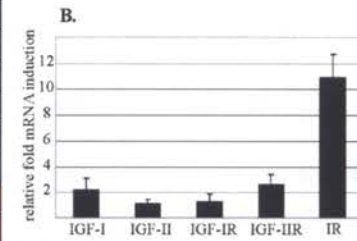
the level of Erk phosphorylation (Figure 7b). This suggests that the IR directly signals via MAPK. Shc is an IR adaptor substrate that is activated upon phosphorylation of IR ultimately leading to the activation of the Ras/MAPK pathway and concomitant stimulation of mitogenic signaling pathways (101, 201). While insulin does stimulate Shc phosphorylation, other growth factor stimuli are stronger activators of this adaptor protein. This may suggest that IGF-II signaling is the major activator of IR phosphorylation, which would be in line with the predominance of the IR-A isoform, which has a higher affinity for IGF-II (28, 29).

FIGURES

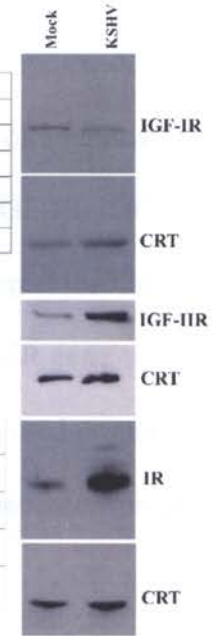
Figure 1.

Gene	Probe Set ID	Infection A	Infection B	Infection C	Infection D
IGF-I	209540_at	A	A	A	A
IGF-I	209541_at	A	A	A	A
IGF-I	209542_x_at	A	A	A	A
IGF-I	211577_s_at	A	A	A	A
IGF-II	210881_s_at	A	A	A	A
IGF-II	202410_x_at	A	A	A	A
insulin	206598_at	A	A	A	A
IGF-IR	203627_at	NC	NC	NC	NC
IGF-IR	203628_at	NC	NC	NC	NC
IGF-IIR	201392_s_at	3.60	NC	NC	3.16
IGF-IIR	201393_s_at	3.03	NC	NC	2.63
IR	207851_s_at	2.66	NC	NC	3.03
IR*	213792_s_at	6.23	4.71	2.14	7.24
IGFBP1*	206302_at	-3.87	-41.68	-3.82	-36.58
IGFBP2*	202718_at	3.60	15.03	5.81	2.66
IGFBP3	210095_s_at	NC	NC	NC	NC
IGFBP3	212143_s_at	NC	NC	NC	NC
IGFBP4	201508_at	NC	NC	NC	NC
IGFBP5	203424_s_at	NC	NC	NC	NC
IGFBP5	203425_s_at	NC	NC	NC	NC
IGFBP5	203426_s_at	NC	NC	NC	NC
IGFBP5	211958_at	NC	NC	NC	NC
IGFBP5	211959_at	NC	NC	NC	NC
IGFBP6*	203851_at	-8.39	-86.34	-5.83	-84.63

A.



C.



D.

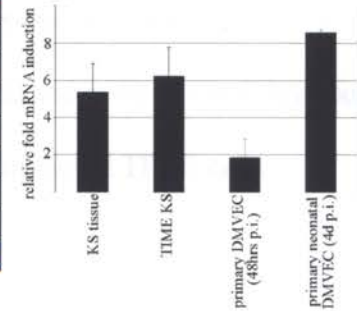


Figure 1. Gene expression profiling of IGF system genes in KSHV-infected and uninfected E-DMVEC. (A) Affymetrix HG_U133A GeneChip data for ligands, receptors, and all 6 IGFBPs obtained from four infected samples compared to their respective controls. Significant changes with a p-value of $p > 0.01$ (ANOVA) are highlighted by “*”. Genes with multiple probe sets are reflected in the table; ‘NC’ indicates no change in gene expression, and ‘A’ scored absent on the microarray. Values given are absolute fold change; blue indicates down-regulated and red up-regulated expression changes. (B) qPCR of selected peptide ligands and their receptors. Values are fold-change over uninfected E-DMVEC. Error bars indicate SEM of 3 replicates. (C) Western Blot analysis comparing levels of protein expression for IGF-IR, IGF-IIR and IR in KSHV infected and uninfected E-DMVEC. To control for equal loading, antibodies to the cellular chaperone calreticulin (CRT) were used. (D) IR gene expression comparing normal skin to KS tissue, two independently infected primary DMVEC compared to uninfected cells, collected at 48 hrs or 4 days post-infection, and KSHV infected TIME cells compared to uninfected TIME cells.

Figure 2.

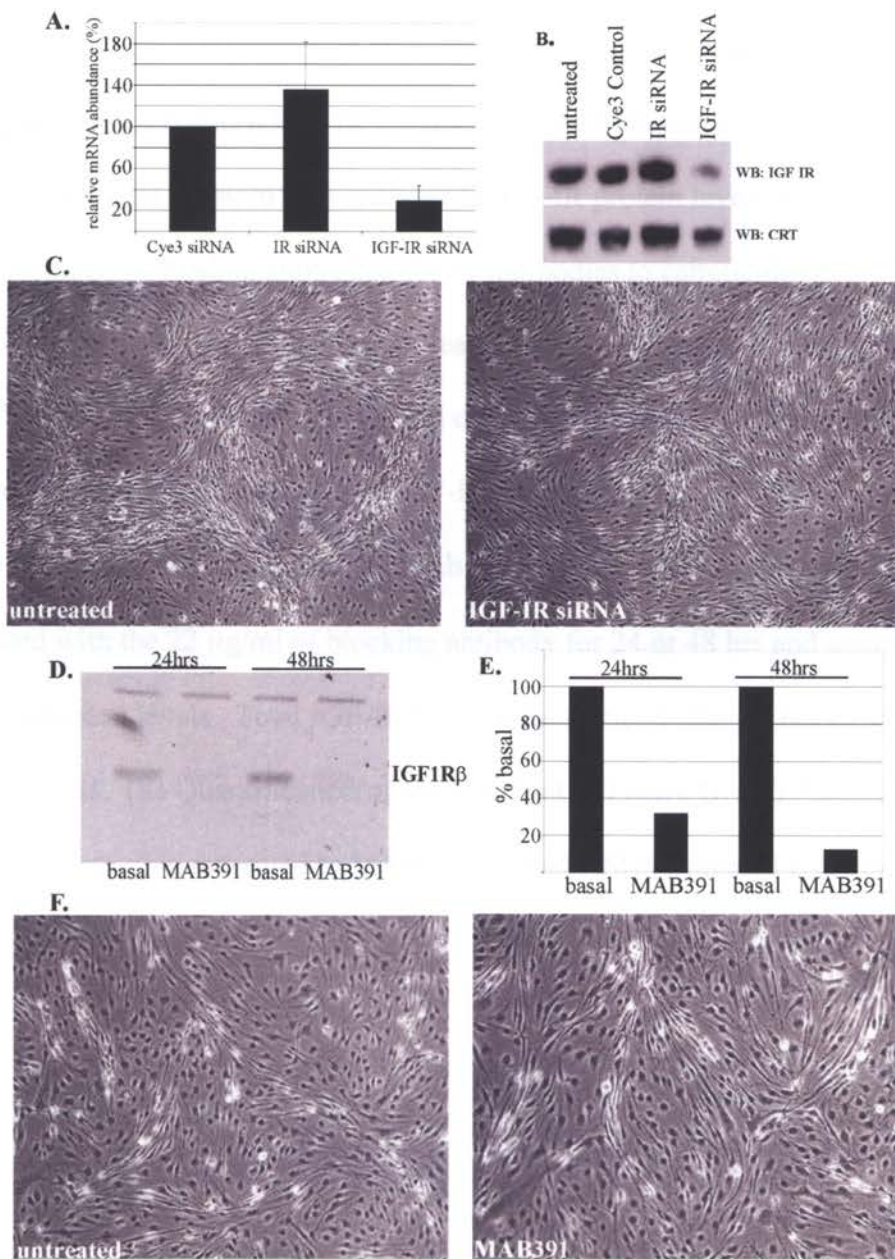


Figure 2. Downregulation of IGF-IR mRNA and protein levels does not affect

KSHV tumorigenesis. (A) qPCR analysis of IGF-IR transcripts from KSHV-infected E-DMVEC treated with nonspecific Cy3-labeled control siRNA, a siRNA targeted against a random gene (control), or a SMARTpool siRNA (Dharmacon) specifically designed against the IGF-IR. Immunofluorescence analysis of Cy3-labeled siRNA-transfectants indicated a transfection efficiency of more than 95% (data not shown). IGF-IR SMARTpool siRNA reduced IGF-IR mRNA levels by 80% compared to untreated or control samples. (B) Western Blot analysis of IGF-IR protein levels after siRNA treatment with equal loading controlled for by antibodies to calreticulin (CRT). (C) Phase-contrast microscopy comparing untreated to IGF-IR siRNA-treated KSHV-infected E-DMVEC. Note that spindle-cell development and contact-independent foci formation occurred in both control and IGF-IR siRNA treated cells. (D) To test the efficiency of the blocking antibody MAb 391, NIH3T3 overexpressing human IGF-IR were treated with the 22 μ g/ml of blocking antibody for 24 or 48 hrs and assayed for IGF-IR expression levels. Total IGF-IR levels were reduced after 24 hrs by 70% and by 90% after 48 hrs. (E) Quantification of Western blot in Figure D. (F) Phase-contrast microscopy comparing untreated to MAb 391-treated KSHV-infected E-DMVEC.

Figure 3.

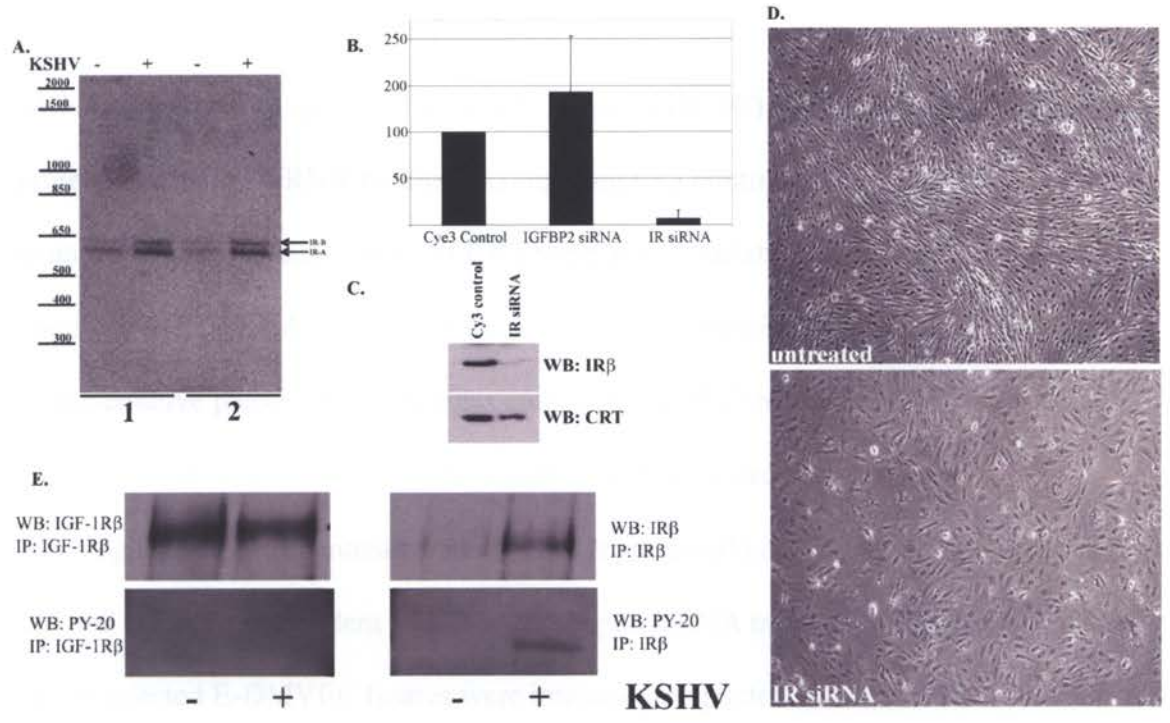


Figure 3. IR is necessary for KSHV-infected E-DMVEC tumorigenesis. (A) RT-PCR to determine expression of IR isoforms in 2 independent uninfected and KSHV-infected E-DMVEC cultures (1 & 2). PCR products were separated on a 2% agarose gel to identify the distinct 36-base-pair difference in length. (B) IR transcript levels measured by qPCR in KSHV-infected E-DMVEC treated with nonspecific Cy3-labeled control siRNA, a siRNA targeted against a random gene (control), or a SMARTpool siRNA (Dharmacon) specifically designed against IR. (C) Western Blot analysis of IR protein levels after siRNA treatment comparing Cy3 control siRNA and IR siRNA-treated samples. Reduced levels of CRT were due to variation in protein loading and unrelated to IR siRNA which does not affect CRT expression (see Fig. 2B). (D) Representative phase-contrast images comparing KSHV-infected E-DMVEC either untreated or treated with IR siRNA. Control siRNA treated samples were indistinguishable from untreated and are not represented here. Note the reduced spindle cell and contact-independent foci formation upon siRNA treatment. (E) KSHV-infected and uninfected E-DMVEC lysates were immunoprecipitated with either IR or IGF-IR and assayed by Western Blot to compare receptor levels (top panel) or to determine the phosphorylation state of IR and IGF-IR using the phosphotyrosine-specific antibody, PY-20 (bottom panel).

Figure 4.

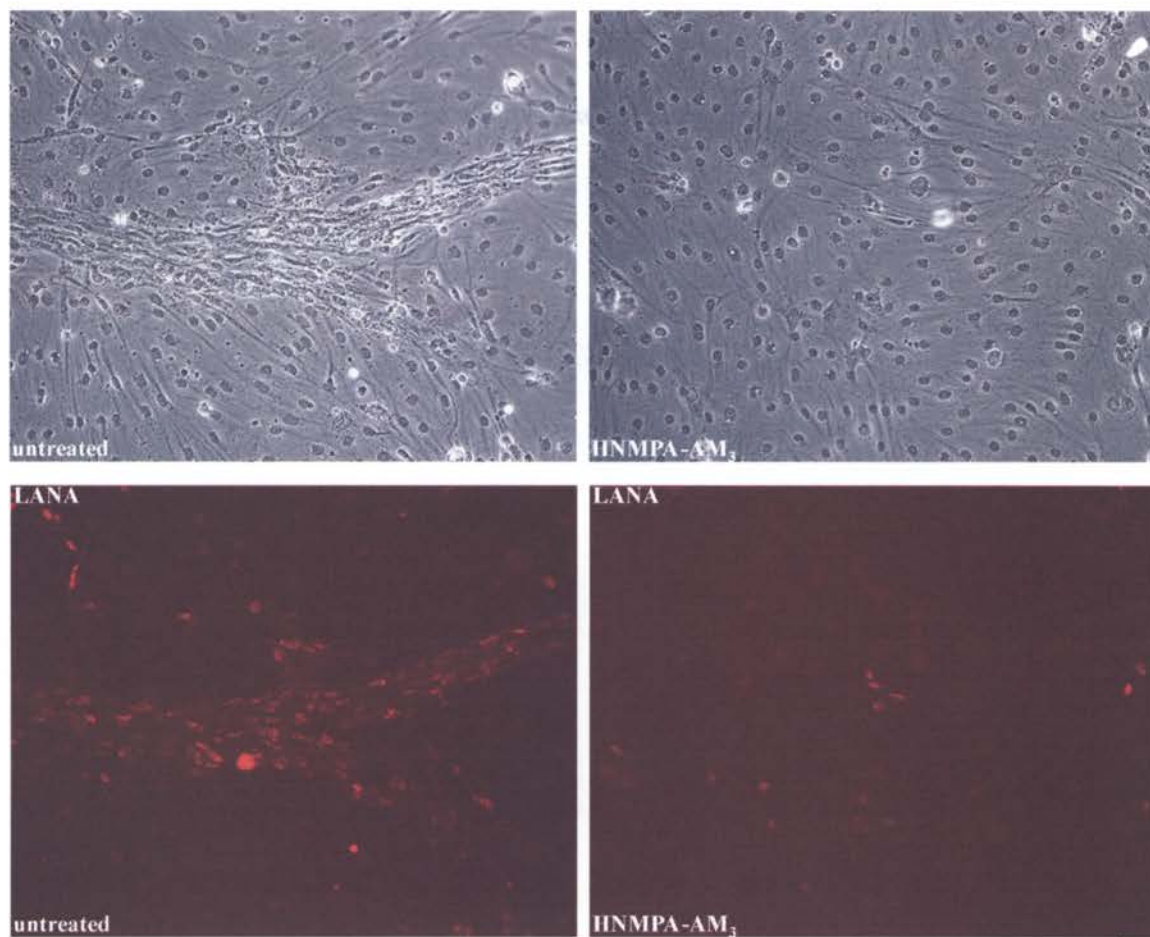
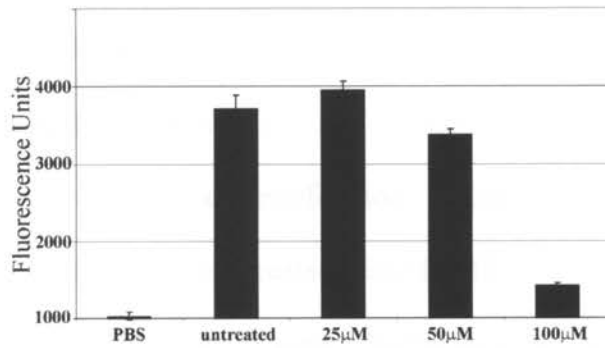


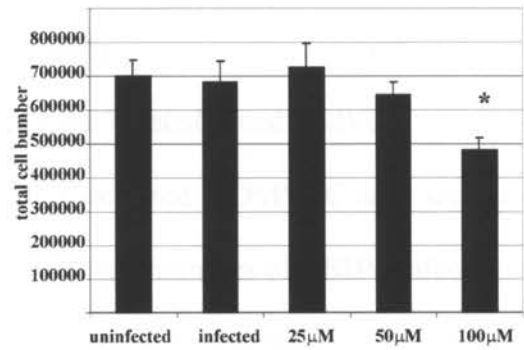
Figure 4. IR-specific tyrosine kinase inhibitor HNMPA-(AM₃) prevents spindle cell and foci-formation in KSHV-infected E-DMVEC. Top panel: Phase-contrast images of HNMPA-(AM₃) [50 μM]-treated and untreated KSHV-infected E-DMVEC showing inhibition of spindle-cell foci following HNMPA-(AM₃) treatment. Bottom panel: Dark-field images of HNMPA-(AM₃) [50 μM]-treated and untreated KSHV-infected E-DMVEC showing expression of LANA-1 in KSHV-infected spindle cells and the selective loss of LANA-1-positive foci following HNMPA-(AM₃) treatment.

Figure 5.

A.



B.



C.

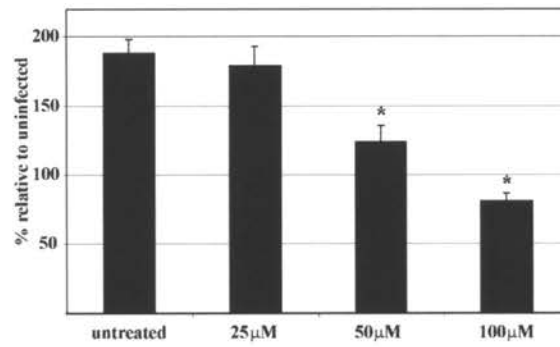


Figure 5. Inhibiting IR signaling does not affect cell viability in KSHV-infected E-DMVEC. In all experiments, KSHV-infected E-DMVEC were left untreated or treated with 25 μ M, 50 μ M, and 100 μ M HNMPA-(AM₃) for 14 days. (A) ATP Cell viability assay cells were lysed and ATP was quantitatively determined using a luciferin bioluminescence assay. PBS was used as negative control to establish background levels. (B) Pre-confluent cell proliferation. Cells were seeded at low density treated with HNMPA-(AM₃). Total cell counts were determined using a hemocytometer and compared to normal cell proliferation of uninfected E6/E7-transformed DMVEC. (C) Post-confluent cell proliferation. Uninfected or KSHV-infected E-DMVEC were seeded at high density and treated with HNMPA-(AM₃). Total cell numbers of KSHV-infected E-DMVEC, counted using a hemocytometer, are presented as a percentage of uninfected E-DMVEC total cell counts to determine differences based on any effect of HNMPA-(AM₃) treatment. “*” indicates significantly different as determined by two-sided t-test, with $\alpha=0.05$.

Figure 6.

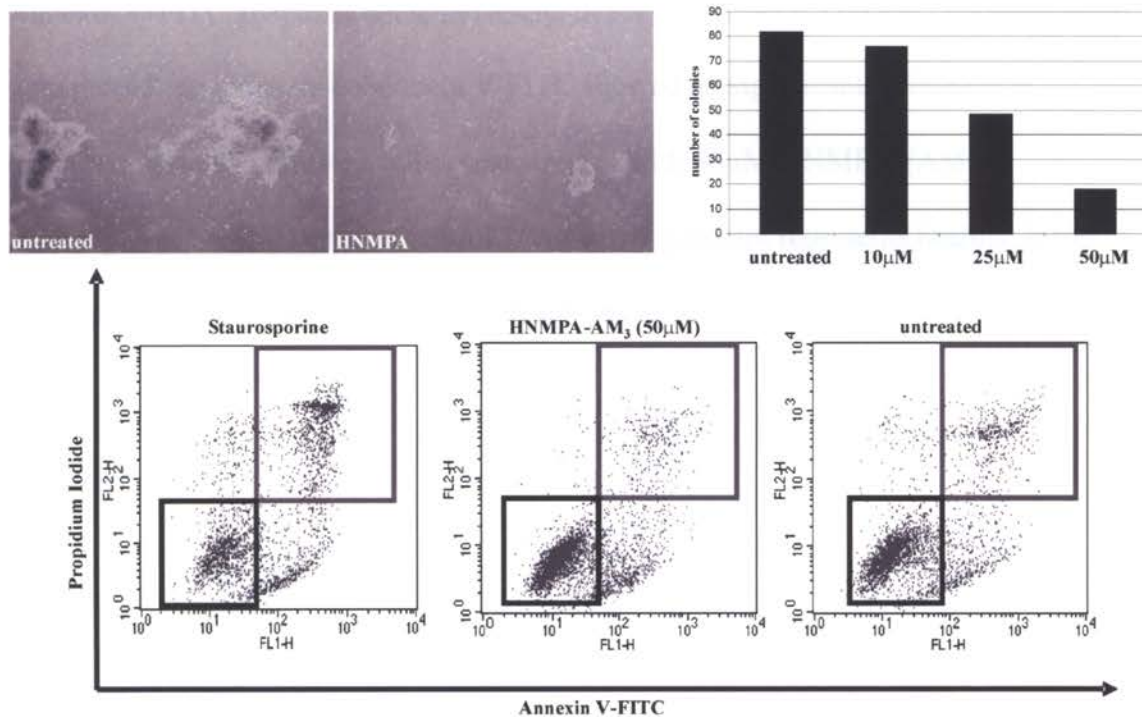
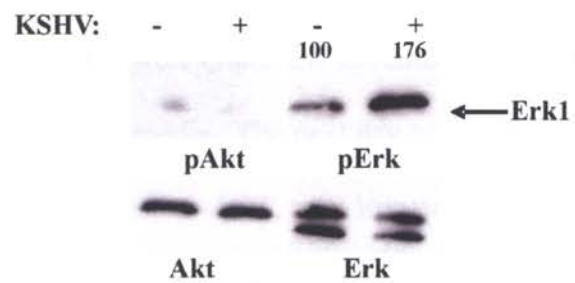


Figure 6. Inhibiting IR activity prevents anchorage-independent growth of KSHV-infected E-DMVEC, but does not affect apoptosis. (A) Soft-agar growth assay. KSHV-infected E-DMVEC were left untreated or treated with 50 μ M HNMPA-(AM₃) for 14 days and transferred to soft-agar containing media. Phase-contrast images are representative. The graph quantifies the number of foci observed in each sample. (B) Annexin V-FITC apoptosis detection assay. KSHV-infected E-DMVEC double-stained with propidium iodide and Annexin V-FITC showed no significant difference in apoptosis between untreated cells versus treated with 50 μ M HNMPA-(AM₃); Staurosporine used as positive control. Lower left quadrant represents healthy, lower right early apoptotic, and upper right late-apoptotic cells.

Figure 7.

A.



B.

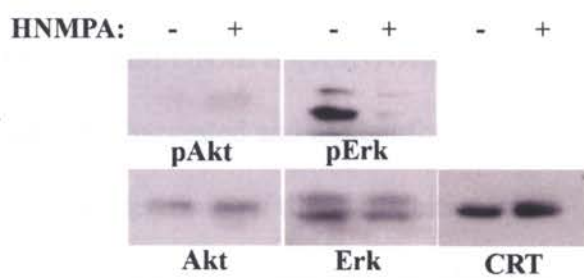
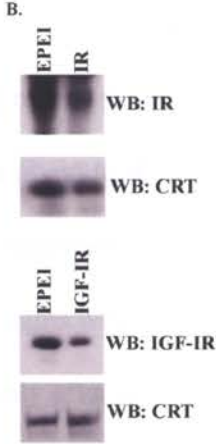
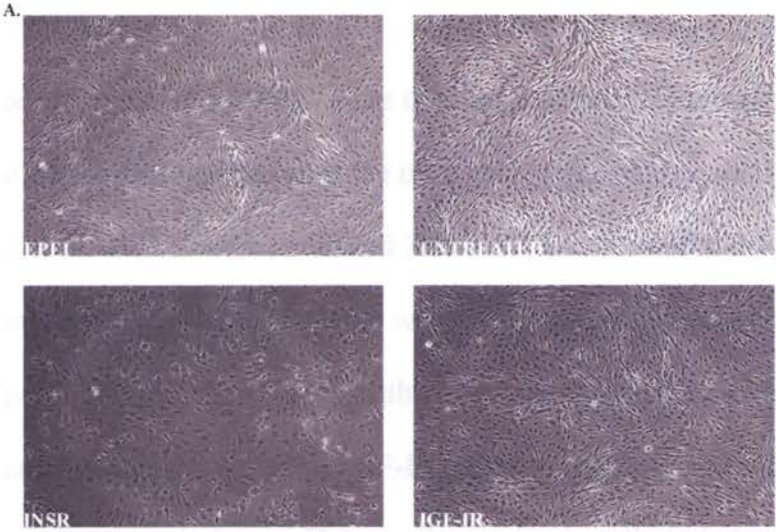


Figure 7. Comparison of known IR signaling pathways indicates IR activation mediated by mitogen-activated protein kinases. (A) Total cell lysate harvested from KSHV-infected and uninfected E-DMVEC blotted for total AKT, phospho-AKT, total Erk, and phospho-Erk to ascertain which IR signaling pathways were activated. There was a 1.5-fold increase in phosphorylated Erk in KSHV-infected versus uninfected E-DMVEC, while there was no change in phospho-AKT levels. (B) KSHV-infected E-DMVEC were either left untreated or treated with 50 μ M HNMPA-(AM₃) overnight in complete media. The next day total cell lysates were harvested and blotted for total AKT, phospho-AKT, total Erk, and phospho-Erk, to determine if direct inhibition of IR signaling affected MAPK phosphorylation. Calreticuling (CRT) was used as a loading control.

Supplemental Figure 1.



Supplemental Figure 1. Morpholino Antisense oligo (PMO) treatment of KSHV infected E-DMVEC. KSHV infected E-DMVEC were seeded at 8×10^5 cells/60mm dish. Cells were washed once with PBS and 2ml OptiMEM (Invitrogen, Carlsbad, CA) was added. In a round-bottom polypropylene tube 980 μ l sterile water was added to 10 μ l (0.5mM stock solution) of morpholino antisense oligo (Gene tools, Philomath, OR) and vortexed lightly. 10 μ l EPEI Special Delivery Solution (200 μ M stock solution) was added to the morpholino/water mix and incubated 20 minutes at room temperature. 2ml of OptiMEM was added to the morpholino mix, which was then given to their respective dishes. Dishes were incubated 3hrs at 37°C, after which the morpholino mix was removed and 3ml fresh media was added. (A) Phase contrast images were taken 7 days post treatment showing an inhibition of spindle cell formation only after IR morpholino antisense treatment, while IGF-IR morpholino antisense treatment had no effect. (B) To measure knock-down efficiency, lysates were collected also 3 days post treatment, normalized by Bradford, and proteins were separated by 8% acrylamide gel. Gels were transferred to PVDF membrane and blotted for IR, IGF-IR (IR (C-19), IGF-IR (HC-20) Santa Cruz Biotechnology, Santa Cruz, CA) or Calreticulin, (CRT, Stressgen, Victoria, BC, Canada) as loading control. EPEI lysates are mock treated with morpholino oligo carrier only to compare against specific PMOs.

DISCUSSION

We report in this study that the IR is essential for KSHV-mediated post-confluent and contact-independent growth of immortalized DMVEC *in vitro*. Gene expression profiling identified the IR as being up-regulated when comparing uninfected and KSHV-infected E-DMVEC. qPCR and Western Blot confirmed the GeneChip results. Inhibition of IR expression with siRNA and of IR signaling with HNMPA-(AM₃) prevented the formation of tumor-like foci *in vitro*. In contrast, similar treatments targeting the IGF-IR had no effect. The latter finding is different from a recent report that demonstrated that autocrine stimulation of the IGF-IR by IGF-II was essential for growth and survival of the KS-derived cell line KSIMM (17). Although originally derived from KS tumors, KSIMM are negative for KSHV (43). In contrast to KS tissues, which are characterized by predominant expression of lymphatic endothelial cell markers, KS-derived cell lines are usually characterized by expression of mesenchymal non-endothelial cell markers, suggesting that they are primitive or poorly differentiated endothelial cells. The individual contribution of KSIMM-like cells and KSHV-transformed ECs in KS development is not known. Within the tumor environment, it is possible that the IR contributes to tumorigenesis of ECs, whereas the IGF-IR is required for the continued growth of undifferentiated non-infected ECs.

Expression of both IGF-IR and IR has been demonstrated in KS tissue. IGF-IR was detected by immunohistochemistry in tumor spindle cells (17). Over-expression of the IR in KS tissue compared to normal skin was reported by Wang et al. in a comprehensive microarray study (204), and we have independently shown that IR gene expression is induced in KSHV-infected primary DMVEC, AIDS-KS tissue, and TIME

cells. Furthermore, we show that the up-regulated IR is phosphorylated and that there is increased activation of the downstream Erk pathway, but not the PI3K pathway, in KSHV-infected cells. We cannot completely rule out that the activation of Erk is a direct effect of KSHV instead of IR, although our data suggests that by inhibiting IR activation we do indeed directly affect Erk phosphorylation. The Erk pathway is a target of KSHV during *de novo* infection to modulate initial gene cellular and viral expression (169), while our analysis of the two IR activated pathways was performed 4 weeks into the latent phase of the infection. Our results do rule out IR activation of PI3K pathway, since there was no change in AKT phosphorylation in KSHV infected E-DMVEC. PI3K is also activated early in KSHV infection (169), while at the latent stage we did not see PI3K activation (Figure 7).

The IR joins a growing list of host cell proteins essential for the transformed phenotype in endothelial cells infected by KSHV *in vitro* (111, 125, 150). It seems that multiple mechanisms are required to support the post-confluent growth of DMVEC. Yet, not every growth factor receptor or oncogene that is expressed or up-regulated in KSHV-infected cells is necessary for KSHV-mediated transformation, exemplified by the IGF-IR, as well as by a number of other KSHV-induced transcripts previously shown to be dispensable for this process (150).

The IR is known to be involved in tumorigenesis, particularly the A isoform that predominates in KSHV-infected DMVEC. A preferential expression of the IR-A isoform has been shown in several types of cancers, including lung, colon, breast, ovarian, and thyroid cancer (reviewed in (29)). Splicing of IR presumably alters the affinity of the receptor for its ligand. While both isoforms have a high affinity for insulin, IR-A has a

higher affinity for IGF-II, which is able to displace insulin and activate predominantly mitogenic rather than typical metabolic signaling pathways. Whereas both ligands are provided by the tissue culture medium, neither ligand is expressed in KSHV-infected cells to appreciable levels thus ruling out an autocrine mechanism. In vivo, exogenous ligands could be provided in a paracrine fashion by KSIMM-like cells or by non-tumor cells, or by IGF-II or insulin present in the blood. Further studies will be required to clarify which of these ligands is present in KS tumors and whether the ligands are produced within the tumor.

In summary, the IR is required to support the contact-independent, post-confluent proliferation of KSHV-infected ECs, thus allowing the development of multi-layered foci in monolayer culture, or colony growth in soft agar. Since these *in vitro* growth characteristics mimic early-stage tumorigenesis, we propose that IR contributes to KS tumor development.

ACKNOWLEDGEMENTS

The work reported in this manuscript was supported by grants PS1-RR00163 and RO1-CA099906 (AVM and KF). Initial support for this project was from Virogenomics, Inc., a company that may have a commercial interest in the results of this research. A potential conflict of interest by KF and AVM has been reviewed and managed by the OHSU Conflict of Interest in Research Committee. PPR was supported by the Molecular Hematology Training Grant T32 HL007781-13 and a Tartar Trust fellowship. This work was also partially supported by an award from the American Heart Association.

CHAPTER 3

Insulin-like Growth Factor II Receptor-mediated intracellular Retention of Cathepsin B is essential for transformation of endothelial cells by Kaposi's sarcoma associated herpesvirus

submitted for publication

Patrick P Rose¹, Matthew Bogyo², Ashlee V. Moses¹, and Klaus Früh^{1,3}.

¹Vaccine and Gene Therapy Institute, Oregon Health and Science University, Portland,
Oregon, United States, 97239.

²Stanford University School of Medicine, Stanford, California, United States, 94305-
5324.

³To whom requests for reprints should be directed at the Vaccine and Gene Therapy
Institute, Oregon Health and Science University, 505 NW 185th Ave, Beaverton, OR,
97006. Phone: 503 418 2735 (KF), 503 417 2712 (AM), Fax: 503 418 2701; email:

fruehk@ohsu.edu

Running Title: Cathepsin B activity in KS tumorigenesis

Keywords: Kaposi sarcoma, herpesvirus, endothelial cell, tumorigenesis, Cathepsin B,
cysteine proteases, mannose-6 phosphate receptor, insulin-like growth factor II receptor

ABSTRACT

Kaposi's Sarcoma-associated Herpesvirus (KSHV/HHV8) is the pathological agent of Kaposi's sarcoma (KS), a tumor characterized by aberrant proliferation of endothelial cell (EC)-derived spindle cells. Since in many cancers tumorigenesis is associated with an increase in the activity of the cathepsin family, we studied the role of cathepsins in KS using an *in vitro* model of KSHV-mediated EC-transformation. Small-molecule inhibitors and small interfering RNA (siRNA) targeting cathepsin B, but not other cathepsins, inhibited KSHV-induced post-confluent proliferation, spindle cell and foci formation of dermal microvascular ECs. Interestingly, neither cathepsin B mRNA nor protein levels were induced in ECs latently infected with KSHV. Secretion of cathepsin B was strongly diminished upon KSHV infection. Increased targeting of cathepsin B to endosomes was caused by KSHV inducing expression of insulin-like growth factor-II receptor, a mannose-6-phosphate receptor (M6PR) which binds to cathepsins. Inhibiting IGF-IIR/M6PR expression by siRNA released cathepsin B for secretion. Unlike the increased cathepsin secretion observed in most other tumors, viral inhibition of cathepsin B secretion via induction of a M6PR is crucial for transformation of ECs.

INTRODUCTION

Kaposi Sarcoma-associated Herpesvirus (KSHV/HHV8) belongs to the γ -herpesviruses subfamily and is the pathological agent of Kaposi sarcoma (KS) and of lymphoproliferative disorders in B cells (84). KS is a mesenchymal tumor generally targeting the skin and soft-tissue organs. The sarcoma is composed of interweaving bands of vascularizing spindle cells that are of endothelial origin, frequently associated with infiltrating inflammatory cells (33, 121). Acquired Immunodeficiency Syndrome (AIDS) has been most commonly associated with KS, although other forms of KS exist independent of HIV infection, e.g. classic, endemic, and iatrogenic KS (65, 121). As antiretroviral treatment effectively reduces the prevalence of AIDS-KS, the incidence of iatrogenic KS has increased 400% relative to the population growth in North America, generating concern over resurging KS (<http://www.emedicine.com/derm/topic203.htm>).

The development of several *in vitro* systems that rely on infection of primary or immortalized endothelial cells (ECs) by KSHV has greatly advanced our understanding of virus/host cell interaction during tumorigenesis (112). Dermal microvascular endothelial cells stably transfected with the oncogenes E6 and E7 of human papillomavirus (E-DMVEC) are immortalized, but remain contact-inhibited, grow as discrete monolayers of cobblestone phenotype and enter senescence if not passaged after attaining confluence (123). Upon infection with KSHV, E-DMVEC develop a spindle-cell phenotype, lose contact inhibition, form foci when cultured post-confluence, and acquire the ability to form colonies in soft agar (123). As in KS tumors, viral gene expression in E-DMVEC is largely restricted to ORFs 71 (vFLIP), ORF72 (vCyclin), ORF73 (LANA) and kaposin, and only a few cells spontaneously enter the lytic cycle of

viral replication. Despite the restricted viral gene-expression program, latent infections are associated with a dramatic reprogramming of the cellular transcriptome and proteome (10, 124, 125, 204). Several virus-induced host cell proteins are required to support post-confluent growth, including c-Kit, hemoxygenase, RDC-1, Neuritin, and the insulin receptor (111, 125, 150, 155).

One of the hallmarks of KS is aberrant neoangiogenesis by proliferating spindle cells, which results in abnormal vasculature. Neoangiogenesis involves the degradation of extracellular matrix by proteases (20, 87, 88, 194). Despite the important role of cathepsins in many cancers, the role of cathepsin function in KS development has not been studied so far. Cathepsins are part of the papain subfamily within the cysteine protease superfamily. Most cathepsins are ubiquitously expressed in lysosomes and play a role in protein degradation and processing. In addition to these house-keeping functions, cathepsins are implicated in wide variety of diseases, including cancer (194, 195). In particular, cathepsin B (CTSB) is linked to a number of human cancers, including prostate carcinoma, breast cancer, and brain tumors (81, 105, 185, 191, 210).

In an effort to characterize cathepsin involvement in KSHV-induced tumorigenesis, we now demonstrate that CTSB is an essential factor for KSHV-induced post-confluent growth of E-DMVEC whereas other cathepsins tested did not play an essential role. Unexpectedly, secretion of CTSB was inhibited in latently infected ECs. CTSB is retained by the insulin-like growth factor-II receptor (IGF-IIR/M6PR), which we previously reported to be transcriptionally induced during KSHV-mediated transformation of E-DMVEC (155). Therefore, unlike the increased secretion of CTSB observed in several other tumor models, CTSB is retained in the endosomal/lysosomal

compartment in KS, where it likely regulates processing of growth factors or growth factor binding proteins. Given the recent progress in developing CTSB-inhibitors for cancer treatment (50), our data suggest that such inhibitors might be a novel treatment for KS.

METHODS AND MATERIALS

Viruses, cell culture, and reagents. KSHV-infected E-DMVEC were established and maintained as previously described (Moses et al., 1999). KSHV-infected DMVEC were used in experiments when >90% of the cells expressed LANA-1. CA-074 (cat# 205530), CA-074ME (cat# 205531), and HNMPA-(AM₃) (cat# 397100) were obtained from EMD Biosciences (San Diego, CA). Antibodies against cathepsin S (cat# IM1003), cathepsin L (cat# 219387) and cathepsin B (cat# IM27L) were purchased from EMD Biosciences (San Diego, CA). Mouse monoclonal anti-calreticulin (SPA-601) was purchased from Stressgen, (Victoria, BC, Canada). Purified human native cathepsin B (cat# JA7741) was obtained from EMD Biosciences (San Diego, CA). Polyclonal IGF-IIR/M6PR antibody (H-20) was obtained from Santa Cruz Biotechnology (Santa Cruz, CA).

Microarray experiments and analysis. cDNA synthesis, hybridization to HG_U133A and B arrays (Affymetrix), and signal intensity normalization were performed at the OHSU microarray core facility (www.ohsu.edu/gmst/amc). GeneChip data were analyzed with Arrayassist (Stratagene). Comparisons were made between passage-matched KSHV-infected E-DMVEC and mock-infected E-DMVEC in 4 separate experiments. A master data table consisting of expression values extracted from all CEL files was created with the Probe Logarithmic Error Intensity Estimate (PLIER) method. To define the baseline from which changes in gene expression data were determined in KSHV-infected samples, a virtual chip comprising all mock-infected control expression data was used. Significant changes with a p-value of p=0.01 was determined by ANOVA with variance stabilization and no p-value correction.

Western Blot and Immunoprecipitations. For immunoprecipitation, cells were washed twice with ice-cold PBS, lysed in NP-40 buffer [1% NP-40, 150 mM NaCl, 10% glycerol, 20 mM Tris-HCl (pH 8.0), 1 mM EDTA (pH 8.0), 0.2% SDS] containing protease inhibitors (Roche Diagnostics; Indianapolis, IN), 1 mM NaVO₄, and 1 mg/ml pepstatin. Lysates were cleared and protein concentration was determined as above. For IGF-IIR/M6PR, 500 µg of whole-cell lysate protein was immunoprecipitated with 10 µg of anti-IGF-IIR/M6PR antibody and incubated overnight at 4°C while rocking. 50 µl of protein A/G-agarose bead slurry (Upstate) was added for 45 minutes while rocking at 4°C. Three washes were performed and the pellet was boiled in 2x SDS sample buffer. The beads were spun down and the supernatant was separated by a 10% SDS-PAGE. For Westerns, cells were directly lysed in 1X SDS Sample buffer [100 mM Tris-Cl (pH6.8), 2% SDS, 10% Glycerol] without dyes or DTT/2-mercaptoethanol and subsequently boiled for 5 minutes. Protein content was normalized and determined using a BCA Protein Assay kit (cat#23227, Pierce, Rockford, IL). Before resolving samples on 10% SDS-PAGE, 100 mM DTT and 0.01% bromophenol blue were added to the lysates and samples were boiled for 5 minutes. Gels were transferred to nylon membranes, blocked for 20 minutes with 10% milk in 1X PBS supplemented with 0.1% Tween-20, and probed with a the respective antibodies. Bound antibodies were detected by enhanced chemiluminescence (Pierce) and exposed to film.

RT-PCR. qPCR was performed on an ABI7700 sequence detection system (Applied Biosystems, Foster City, CA). Target gene expression was compared to the

housekeeping gene GAPDH. Total RNA was purified from primary DMVEC using RNeasy spin columns (Qiagen Inc, Valencia, CA). Human tissue was a generous gift from H. Koon and B. J. Dezube and prepared as previous described (150). Total RNA was treated with DNase I (DNase Free: Ambion, Austin, TX) before synthesis of cDNA with random hexamers and Superscript III (Invitrogen, Carlsbad, CA). The following primers were selected by using the software Primer Express (Applied Biosystems): IGF-IIR/M6PR 6333F: GCAGAAGCTGGGTGTCATAGG, 6420R: 5'CACGGAGGATGCGGTCTTAT; IGF-IR 2184F: GGAGGAGGCTGAATACCGC, 2252R: 5'TCAGGTCTGGGCACGAAGAT. Reactions were performed using SYBR green PCR core reagents. Relative expression values between uninfected and KSHV infected, normal skin, and KS tissue were calculated by the comparative C_t method (106). Dissociation curves were performed on human reference RNA after each amplification run to control for primer-dimers. For analyzing CTSB splicing, the following primers were used as previously published for PCR: CTSB full length fwd: 5'CAGCGCTGGGCTGGTGTG, CTSB(-2) fwd: 5'CAGCGCTGGGTGGATCTA, CB(-2/3) fwd: 5'CAGCGCTGGGCCGGGCAC, CB EXON 11 rev: 5'CCAGGACTGGCACGACAGGC. PCR to determine CTSB isoforms was performed by standard approaches (95°, 5 minutes, [95°, 1 minute, 55°, 1 minute, and 72°, 2 minutes] for 30 cycles, 72°, 10 minutes).

siRNA treatments. KSHV-infected E-DMVEC were seeded the day prior to siRNA treatment at 30% confluency in 35-mm polystyrene dishes (Corning). On the day of treatment, for each sample, 3 μ l Oligofectamine (Invitrogen) was mixed with 12 μ l

OptiMEM (GIBCO-Invitrogen) for 5 minutes at room temperature. A mix of 200nM SMARTpool siRNA (Dharmacon) and 180 μ l OptiMEM were added to Oligofectamine mix and incubated 20 minutes at room temperature. For IGF-IIR/M6PR siRNA treatment, single siRNA were employed, sense strand: AGACCAGGCUUGCUCUAUAAU [On-Targetplus Set (6)], CAACUUUCCUCCAUCACAAU [On-Targetplus Set (7)], and CGAUACCUCUCAAGUCAAAU [On-Targetplus Set (8)], cat #J-010601-06, Dharmacon). Cells were washed once in OptiMEM and 800 μ l OptiMEM was added to the dish prior to adding 200 μ l siRNA mix. Cells were incubated 6 hours before receiving a second treatment of siRNA as before. Cells were incubated overnight and the siRNA mix was removed and replenished with 2 ml complete media. siRNA treated cells were incubated 4-6 days to determine the peak of downmodulation at which point protein levels were assayed by Western Blot. For long-term observation of phenotypic changes, siRNA-treated cells were treated again with siRNA one week after the first treatment to ensure efficient knockdown. One day after the second treatment series CTSB activity was measure by zymogen assay.

Focus inhibition assay. KSHV-infected E-DMVEC were seeded at 30-50% confluency on 35-mm dishes (Corning) and treated either with siRNA or the CTSB small-molecule inhibitors, CA-074 or CA-074ME for a two week period. 10 μ M of inhibitors were added during change of medium (every 2 days), whereas a second round of siRNA treatment was performed 7 days after the first treatment to maintain knockdown of specified genes. For siRNA rescue, 10ng/ml of native human CTSB was added every 2 days after initial

siRNA treatment and continued for two weeks total. Cells were examined for spindle-cell formation, loss of contact inhibition (a result of adherent foci in the monolayer), or virus-induced cytopathic effect by microscopy. Cells were washed twice in PBS and fixed in 3.7% paraformaldehyde for 20 minutes before washing again and adding a coverslip over 80 μ l glycerol.

Immunofluorescence microscopy. Cells were washed twice with 1X PBS, and fixed with 3.7% formaldehyde (in PBS) for 20 minutes at room temp. Cells were washed twice with 1X PBS and permeabilized with 0.1% Triton X-100 (in PBS), for 5 minutes. Subsequently, cells were washed three times with 2% PBA (BSA in PBS). To measure KSHV infection after inhibitor treatment, cells were probed with a primary rabbit polyclonal anti-LANA-1 (ORF73) (a gift from Dr. Bala Chandran; Rosalind Franklin University, Chicago, IL) at 1:500 for 2 hrs at 37 $^{\circ}$ C. Cells were washed three times with 2% PBA (BSA in PBS) and incubated with goat anti-rabbit 594 Alexa Fluor secondary (Molecular Probes, Eugene, OR), 1:500 for 45 min at 37 $^{\circ}$ C. Images were analyzed with a Nikon fluorescence microscope. For live-staining, KSHV-infected E-DMVEC were seeded at confluency on Lab-Tek II 1.5 Borosilicate chambered coverglass slides (cat# 155382, Electron Microscopy Sciences, Hatfield, PA). The next day cells were left untreated or treated with CA-074 (10 μ M), CA-074ME (10 μ M), or HNMPA-(AM₃) (50 μ M) overnight before being probed with GB-111 FL (1 μ M) for 60 minutes. Images were acquired by Aurelie Snyder of the OHSU-MMI Research Core Facility (<http://www.ohsu.edu/research/core>) with an Applied Precision Deltavision RTTM image restoration system. This includes the API chassis with precision motorized XYZ stage,

an Olympus IX-71 inverted fluorescent microscope with standard filter sets, mercury illumination with an API light homogenizer, a Nikon CoolSnap Camera and DeltaVision software. Deconvolution using the iterative constrained algorithm of Sedat and Agard and additional image processing was performed on a Linux OS platform with the SoftWoRx program. More scope tech specs can be found at:
http://www.api.com/pdfs/lifescience/DeltaVision_RT_specs.pdf.

Cell viability assay. Cell viability by ATP determination was measured according to the manufacturer's protocol (Molecular Probes, Cat #A-22066). KSHV-infected E-DMVEC were treated with CA-074 (10 μ M), CA-074ME (10 μ M), or HNMPA-(AM₃) (100 μ M) for 4 days in 35-mm dishes and lysed in 1% Triton X-100 for 10 minutes. 5 μ l of D-luciferin/luciferase mix was added per sample and immediately read in a luminometer.

Annexin V-FITC apoptosis detection assay. Apoptosis in uninfected and KSHV-infected E-DMVEC was analyzed with the R&D System Annexin V-FITC Apoptosis Detection kit (cat # TA4638). Cells were washed once in PBS and resuspended in serum-free medium, followed by treatment with Staurosporine (1 μ M), CA-074 (10 μ M), CA-074ME (10 μ M) or left untreated overnight. Cells were trypsinized and washed in 2% PBA before each sample was resuspended in 100 μ l Annexin Reagent (10 μ l 10X Binding Buffer, 10 μ l Propidium Iodide, 1 μ l Annexin V-FITC, and 79 μ l ddH₂O) for 15 minutes at room temperature. 400 μ l 1x Binding Buffer was added before samples were analyzed by flow cytometry.

Proliferation Assay. Uninfected or KSHV-infected E-DMVEC were seeded at 3×10^5 cells for pre-confluency or 5×10^5 cells for post-confluency per 35-mm dish. Cells were grown in the presence or absence of CA-074 (10 μ M), CA-074ME (10 μ M), or HNMPA-(AM₃) (50 μ M) for 5 days before being trypsinized, stained with trypan blue and counted. For the post-confluency assay, cell numbers were normalized to cell numbers in a confluent monolayer of uninfected E-DMVEC (set at 100%) and are presented as a percentile of the uninfected E-DMVEC.

Soft agar assay. Forty thousand KSHV-infected E-DMVEC treated with CA-074, CA-074ME or left untreated for 14 days were plated in 1.5 ml endothelial-SFM growth medium supplemented with 10% human AB serum, 25 μ g/ml endothelial cell growth supplement, and 0.4% melted agarose onto a 3-ml bottom layer of 0.5% agarose medium per well of a 6-well dish. The cells were fed several drops of medium every 3 days, and colonies were photographed after 3 weeks.

Zymogen Assay. CTSB activity was measured with the InnoZyme Cathepsin B Activity Assay Kit (cat# CBA001, EMD Biosciences, San Diego, CA). To test CA-074 and CA-074ME inhibition on native CTSB, 10 μ M of either inhibitor were combined with 50ng of native CTSB enzyme, *in vitro*. Fluorogenic substrate Z-Arg-Arg 7-amino-4-methylcoumarin (AMC) was added and the release of AMC was assayed as recommended by the manufacturer. To measure CTSB enzymatic activity in uninfected and KSHV-infected E-DMVEC lysates and supernatants, cells were seeded in 35-mm

dishes (Corning) in 200 μ l media. Dishes were rocked constantly to cover all cells with media. The media was collected and cells were lysed as suggested in the protocol. Fluorescence was measured using the Flexstation Plate Reader and analyzed using the Softworx Pro 4.0.1 software (Molecular Devices, Sunnyvale, CA).

RESULTS

Cathepsins expressed in KSHV-infected E-DMVEC are involved in tumorigenesis.

As cathepsins have been implicated in a variety of human cancers, we wanted to assess the role of cathepsins in KSHV-induced tumorigenesis. We initially monitored post-confluent growth of E-DMVEC latently infected with KSHV in the presence or absence of the broad-spectrum cysteine protease inhibitor (2S, 3S)-trans-epoxysuccinyl-L-leucylamido-3-methylbutane ethyl ester loxistatin (EST). KSHV-infected E-DMVEC were seeded at 30% confluency and treated with EST (58 μ M) for two weeks whereby the inhibitor was refreshed every 3rd day. While untreated cells develop a spindle-cell phenotype and form foci, EST prevented post-confluent growth and caused KSHV-infected E-DMVEC to remain cobblestone-like as a single monolayer (Figure 1a). Similar observations were made with a series of other broad-spectrum cysteine protease inhibitors (data not shown). These studies suggested that cysteine proteases, presumably cathepsins, are important for the continuous growth of KSHV-infected E-DMVEC upon reaching confluency.

To determine which cathepsins are expressed in KSHV-infected DMVEC, the gene-expression profiles were extracted for all known cathepsin transcripts from complete genome expression arrays (Affymetrix U133A and B). Four independent experiments of KSHV-infected E-DMVEC cultures were compared with their passage- and age-matched cultures of uninfected E-DMVEC. Cathepsin transcripts were scored with the Stratagene algorithm, Probe Logarithmic Error Intensity Estimate (PLIER) method. Only cathepsin S, represented by two Affymetrix probe sets, was induced upon KSHV infection (Supplemental Figure 1).

siRNA screen against cathepsin S, L, and B suggests cathepsin B involvement in KSHV-induced tumorigenesis.

Using a series of more selective cathepsin inhibitors, we narrowed down the list of potential candidates responsible for the inhibitory effects, which were observed with broad-spectrum inhibitors. In particular, the vinyl sulfone LHVS (N-morpholinurea-leucine-homophenylalanine-vinylsulfone-phenyl) has specificity for cathepsins S, L, and B (40, 134, 190). KSHV-infected E-DMVEC were treated with LHVS (25 μ M) as above. Similar to the broad-spectrum inhibitors, an inhibition of post-confluent growth was observed (Figure 1a) suggesting that at least one of these proteases is important for KSHV-mediated transformation of E-DMVEC. Gene expression profiling suggested that all three cathepsins are present in E-DMVEC, but only cathepsin S is induced (Supplemental Figure1). This expression profile was confirmed at the protein level using specific antibodies in immunoblots (Figure 1b). To distinguish which of these three cathepsins are necessary for KSHV-induced tumorigenesis, SMARTpool siRNAs were employed against each candidate protease. KSHV-infected E-DMVEC were treated separately with SMARTpool siRNAs against cathepsin S, L, and B, or mock-treated with a Cy5-labeled siRNA against luciferase. siRNA treated KSHV-infected cultures were monitored over two weeks for spindle-cell and foci formation. Transfection efficiency was visualized with the Cy5-label conjugated to the luciferase siRNA and estimated to be consistently around 95%. Western blot analysis of siRNA treated cultures revealed that all three SMARTpool siRNAs efficiently reduced target protein levels (Figure 2a). Furthermore, cathepsin L siRNA inhibited its target cathepsin, but did not affect protein expression of CTSB and vice versa. As shown in Figure 2, despite efficient gene

knockdown, cathepsin S and L SMARTpool siRNAs did not impede KSHV-induced tumorigenesis, similar to Cye3-luciferase treated (data not shown) or untreated cultures. In contrast, CTSB siRNA dramatically inhibited spindle-cell and foci development in KSHV-infected E-DMVEC (Figure 2b). These data suggested that CTSB was responsible for the inhibition of KSHV-mediated E-DMVEC transformation by cathepsin inhibitors.

Intracellularly active CTSB is essential for KSHV-induced tumorigenesis.

Previous studies on CTSB involvement in human tumors showed that secreted or extracellular-matrix associated CTSB was involved in tumorigenesis by degrading extracellular matrix components or activating matrix-metallo-proteases, respectively (99, 116, 185). Therefore, we initially hypothesized that exogenous CTSB is required for KSHV-induced tumorigenesis. To test this hypothesis, we examined whether post-confluent growth of CTSB-siRNA-treated cells could be rescued by exogenously adding native human CTSB to the media of KSHV-infected E-DMVEC. Even after prolonged treatment with 10ng/ml native human CTSB, the siRNA treatment still inhibited post-confluent growth of spindle-cells (Figure 3a) suggesting that endogenous, rather than secreted CTSB is essential for KSHV-induced tumorigenesis.

The role of intracellular versus extracellular CTSB was further examined by using two different versions of the activity-based CTSB suicide inhibitor CA-074. CA-074 is unable to cross the cell membrane and consequently can only inhibit extracellular CTSB activity. A methyl ester-modified version of CA-074, proinhibitor CA-074ME, can cross the membrane and inhibit intracellular CTSB, although the modification reduces

selectivity for CTSB (117). To ensure that both versions of CA-074 inhibited CTSB activity, they were tested against native human CTSB *in vitro*. At the concentration of 10 μ M, the inhibitors were combined with native human CTSB in the presence of the fluorogenic synthetic CTSB substrate, Z-Arg-Arg 7-amino-4-methylcoumarin (AMC). The release of AMC was measured by fluorescence. Compared to untreated CTSB activity both versions of CA-074 successfully reduced CTSB activity (Figure 3b). To examine whether CA-074 or CA-074ME inhibited KSHV-mediated transformation of E-DMVEC, uninfected or KSHV-infected E-DMVEC cultures were treated with 10 μ M of the respective CTSB inhibitors over a period of two weeks. Untreated KSHV-infected E-DMVEC developed spindle-cell morphology and formed foci (Figure 3c, panel 1). The non-permeable version CA-074 was unable to inhibit spindle-cell and foci formation (Figure 3c, panel 3). In contrast, the development of spindle cell morphology was inhibited by CA-074ME (Figure 3c, panel 2). This result supports the conclusion that intracellular, rather than secreted CTSB is required for KSHV-induced tumorigenesis.

To locate enzymatically active CTSB in live cells, a fluorescein-conjugated activity-based probe, GB-111 FL, which binds to both active cathepsins L and B, was exploited. Prior to probing with GB-111 FL, KSHV-infected E-DMVEC were treated with CA-074 (10 μ M) or CA-074ME (10 μ M). As a control, a non-competitive inhibitor of the insulin receptor, hydroxy-2-naphthalenyl-methyl phosphonic acid trisacetoxymethyl ester (HNMPA-(AM₃)) was used. In Figure 3d panel 1, untreated cells were probed with GB-111 FL, indicating active cathepsin L and B are localized to small vesicles. In Figure 3d panel 2, E-DMVEC treated with the non-competitive inhibitor HNMPA-(AM₃) showed no difference in the staining pattern compared to untreated cells.

Probe staining of most cells treated with the non-permeable inhibitor CA-074 was similar to untreated cells. Some cells did display a reduced vesicular staining (Figure 3d panel 3). This could be due to the ability of unmodified CA-074 to enter the endocytic compartment during long-term treatment, as has been previously documented (185). The amount that is internalized does not seem to be effective at inhibiting post-confluent growth. In contrast, the membrane-permeable inhibitor CA-074ME completely eliminated vesicular staining (Figure 3d panel 4), which is consistent with its efficient inhibition of post-confluent growth. We conclude from these findings that CTSB inhibitors can efficiently neutralize CTSB activity, and that intracellular active CTSB is essential for KSHV-induced tumorigenesis.

CTSB inhibitor CA-074ME reduces the number of LANA-positive E-DMVEC.

CTSB activity appears essential for KSHV-induced tumorigenesis, and only treatment with the membrane permeable version of the CTSB suicide inhibitor was successful at inhibiting spindle-cell and foci formation. In our cell culture system, most but not all E-DMVEC are latently infected with KSHV. Therefore, we wanted to explore whether treatment with the CTSB-inhibitor changed the ratio of infected versus uninfected E-DMVEC. Cells were stained for the latent nuclear antigen, LANA-1, which tethers the viral genome to the cellular chromosome thus giving a characteristic punctuate staining pattern. KSHV-infected E-DMVEC were left untreated or treated for 14 days with either CA-074 (10 μ M) or CA-074ME (10 μ M) and stained with a polyclonal antibody against LANA-1 (Figure 4, left panels). CA-074ME treatment resulted in a dramatic 89% reduction in the number of LANA-1 positive cells compared to untreated

KSHV-infected E-DMVEC (Figure 4, middle and upper panels), whereas the non-permeable inhibitor CA-074 did not change the ratio of LANA-1 positive versus negative cells (Figure 4, bottom panel). The number of LANA-1 positive cells was quantified by counting individual nuclei as shown in Figure 4b. These observations indicated that KSHV-infected E-DMVEC have lost their growth advantage and fail to proliferate when CTSB activity is inhibited with CA-074ME.

CTSB inhibitors are non-toxic and do not sensitize KSHV-infected E-DMVEC to apoptosis.

To address whether CTSB inhibitors are toxic to cells, an ATP cell-viability assay was performed. KSHV-infected E-DMVEC were cultured in the presence of CA-074 (10 μ M), CA-074ME (10 μ M) or left untreated for two weeks. As a positive control, a previously identified inhibitor of KSHV-induced tumorigenesis, HNMPA-(AM₃), was used at a concentration (100 μ M), which is toxic to the cells (155). During this time, the cells reached confluency and formed spindle cell-containing foci, except in the presence of CA-074ME. Treated cells were lysed and ATP was quantitatively determined by luciferin bioluminescence assay. A decrease in ATP concentration was only seen with HNMPA-(AM₃), as previously described (155). In contrast, neither CA-074 nor CA-074ME seemed to inhibit cell viability (Supplemental Figure 2a).

Additionally, CTSB inhibitor-treated cells were assayed by flow cytometry for phospholipid flipping as an indication of apoptosis using an Annexin V-FITC apoptosis detection kit. Cells and supernatants were collected after 14 days of treatment with CA-074 (10 μ M) or CA-074ME (10 μ M) and stained with Annexin V-FITC and propidium

iodide. The staining pattern distinguishes between early apoptotic cells (Annexin V-positive) and late apoptotic cells (propidium iodide- and Annexin V-positive). While neither treated (Supplemental Figure 2b panels 3 and 4 for uninfected, and panels 7 and 8 for KSHV-infected E-DMVEC) nor untreated E-DMVEC (Supplemental Figure 2b, panels 1 and 5) showed any significant change in the amount of viable cells, a large double-positive cell population was visible when treating with the apoptosis-inducing compound Staurosporine (Supplemental Figure 2b, panels 2 and 6). The ATP-viability assay and the Annexin V stain show that the CTSB inhibitor concentrations are not toxic to cells.

Cathepsin B supports post-confluent foci formation and loss of contact inhibition.

Next, we examined whether CTSB inhibitors affected the proliferation of KSHV-infected E-DMVEC prior to reaching confluency. Cells were seeded at low density and allowed to grow to confluency while treated with CA-074 (10 μ M), CA-074ME (10 μ M), or HNMPA-(AM₃) (100 μ M). Cells were trypsinized, stained with trypan blue and counted using a hemocytometer. Treatment with either version of the CTSB inhibitor CA-074 did not reduce cell numbers (Figure 5a). As expected, HNMPA reduced cell numbers. These results support the notion that proliferation of KSHV-infected E-DMVEC is not affected by CTSB inhibitors.

To determine whether post-confluent growth of KSHV-infected E-DMVEC was affected, cells were seeded at confluency and treated with CA-074 (10 μ M), CA-074ME (10 μ M) or HNMPA-(AM₃) (50 μ M) for two weeks. Cells were trypsinized, stained with trypan blue and counted using a hemocytometer. Inhibiting intracellular CTSB activity

with the methyl ester version of CA-074 reduced the number of cells to levels of uninfected E-DMVEC, which remain as a single monolayer at confluency. In contrast, KSHV-mediated post-confluent proliferation was not affected by the unmodified version of CA-074, which was comparable to untreated KSHV-infected E-DMVEC (Figure 5b). HNMPA-(AM₃) at 50 μ M was used as a positive control, since it was previously shown that at this non-toxic concentration HNMPA-(AM₃) efficiently inhibits KSHV-induced tumorigenesis (155).

KSHV-infected E-DMVEC have the ability to form colonies in soft agar, a hallmark of transformation (123, 155). In order to establish whether KSHV infected E-DMVEC were able to form colonies upon CTSB inhibition, cells were treated with CA-074 (10 μ M), CA-074ME (10 μ M) or left untreated for 14 days before transfer to soft agar. The non-permeable inhibitor CA-074 and untreated KSHV-infected E-DMVEC efficiently formed colonies in soft agar. In contrast, the membrane-permeable CA-074ME inhibited colony formation (Figure 5c). The total amount of colonies formed under each condition is quantified in Figure 5d. Taken together, the results suggest that CTSB is not required for E-DMVEC proliferation prior to reaching confluency. Instead CTSB is essential for supporting post-confluent and anchorage-independent growth.

CTSB activity is retained intracellularly in KSHV-infected E-DMVEC.

As latent KSHV infection in E-DMVEC does not alter CTSB gene expression or protein levels and intracellular CTSB is essential for post-confluent growth, the subcellular distribution of CTSB activity was analyzed. A CTSB zymogen assay compared extracellular and intracellular CTSB activity between uninfected and KSHV-

infected E-DMVEC. Cells were cultured overnight in a minimal amount of media at which time both the supernatant and whole cell lysates were collected. Lysates and supernatant were mixed with the fluorogenic synthetic CTSB substrate AMC and released AMC was measured by fluorescence. While most of active CTSB in uninfected E-DMVEC was secreted, almost all of the active CTSB was retained intracellularly in KSHV-infected E-DMVEC (Figure 6a). The altered distribution was also seen when comparing uninfected E-DMVEC with KSHV-infected E-DMVEC using the activity based probe, GB-111 FL. There were more organized vesicles visible concentrated with protease activity in KSHV-infected E-DMVEC (Figure 6b).

One possible reason for the differential distribution of CTSB was alternative splicing of the CTSB transcript, which contains 13 exons (5, 8, 114, 210). Tumors can contain different species of CTSB mRNA, which can have a dramatic effect on translational efficiency (5) or on cellular trafficking of the translated protein (114). To examine CTSB mRNA splicing, total RNA from uninfected and KSHV-infected E-DMVEC was isolated and analyzed by reverse-transcriptase (RT)-PCR. Primers were designed against the most dominant CTSB mRNA products as identified in other tumor models: full-length CTSB, CTSB without exon 2 [CB(-2)], or CTSB without exons 2 and 3 [CB(-2/3)] (114). The dominant species in E-DMVEC appeared to be CTSB mRNAs missing exon 2 or both exon 2 and 3, while the full-length transcript was absent. The same splicing pattern was observed in both KSHV-infected and uninfected E-DMVEC (Figure 6c), suggesting that differential splicing is most likely not responsible for subcellular distribution of CTSB.

The KSHV-induced mannose 6-phosphate receptor, IGF-IIR/ M6PR, is required for retaining cathepsin B.

Fluorescent probes revealed a perinuclear vesicular staining pattern for active CTSB consistent with an endosomal/lysosomal localization (Figure 3d). To further determine whether CTSB located to these compartments, we disrupted endocytosis by neutralizing the lysosomal pH with NH₄Cl. Treatment with NH₄Cl did not inhibit the enzymatic activity of CTSB *in vitro* (Figure 7a). Instead, the absolute intracellular CTSB activity was reduced both in uninfected and KSHV-infected E-DMVEC to the same extent (Figure 7b), consistent with a lysosomal/endosomal targeting of CTSB.

Lysosomal targeting of CTSB occurs via mannose 6-phosphate receptors. The major receptor for sorting CTSB to lysosomes is the IGF-IIR/M6PR (64, 158). Interestingly, we previously observed that IGF-IIR/M6PR expression was highly induced in E-DMVEC latently infected by KSHV (155). Moreover, IGF-IIR/M6PR is highly expressed in KS tissue (Figure 7c). To determine whether CTSB associated with IGF-IIR/M6PR, we immunoprecipitated IGF-IIR/M6PR and probed for CTSB using specific antibodies. CTSB was clearly present in IGF-IIR/M6PR immunoprecipitates (Figure 7d). The KSHV-mediated increase in IGF-IIR/M6PR expression resulted in a concomitant increase of co-immunoprecipitated CTSB. To assess whether induced IGF-IIR/M6PR expression was responsible for the increased CTSB retention in the endosomal/lysosomal compartment in KSHV-infected cells, we treated KSHV-infected DMVEC with siRNA against IGF-IIR/M6PR. As shown in Figure 7e, treatment with siRNA to IGF-IIR/M6PR efficiently reduced mRNA expression levels and had no effect on IGF-IR mRNA. Moreover, cell-associated CTSB activity was significantly reduced in cells treated with

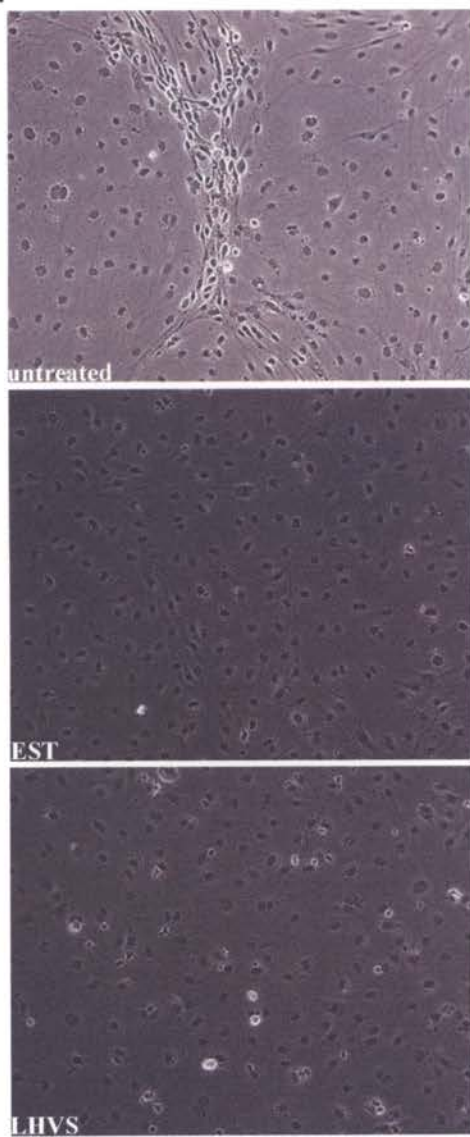
IGF-IIR/M6PR siRNA (Figure 7f). Therefore, we conclude that the IGF-IIR/M6PR is responsible for retaining active CTSB intracellularly by targeting CTSB to the endosomal/lysosomal compartment.

IGFII-R/M6PR is essential for KSHV-induced tumorigenesis.

To determine whether the IGF-IIR/M6PR-mediated retention of CTSB was essential for post-confluent growth and foci-formation, we treated KSHV-infected DMVEC with IGF-IIR/M6PR siRNA. Cells were seeded at 30% confluency and incubated with three different siRNAs designed against IGF-IIR/M6PR. One week after the first treatment, cells were treated a second time with siRNA. At the end of two weeks, E-DMVEC treated with control siRNA (Cye3-labeled siRNA to luciferase) displayed the KSHV-mediated phenotypic change to a spindle-cell phenotype. In contrast, all three individual IGF-IIR/M6PR-specific siRNAs efficiently inhibited spindle cell and foci formation (Figure 8). Taken together with the finding that IGFII/M6PR retained CTSB and that CTSB-specific siRNA inhibits KSHV-mediated post-confluent growth, these data strongly suggest that retention of CTSB by the IGF-IIR/M6PR is essential for the development of the KSHV-induced tumorigenic phenotype.

Figure 1. Cysteine protease inhibitors effectively prevent KSHV-induced tumorigenesis.

A.



B.

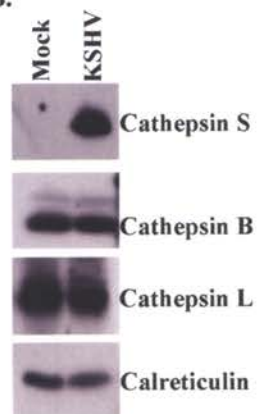
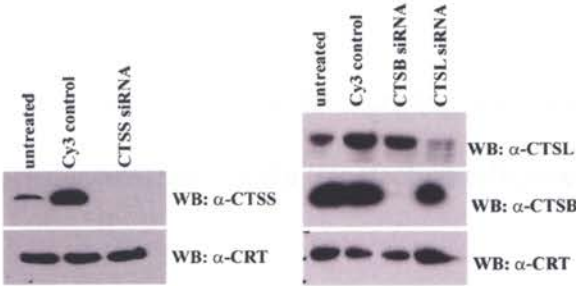


Figure 1. Cysteine protease inhibitors effectively prevent KSHV-induced tumorigenesis. (A) Phase-contrast images of KSHV-infected E-DMVEC treated with cysteine protease inhibitors EST and LHVS. Both compounds effectively inhibit spindle-cell and foci formation. (B) Western blot analysis comparing levels of protein expression for cathepsin S, L and B in KSHV infected and uninfected E-DMVEC. To control for equal loading, antibodies to the cellular chaperone calreticulin (CRT) were used.

Figure 2. Downregulation of CTSB mRNA inhibits KSHV-mediated foci formation.

A.



B.

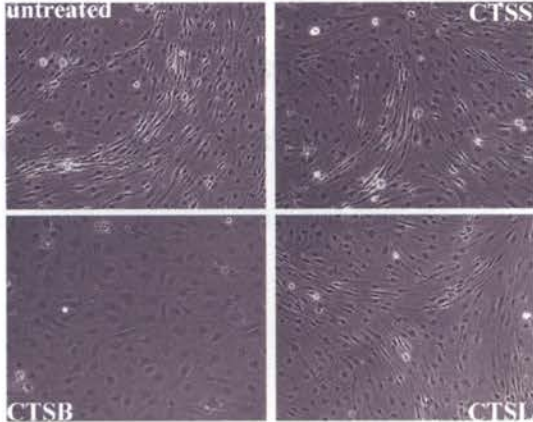


Figure 2. Downregulation of CTSB mRNA inhibits KSHV-mediated foci formation.

(A) Western blot analysis of cathepsin S, L and B protein levels after siRNA treatment with equal loading controlled for by an antibody to calreticulin (CRT). siRNAs to cathepsin L and B were target-specific as determined by Western Blot. (B)

Representative phase-contrast microscopy comparing untreated samples to cathepsin S, L, or B siRNA treated KSHV-infected E-DMVEC. Control siRNA-treated samples were indistinguishable from untreated and are not represented here. Only cathepsin B siRNA reduced foci formation. Immunofluorescence analysis of Cy3-labeled siRNA-transfectants indicated a transfection efficiency of more than 95% (data not shown).

Figure 3. Intracellular CTSB is essential for KSHV-induced spindle-cell and foci formation.

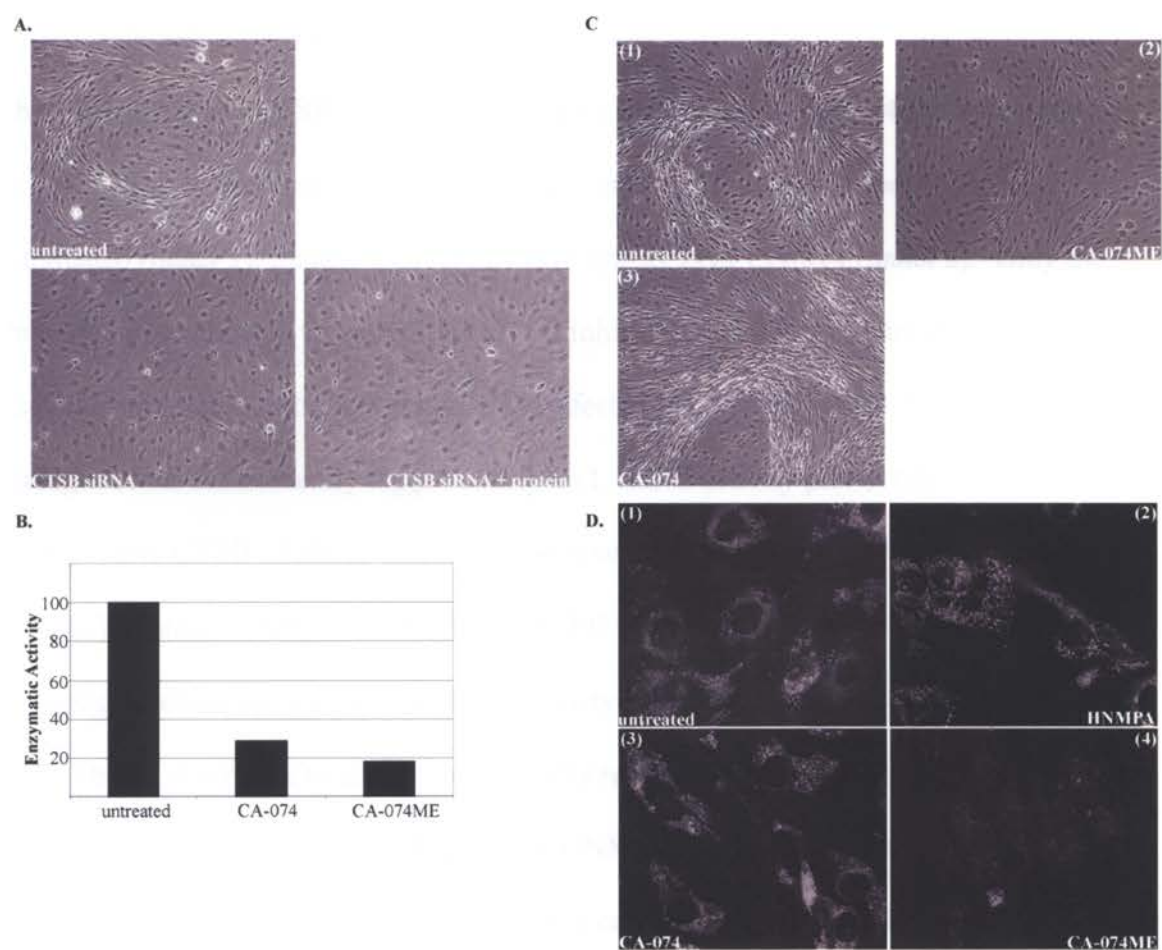


Figure 3. Intracellular CTSB is essential for KSHV-induced spindle-cell and foci formation. (A) Phase-contrast images of the CTSB siRNA-treated cultures incubated with purified human native CTSB. Treatment of KSHV-infected E-DMVEC with 10ng/ml native CTSB (rescue) did not reverse the effect of CTSB siRNA knockdown, compared to only CTSB siRNA-treated samples (siRNA). The upper left panel shows KSHV-infected E-DMVEC without treatment. (B) Zymogen assay to determine effectiveness of the two inhibitors on CTSB enzymatic activity. Both inhibitors effectively reduced CTSB activity as compared to untreated active CTSB, when analyzed by cleavage of the CTSB fluorogenic substrate Z-Arg-Arg 7-amino-4-methylcoumarin (AMC). (C) Representative phase-contrast images of KSHV-infected E-DMVEC untreated (panel 1), treated with CA-074ME (panel 3) or CA-074 (panel 2). Only the membrane-permeable version of the CTSB inhibitor, CA-074ME, was able to inhibit spindle-cell and foci formation in KSHV-infected E-DMVEC (panel 2). (D) Microscopy images of the fluorescently tagged cathepsin L and B activity probe, GB-111 FL, after competitive CTSB inhibitor or non-competitive insulin receptor inhibitor [HNMPA-(AM₃)] treatment. KSHV infected E-DMVEC were treated with the various inhibitors overnight before being probed with the activity based small-molecule inhibitor GB-111 FL. Only CA-074ME treatment dramatically reduced the staining pattern of GB-111 FL (panel 4). Meanwhile untreated (panel 1), HNMPA-(AM₃) (panel 2), and CA-074 (panel 3) showed no change in their staining. Some cells treated with CA-074 did show a reduction in vesicular staining similar to CA-074ME, and it has been documented that CA-074 can permeate the cells; however, at this concentration the inhibitor had no effect on KSHV-induced tumorigenesis.

Figure 4. The membrane-permeable CTSB inhibitor CA-074ME reduces the number of LANA-1 positive E-DMVEC.

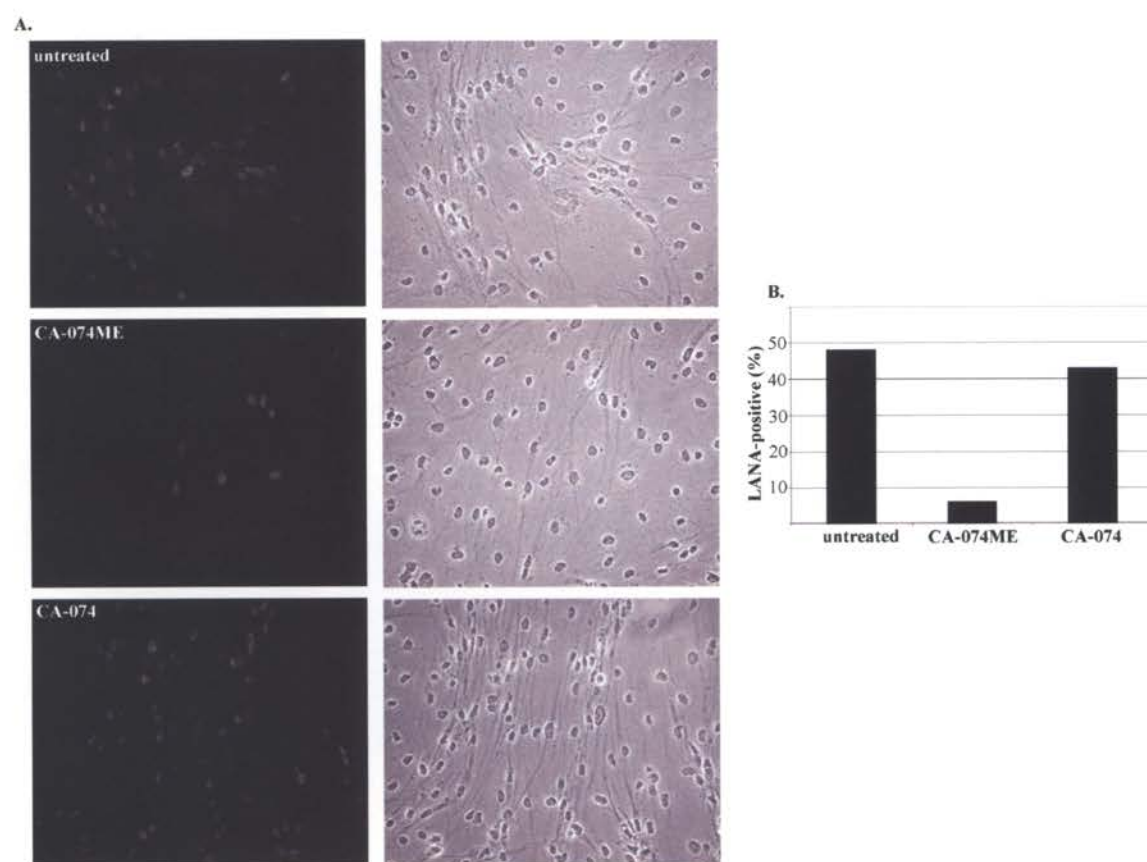


Figure 4. The membrane-permeable CTSB inhibitor CA-074ME reduces the number of LANA-1 positive E-DMVEC. (A) Phase-contrast and dark-field images of untreated (upper panel), CA-074ME (10 μ M) (middle panel) or CA-074 (10 μ M) (lower panel) treated KSHV-infected E-DMVEC showing expression of LANA-1 in KSHV-infected spindle cells and the selective loss of 89% of LANA-1-positive foci following CA-074ME treatment. (B) Graph quantifying LANA-1 positive cells for each field visualized.

Figure 5. Inhibiting intracellular CTSB activity prevents post-confluent anchorage-independent growth of KSHV-infected E-DMVEC.

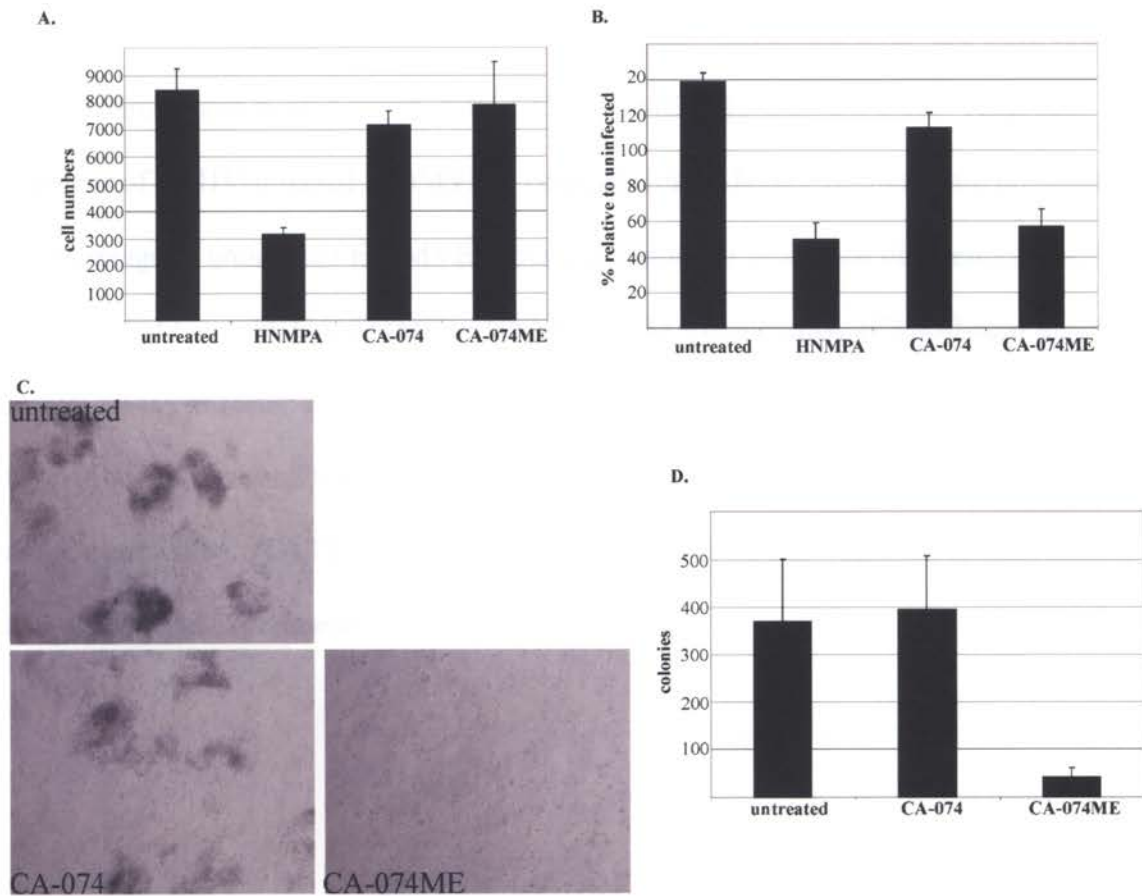


Figure 5. Inhibiting intracellular CTSB activity prevents post-confluent anchorage-independent growth of KSHV-infected E-DMVEC. (A) Pre-confluent cell proliferation. Cells were seeded at low density and left untreated or treated with CA-074, CA-074ME, or HNMPA-(AM₃). Total cell counts were determined using a hemocytometer and compared to normal cell proliferation of untreated E-DMVEC. (B) Post-confluent cell proliferation. Uninfected or KSHV-infected E-DMVEC were seeded at high density and treated with CA-074, CA-074ME or HNMPA-(AM₃). Total cell numbers of KSHV-infected E-DMVEC, counted using a hemocytometer, are presented as a percentage of uninfected E-DMVEC total cell counts to determine differences based on any effect of CA-074, CA-074ME or HNMPA-(AM₃) treatments. (C) Soft-agar growth assay. KSHV-infected E-DMVEC were left untreated or treated with CA-074 or CA-074ME for 14 days and transferred to soft-agar containing media. Phase-contrast images are representative. (D) The graph quantifies the number of foci observed in each sample and of replicate experiments.

Figure 6. Active CTSB is retained in KSHV-infected E-DMVEC, and both uninfected and KSHV-infected E-DMVEC express the same CTSB mRNA species.

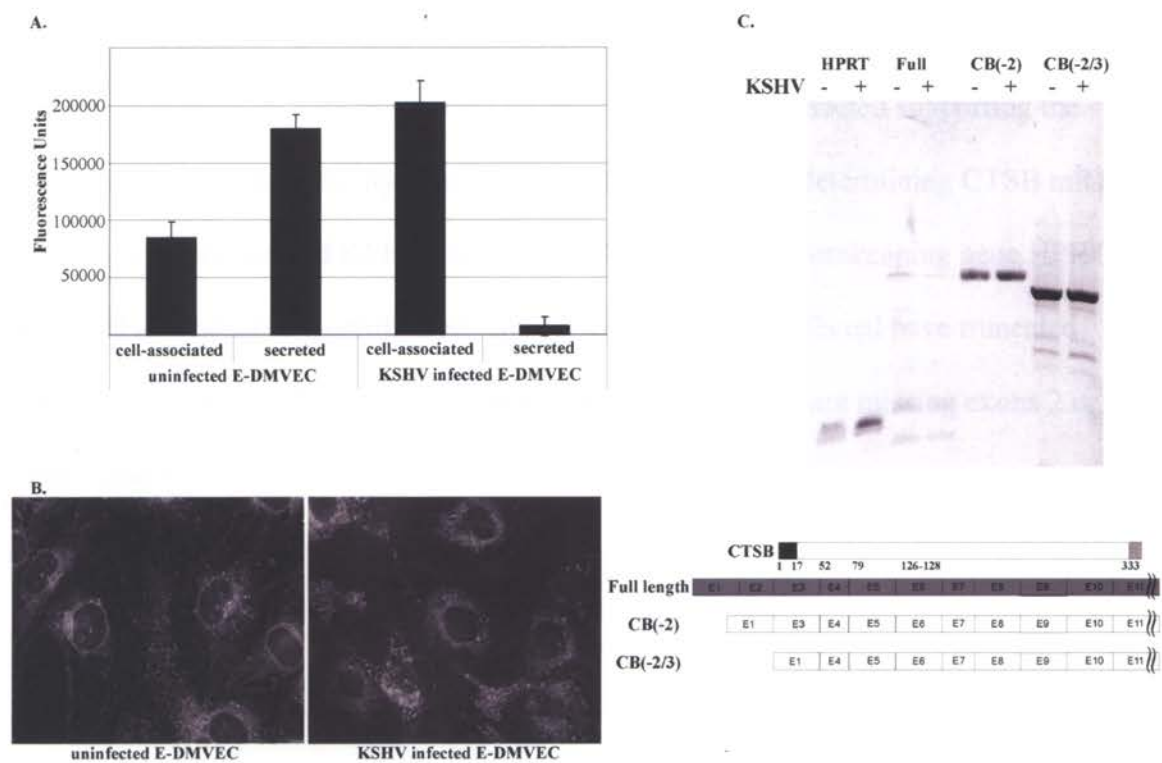


Figure 6. Active CTSB is retained in KSHV-infected E-DMVEC, and both uninfected and KSHV-infected E-DMVEC express the same CTSB mRNA species.

(A) Zymogen Assay comparing CTSB enzymatic activity of uninfected and KSHV-infected E-DMVEC cultures in lysates and supernatant. Uninfected E-DMVEC secrete the majority of active CTSB, while KSHV-infected E-DMVEC retain almost all of the active CTSB intracellularly as very little is secreted. (B) KSHV-infected and uninfected E-DMVEC were probed with the activity-based small-molecule inhibitor GB-111 FL to visualize CTSB activity. In KSHV-infected E-DMVEC, there were more organized vesicles concentrated with fluorescent probe compared to uninfected supporting the increased intracellular activity measured in (A). (C) RT-PCR determining CTSB mRNA species in uninfected and KSHV-infected E-DMVEC. The housekeeping gene HPRT was used as a positive control. Both uninfected and KSHV-infected have truncated versions of CTSB mRNA as the dominant species; they either are missing exons 2 or exon 2 and 3.

Figure 7. IGF-IIR/M6PR is responsible for increased endo-lysosomal trafficking of CTSB.

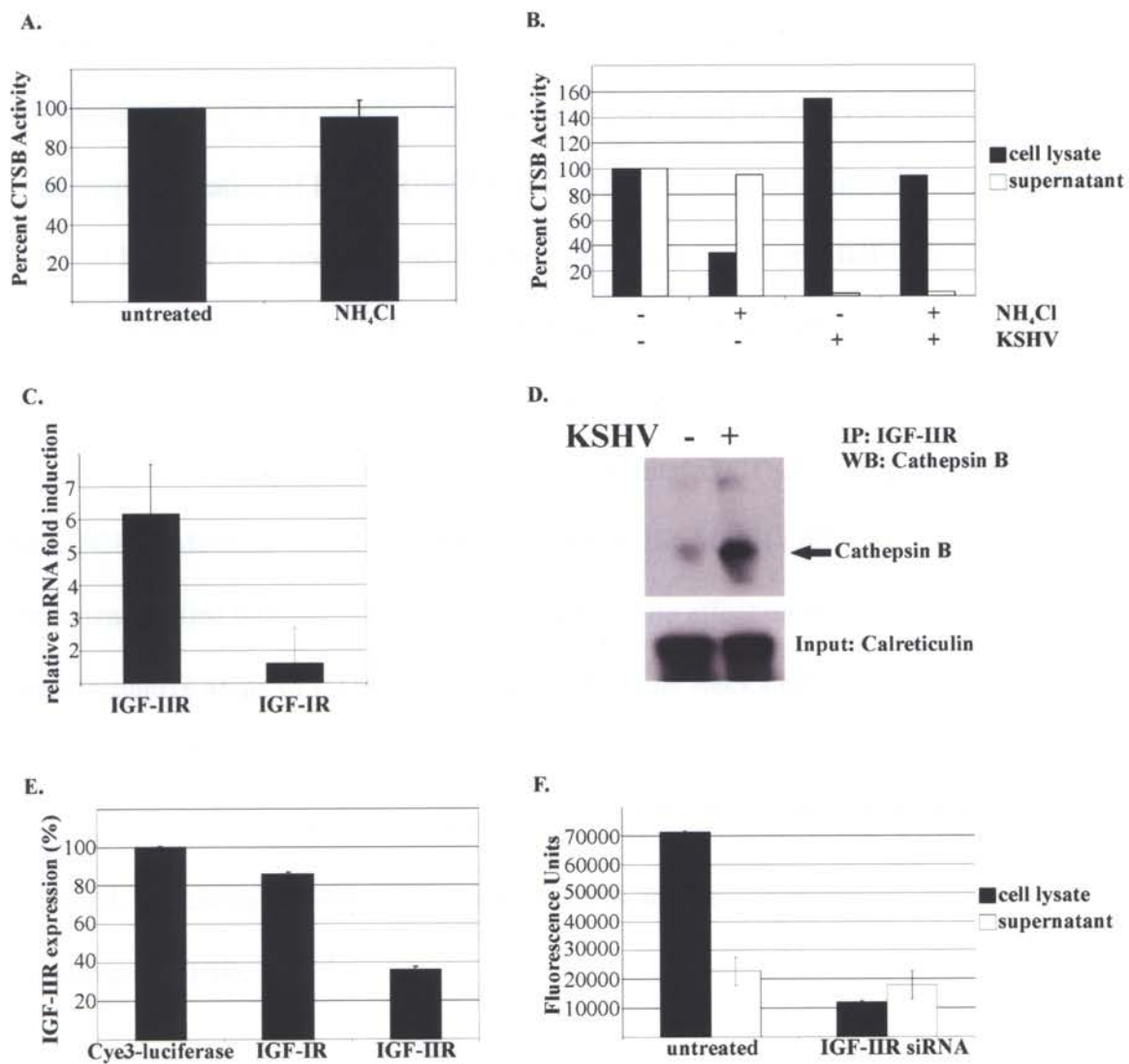


Figure 7. IGF-IIR/M6PR is responsible for increased endo-lysosomal trafficking of

CTSB. (A) CTSB activity assay after disruption of lysosomes with NH_4Cl . Uninfected and KSHV-infected E-DMVEC lysates and supernatants were collected 24-hrs after NH_4Cl treatment, and CTSB activity was compared to untreated samples. NH_4Cl efficiently disrupted intracellular CTSB activity. (B) CTSB zymogen assay controlling for activity in the presence of NH_4Cl . NH_4Cl had no effect on actual CTSB activity. (C) Quantitative real-time PCR comparing IGF-IR and IGF-IIR/M6PR expression levels in KS tissue. Only IGF-IIR/M6PR was significantly induced in KS tissue. (D) Co-immunoprecipitation of IGF-IIR/M6PR and CTSB. Lysates of uninfected and KSHV-infected E-DMVEC were lysed and immunoprecipitated with anti-IGF-IIR/M6PR. Samples were resolved on a 10% acrylamide gel and blotted with a anti-CTSB antibody. Proportional to the increase in IGF-IIR/M6PR expression after long-term KSHV infection, there was an increase in coimmunoprecipitated CTSB. (E) Quantitative real-time PCR confirming efficient knockdown of IGF-IIR/M6PR mRNA after siRNA treatment against IGF-IIR/M6PR. The siRNA had no effect on IGF-IR. (F) Representative assay of CTSB activity assay after one week of IGF-IIR/M6PR siRNA treatment. Cells were treated again using the two-hit combination one day prior to testing CTSB activity. In the presence of IGF-IIR/M6PR siRNA intracellular CTSB activity was depleted, indicating IGF-IIR/M6PR is responsible for the increased endo-lysosomal targeting of CTSB.

Figure 8. IGF-IIR/M6PR siRNA inhibits spindle cell and foci formation in KSHV-infected E-DMVEC.

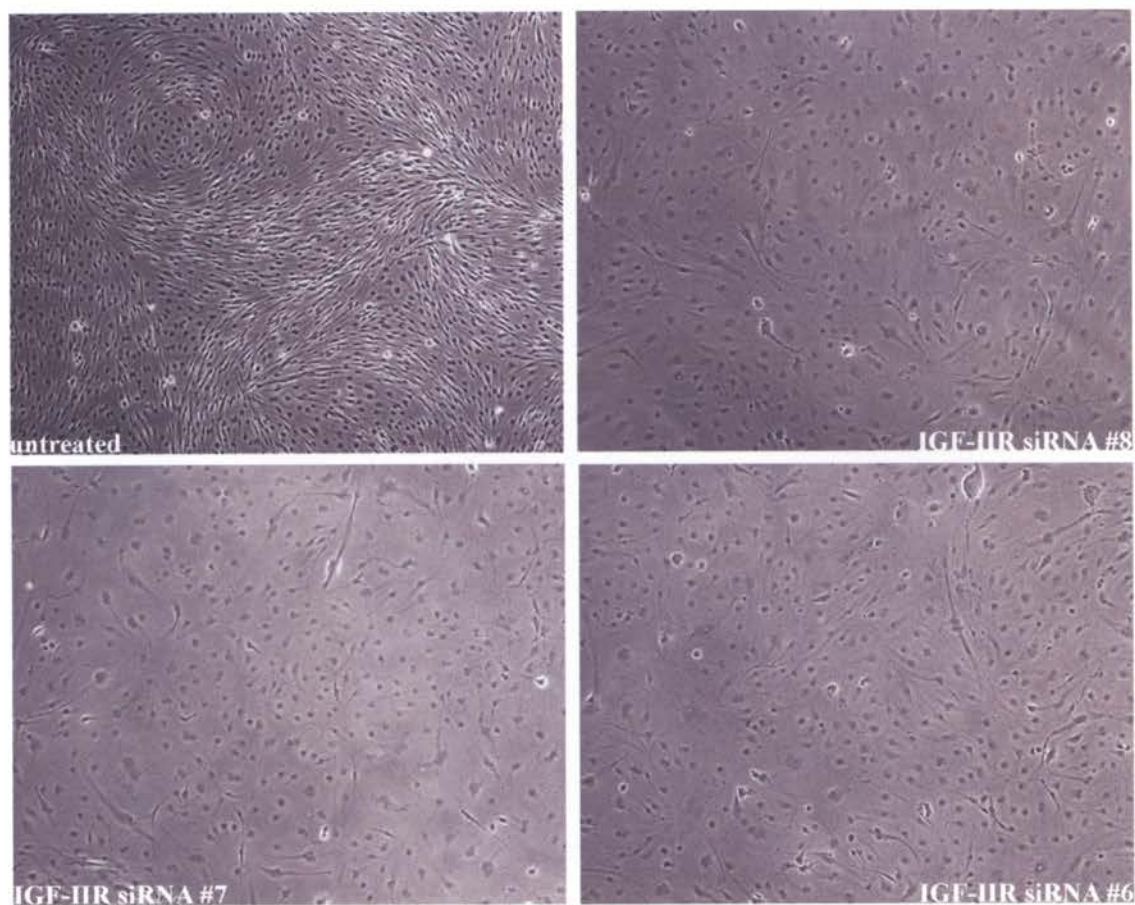


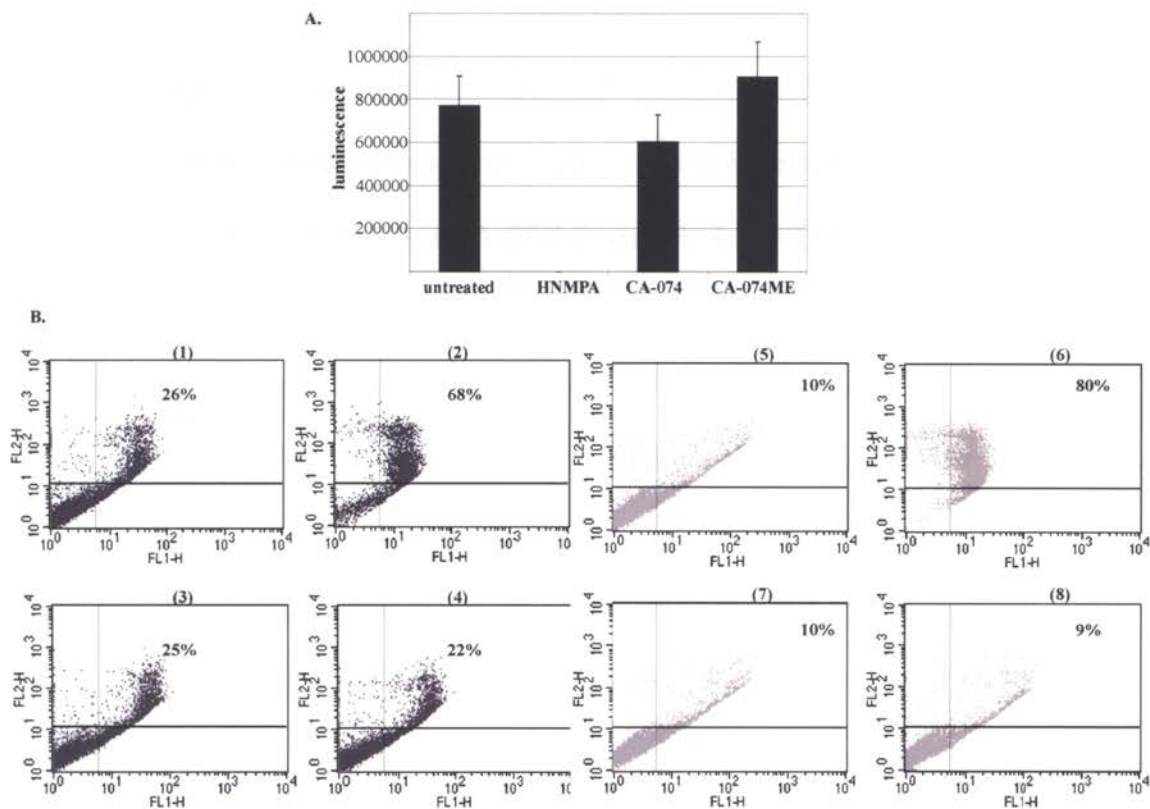
Figure 8. IGF-IIR/M6PR siRNA inhibits spindle cell and foci formation in KSHV-infected E-DMVEC. Representative phase-contrast microscopy comparing untreated samples to IGF-IIR/M6PR siRNA treated KSHV-infected E-DMVEC. Control siRNA treated samples were indistinguishable from untreated and are not represented here. IGF-IIR/M6PR siRNA reduced foci formation. Immunofluorescence analysis of Cye3-labeled siRNA-transfectants indicated a transfection efficiency of more than 95% (data not shown).

Supplemental Figure 1. Gene expression profiling of cathepsin genes in KSHV-infected and uninfected E-DMVEC.

Gene	Probe Set ID	Infection A	Infection B	Infection C	Infection D
cathepsin B	200838_at	NC	NC	NC	NC
cathepsin B	200839_s_at	NC	NC	NC	NC
cathepsin B	213274_s_at	NC	NC	NC	NC
cathepsin B	213275_x_at	NC	NC	NC	NC
cathepsin C	201487_at	NC	NC	NC	NC
cathepsin F	203657_s_at	NC	NC	NC	NC
cathepsin H	202295_s_at	NC	NC	NC	NC
cathepsin K	202450_s_at	NC	NC	NC	NC
cathepsin L	202087_s_at	NC	NC	NC	NC
cathepsin O	203758_at	NC	NC	NC	NC
cathepsin S*	202901_x_at	I	I	I	I
cathepsin S*	202902_s_at	I	I	I	I
cathepsin V	210074_at	NC	NC	NC	NC
cathepsin W	214450_at	A	A	A	A
cathepsin Z	210042_s_at	A	A	A	A
cathepsin Z	212562_s_at	A	A	A	A
cathepsin D	200766_at	NC	NC	NC	NC
cathepsin G	205653_at	A	A	A	A
cathepsin E	205927_s_at	NC	NC	NC	NC

Supplemental Figure 1. Gene expression profiling of cathepsin genes in KSHV-infected and uninfected E-DMVEC. (A) Affymetrix HG_U133A GeneChip data for cathepsins were obtained from four infected samples and compared to their respective controls. Significant changes with a p-value of $p > 0.01$ (ANOVA) are highlighted by “*”. Genes with multiple probe sets are reflected in the table; ‘NC’ indicates no change in gene expression, and ‘A’ scored absent on the microarray. Values given are absolute fold change; red indicates up-regulated expression changes.

Supplemental Figure 2. CTSB inhibitors are non-toxic and do not induce apoptosis.



Supplemental Figure 2. CTSB inhibitors are non-toxic and do not induce apoptosis.

(A) ATP cell viability assay. KSHV-infected E-DMVEC were left untreated or treated with 10 μ M CA-074, CA-074ME, or HNMPA-(AM₃) (100 μ M), after which cells were lysed and ATP was quantitatively determined using a luciferin bioluminescence assay. Neither CA-074 nor CA-074ME were toxic to the cells. (B) Annexin V-FITC apoptosis detection assay. Uninfected (panels 1-4) and KSHV-infected E-DMVEC (panels 5-8) were double-stained with propidium iodide and Annexin V-FITC showing no significant difference in apoptosis between untreated (panels 1 and 5) cells versus cells treated with 10 μ M CA-074 (panels 3 and 7) or CA-074ME (panels 4 and 8); Staurosporine was used as positive control (panels 2 and 6). Lower left quadrant represents healthy, lower right early apoptotic, and upper right late-apoptotic cells.

DISCUSSION

CTSB involvement in tumorigenesis has been recognized in a variety of human tumors (176, 185, 191, 210), but this is the first time that CTSB has been implicated in KS. Latent infection by KSHV transforms immortalized DMVEC in a characteristic way that is reminiscent of observations in KS tumors: formation of LANA-positive spindle cells, loss of contact inhibition, continued proliferation post-confluency, formation of disorganized foci, and the ability to grow in soft-agar. An essential function for CTSB in this transformation of E-DMVEC by KSHV was indicated by the finding that each of these steps was inhibited by the membrane permeable methyl ester-modified CA-074ME, but not by the non-permeable CA-074. Both versions of CA-074 are specific for CTSB *in vitro* (Figure 3b); however, the methyl ester modification reduces the specificity of CA-074ME for CTSB and also reacts with cathepsin L in tissue culture and *in vivo* (117). Treatment with siRNA specific for the cathepsins L, B, or S revealed that only the inhibition of CTSB expression prevented KSHV-mediated post-confluent growth. These data strongly suggest that the inhibition of CTSB activity, but not cathepsin L, was responsible for the effect of CA-074ME. Interestingly, others have shown that antisense treatment to CTSB efficiently inhibited tumor invasion and angiogenesis *in vitro* and in mice (96, 99).

In most tumors and tumor models, increased secretion of CTSB has been documented (27, 114, 176); however, CTSB retention has also been reported in some instances. It was found that intracellular active CTSB can also facilitate tumor invasion by acting intracellularly instead of being secreted (68, 185). In E-DMVEC latently infected with KSHV, we observed decreased secretion and an increased intracellular

retention of CTSB concomitant with an increase in intracellular protease activity. CTSB splicing, transcript levels, and protein levels were unchanged by KSHV, with two dominant splice products being present, both missing exon 2 and one also missing exon 3 (Figure 6b). The absence of exon 2 has previously been linked to a 15-fold increase in translational efficiency (5), whereas CTSB lacking the sequence encoded by both exons does not enter the secretory pathway, since its signal sequence is also missing (114). Probing for active CTSB revealed that the majority of CTSB activity is located in vesicles, suggesting that CTSB is able to enter the vesicular sorting system and is likely sorted to the endosomal/lysosomal compartment. This is also supported by the finding that cell-associated CTSB activity is depleted upon disrupting lysosomal trafficking with NH_4Cl . Therefore, E-DMVEC latently infected by KSHV display an increased diversion of CTSB from the exocytic route to the endo-lysosomal compartment.

Our data further suggest that increased endo-lysosomal targeting of CTSB resulted from increased retention by the IGF-IIR/M6PR which is transcriptionally induced by in KSHV-infected cells. IGF-IIR/M6PR is not associated with any known downstream signaling cascade because the receptor does not possess any signal transduction capacity. One of the functions of the IGF-IIR/M6PR is to regulate IGF-II levels (122, 163). Increased release of IGF-II due to a loss of IGF-IIR/M6PR function has been implicated in the promotion of tumor growth in a variety of cancers (62, 64, 107, 130, 205). In addition, the IGF-IIR/M6PR is known as the major cation-independent mannose 6-phosphate receptor in endocytosis and intracellular trafficking of mannose 6-phosphate-tagged proteins, including endo-lysosomal proteases (62). The increased release of active proteases due to decreased expression of the IGF-IIR/M6PR

can contribute to tumor invasion of surrounding tissues, as well as degradation of basement membrane proteins to allow cells to become metastatic. This has been observed in human breast carcinoma, where increased secretion of cathepsin D correlated with a reduction in IGF-IIR/M6PR expression (9, 64, 107).

In contrast to the IGF-IIR/M6PR downregulation observed in many cancers, we previously noted an upregulation of the IGF-IIR/M6PR in the context of a general KSHV-mediated dysregulation of the IGF system (155). We now demonstrate that this transcriptional increase of the IGF-IIR leads to increased retention of CTSB. This conclusion is supported by co-immunoprecipitation and by the finding that siRNA treatment against IGF-IIR/M6PR depleted the concentration of active CTSB in KSHV-infected E-DMVEC (Figure 7f). Furthermore, inhibition of IGF-IIR/M6PR expression by siRNA inhibited KSHV-mediated spindle cell and foci formation. Thus, intracellular retention of CTSB by IGF-IIR is essential for KSHV-mediated post-confluent growth.

What is the potential role of intracellular CTSB for the development of KS spindle cells? Lysosomal CTSB is released into the cytosol in the presence of extrinsic stimuli of apoptosis, particularly TNF and TNF-related ligands, and cytosolic CTSB can act as an effector protease of programmed cell death in tumor cells (14, 58, 102). CTSB has also been identified as an inhibitor of p53-dependent apoptosis in a genome-wide screen of p53 modulators (78); however, death receptor-mediated apoptosis is inhibited by the KSHV protein vFLIP, which is expressed during latency (56). Moreover, if CTSB were promoting apoptosis, we would expect that inhibiting CTSB would prevent apoptosis. Inhibiting CTSB activity did not change the level of apoptosis in KSHV-

infected cultures (Supplemental Figure 2b). Consequently, regulation of apoptosis is likely not to be involved in the observed function of CTSB in KS.

Another possible effect of CTSB inhibition could be an interference with growth-promoting signal transduction cascades. This includes the regulation of IGF-dependent signaling, as cathepsins have been implicated in the cleavage of IGF-binding proteins (163). Indeed, we observed that cathepsins cleave the KSHV-induced IGFBP-2 (our unpublished observations). Therefore, it is conceivable that CTSB is involved in the previously described regulation of the IGF system by KSHV (155). Alternatively, CTSB could be involved in the regulation of some of the other KSHV-induced pro-tumorigenic host cell or viral factors. For instance, CTSB controls processing and release of VEGF (211), which plays an important role in KS (81), and urokinase plasminogen activator (54, 87).

Finally, CTSB could be involved in regulating the activity of matrix-metalloproteases (87) or other proteolytic processes. Matrix-metallo- and cysteine proteases play an important role in tumor invasion and angiogenesis by degrading various components of extracellular matrix (98), and CTSB has been shown to activate matrix-metalloproteases (MMP) (87). CTSB activity is generally a tightly controlled process and deregulating CTSB during tumor growth may facilitate angiogenesis, invasion, or even loss of contact inhibition (79, 158, 175). Interestingly, MMP-1 and MMP-9 are induced in KSHV-infected E-DMVEC and have been shown to be essential for degrading various components of extracellular matrix (Ashlee Moses, unpublished observations). Moreover, a matrix-metallo-protease inhibitor is in clinical trials for KS (22).

An imbalance in protease activity has been described for a wide range of diseases, including rheumatoid arthritis, osteoarthritis, cancer, neurological disorders, osteoporosis, and lysosomal storage diseases (87, 88, 194). Not surprisingly 4 of the 11 characterized human cathepsins have been crystallized in an effort to aid structure-based drug design (193). Based on the data presented here, we suggest that CTSB would be a good target for treating KS.

ACKNOWLEDGEMENTS

The work reported in this manuscript was supported by grants 5R01-CA099906 and 5R01-CA94011-01 (AVM and KF, respectively). Matthew Bogyo was supported by grants R01-EB005011 and U54-RR020843. PPR was supported by the Molecular Hematology Training Grant T32 HL007781-13 and an award from the American Heart Association. Microarray assays (and/or data analysis) were performed in the (Affymetrix Microarray Core/Spotted Microarray Core/Bioinformatics and Biostatistics Core) of the OHSU Gene Microarray Shared Resource. We would also like to thank Aurelie Snyder of the OHSU-MMI Research Core Facility (<http://www.ohsu.edu/research/core>) for her help with microscopy and Dr. Bala Chandran for his kind gift of the LANA polyclonal antibody.

CHAPTER 4

Discussion

Profiling KSHV-driven cellular changes by microarray analysis.

The goal of this dissertation was to analyze the mechanisms of virus-driven tumorigenesis in KS. We wanted to identify cellular pathways that are hijacked by KSHV and characterize the function of these pathways during the latent phase of the viral life-cycle. To establish a profile of KSHV-induced cellular changes, we began with a comparison of age- and passage-matched long-term KSHV infected and uninfected E-DMVEC. This was accomplished by mapping the cellular transcriptome using microarray gene chip analysis.

E6/E7-immortalized endothelial cells (123), not unlike primary endothelial cells (23, 45), show dramatic morphological changes, usually referred to as a spindle-cell phenotype, upon infection with KSHV. This transformation is observed several weeks post-infection with KSHV. During this time, the virus establishes a restricted program of gene expression that encompasses both latent genes and a limited set of lytic genes (95). As a result of viral gene expression, the transcriptional program of the host cell is dramatically altered.

There are many changes in the cellular transcriptome that are directly related to the KSHV infecting endothelial cells. The cell also responds to foreign invasion, and as a consequence the cell changes the transcription profile of many genes to combat the invasion. IFN and TNF- α , for example, are immediate response mediators of the innate

host defense, which precedes the activation of the adaptive immune system to react to the viral infection. As part of the cellular defense mechanism, interferons activate signal-transducing activators of transcription (STATs), which leads to increased expression of many cellular proteins that contribute to the inhibition of viral replication. TNF- α induces pro-inflammatory cytokines via NF κ B (82). In order to discern which cellular changes were caused by the virus directly and which were in response to the viral infection, uninfected E-DMVEC were also treated either with IFN or TNF- α for 6, 12, and 24 hours in culture.

In the long-term KSHV infected cultures, at the time of harvesting RNA for microarray analysis, over 90% of the cell population was positive for the latent gene marker LANA-1 (124, 125). This indicated that the majority of cells were infected and in the latent phase of viral replication. About five percent of KSHV-infected cells will leave the latent phase and autoreactivate into the lytic phase at any given time (124). These lytic cells produce infectious progeny and expose the culture to viral and cellular cytokines. The small proportion of uninfected cells in this culture responds to both viral resistance factors (e. g. interferon) being secreted from latently infected cells, as well as viral and cellular cytokines released from cells destroyed in the lytic phase.

IFN and TNF- α treatments, although not comprehensive, represent an example of host cell-imposed anti-viral transcriptional changes. In Appendix I, table 2 lists genes commonly induced after IFN, TNF- α treatment, and KSHV infection. Some of the viral resistance factors represented in this table are MHC class I (antigen presentation), cathepsin S (responsible for MHC class II processing), toll-like receptor 3 (recognizes foreign exogenous mRNA), and caspase 1 (involved in programmed cell death). This

table does not represent every cellular pathway because not all cellular transcription needs to be induced 2-fold to cause significant changes; however, the changes listed in tables 1 and 2 helped in segregating the cellular response from virus-driven changes during KSHV infection.

The list of genes most likely changed due to direct involvement of viral proteins is extensive although still incomplete. The requirements for the lists created in Appendix I was very stringent. Genes had to be significantly changed ($p=0.01$) 2-fold or higher (\log_2) in all 4 replicate experiments in KSHV infected samples. As a consequence, many genes were excluded that could be equally as important. The reason for this approach was to diminish chances of identifying false positives among the true positive genes. The criteria furthermore created an opportunity to discover genes that were vital for Kaposi sarcoma development. It is not immediately clear what role many of the genes included in the tables have in KSHV tumorigenesis. It becomes difficult to determine how important changes in expression of one particular gene will be. It was, therefore, very interesting to learn that five members of the same signaling axis, the IGF system, were deregulated upon KSHV infection. It thus appeared very likely that this signaling axis played a significant role in KSHV-induced tumorigenesis, and we pursued studying individual members of the IGF system to assess how they were involved in mediating tumorigenesis.

Insulin-like Growth Factor Involvement in KS tumorigenesis.

IGF-I, IGF-II, and insulin expression were not detected by microarray in either uninfected or KSHV-infected endothelial cells. IGF-I and IGF-II mRNAs were barely

measurable by quantitative RT-PCR, while insulin mRNA was undetectable. In tissue culture, these three ligands are provided by human serum added to the culture medium. All three ligands are almost ubiquitously present throughout the body and circulate in the bloodstream. It is not surprising that insulin was not detected because insulin is almost exclusively produced in the pancreas. Therefore, it would be unusual to find insulin other than as provided in the reconstituted media.

KS tumors are highly vascularized, and it is conceivable that a similar exogenous stimulation by insulin or IGF-II present in the patient's blood takes place *in vivo*. Alternatively, tumor cells not infected with KSHV (i.e. KSIMM) or non-tumor cells might provide ligands in a paracrine fashion (75). Further studies in KS samples will be required to clarify this point. It is important to stress that the absence of an autocrine loop *in vitro* does not preclude a significant role for growth factor ligands in KS *in vivo*. Moreover, three of the six insulin-like growth factor binding proteins (IGFBP-1, IGFBP-2, and IGFBP-6) are deregulated by KSHV. Consequently, the ligand bioavailability and signal intensity could be managed by these IGFBP.

Potential Implications for Insulin-like Growth Factor Binding Proteins.

The vast majority of IGF ligands in circulation and in the extracellular fluid are complexed with IGFBP. All six IGFBP have a higher affinity for IGF ligands than their receptors. Therefore, IGFBP are able to prevent binding of IGF ligands to their receptors. Sequestering IGF ligands by IGFBP becomes the major mechanism of regulating IGF bioavailability. Conversely, IGFBP can also act as transporters of IGF-I and IGF-II ligands through the cell membrane, and thereby prolong IGF ligand

persistence in circulation to potentiate IGF effects. To balance the system, IGFBP are sensitive to proteolysis by cysteine proteases, thereby releasing bound IGF ligands (7, 42, 80, 152).

IGFBP-2 was consistently induced upon KSHV infection. Given the suspected role of IGFBP-2 in cancer development (69, 71, 74, 126), we examined if inhibiting IGFBP-2 expression by antisense molecules would interfere with KSHV-mediated transformation. Untreated E-DMVEC grew in disorganized foci characteristic of KSHV-transformation, while those treated with the IGFBP-2 siRNA or morpholino-antisense oligomers (PMO-AS) were inhibited in post-confluent growth and foci formation (Appendix II, Figure 1). The result suggests that IGFBP-2 is involved in the transformation of endothelial cells by KSHV. Even though there is no increase in IGF ligand expression, IGFBP-2 may be relevant in prolonging IGF ligand bioavailability.

Unexpectedly, Western blots using antibodies against IGFBP-2 did not show a strong induction of the protein. Instead, antibodies directed against the C-terminus, but not the N-terminus, revealed a smaller molecular-weight derivative of IGFBP-2 that appeared only in KSHV-infected cells (Appendix II, Figure 2a). The smaller product disappeared from KSHV-infected E-DMVEC when cells were treated with the cysteine protease inhibitor N-morpholinurea-leucine-homophenylalanine-vinylsulfone-phenyl (LHVS) (Appendix II, Figure 2b). LHVS inhibits cathepsins L, S, and B, and it appears that IGFBP-2 is cleaved by one of these cysteine proteases in KSHV-infected cultures.

This result complicates understanding what role IGFBP-2 has in KSHV-mediated tumorigenesis because early proteolytic cleavage would limit IGFBP-2 from being able to regulate IGF bioavailability. While IGFBP-2 fragments are still capable of binding

IGF ligands but with a much lower affinity, proteolysis of IGFBP-2 could alternatively increase the signal potential of the insulin receptor with more free IGF-II available to stimulate tumor growth (42, 71, 72). Interestingly, control of ligand persistence has not been the only role described for IGFBP-2. It is possible that an IGF-independent role may be more essential in the context of KSHV-mediated tumorigenesis (13, 70, 73). IGFBP-2 contains an integrin binding motif in its carboxyl terminus, and studies have suggested an IGF-independent interaction with integrins may regulate migration and proliferation (141, 164). Instead of IGF-II regulation, IGF-independent effects of IGFBP-2 seem to be more relevant in our system.

Both IGFBP-1 and IGFBP-6 gene expression were significantly repressed in KSHV-infected E-DMVEC. IGFBP-6 strongly binds to IGF-II and removes IGF-II from the circulation (203). It was found that adding exogenous IGFBP-6 also inhibited spindle cell and foci formation (unpublished observations by Ashlee Moses). Similar to IGFBP-6, IGFBP-1 removes IGF-I from circulation because it has a higher affinity for IGF-I (203). To date, the importance of IGFBP-1 in KS has not been further investigated. Downregulating IGFBP-1 and IGFBP-6 may be required to increase the IGF ligand signaling capacity without increasing ligand expression.

The insulin receptor is required in KS Tumorigenesis.

Analysis of the IGF system revealed that the insulin receptor is essential for KSHV-mediated post-confluent and contact-independent growth of immortalized DMVEC *in vitro*. Inhibition of IR expression with siRNA or inhibiting IR signaling with the small-molecule inhibitor HNMPA-(AM₃) prevented the post-confluent proliferation

of KSHV-infected cells and foci formation. In contrast, treatments of siRNA or blocking antibodies targeting the IGF-IR had no effect on *in vitro* tumorigenesis of E-DMVEC. This is important because the insulin receptor and IGF-IR are able to heterodimerize to form hybrid receptors. These hybrid receptors have altered affinities for insulin and IGF-II ligands, which changes the signaling capacity of these tyrosine-kinase receptors (29, 128). Our finding is different from a report that demonstrated that autocrine stimulation of the IGF-IR by IGF-I was essential for growth and survival of the KS-derived cell line KSIMM (17). Although originally derived from KS tumors, KSIMM are negative for KSHV (2, 43, 108, 148, 173). The contribution of KSIMM cells to KSHV-transformed endothelial cell development remains unclear. It is possible that paracrine stimulation via the IR contributes to the contact-independent growth of KSHV-infected endothelial cells, whereas autocrine stimulation via IGF-I/IGF-IR is required for the continued growth of undifferentiated uninfected endothelial cells (75).

Expression of both IGF-IR and IR has been demonstrated in KS tissue. Overexpression of the IR in KS tissue compared to normal skin was previously reported by Wang et al. in a comprehensive microarray study (204). We have independently shown that IR gene expression is induced in KSHV-infected primary endothelial cells, AIDS-KS tissue, as well as in telomerase-immortalized endothelial cells. Our attempts to stain for IR in AIDS-KS tissue by immunohistochemistry were unsuccessful. IGF-IR was detected by immunohistochemistry in KS spindle cells (17), which is in agreement with our data that IGF-IR was clearly expressed in both uninfected and infected endothelial cells. Phosphorylation of IGF-IR was not detected *in vitro*, and it is not known if IGF-IR is stimulated *in vivo*.

KSHV target cells can be separated into lymphatic or blood endothelial cells prior to infection by KSHV. Upon virus infection, the distinct expression pattern delineating lymphatic or blood endothelial cells changes and results in a transcriptional phenotype characterized by the prominent expression of lymphatic transcripts (76, 204). A comparison of transcriptional profiles between lymphatic and blood endothelial cells revealed that each cell type expressed IGF-IR equally. Meanwhile, the IR was highly expressed in blood endothelial cells but not in lymphatic endothelial cells (145). Therefore, it seems that induction of IR is not part of the lymphatic reprogramming of KSHV-infected endothelial cells.

The IR is known to be involved in tumorigenesis, particularly the isoform missing exon 11 (IR-A) (29, 135). Splicing of the insulin receptor presumably alters the affinity of the receptor for its ligand. The two isoforms of IR have distinct functions (28, 29). IR-A is expressed predominantly in fetal tissues and is responsible for cell proliferation, while IR-B is prominently expressed in differentiated adult liver and insulin-responsive tissues to manage cell metabolism (77, 135). A preferential expression of the IR-A isoform has been shown in several types of cancers, including lung, colon, breast, ovarian, and thyroid cancer (29, 49, 89, 91, 166, 167, 197). While both isoforms have a high affinity for insulin, IR-A also has a high affinity for IGF-II, which is able to activate predominantly mitogenic rather than typical metabolic signaling pathways (28, 29).

In KSHV-infected E-DMVEC, IR-A is the more prominent isoform. Not only is the IR highly induced in KSHV-infected E-DMVEC but is also phosphorylated, possibly activating downstream signaling cascades. Phosphorylation of IR-A via insulin activates glycogen synthesis. Glucose regulation occurs through the PI3 kinase pathway and

subsequent downstream phosphorylation of PKB/Akt, followed by phosphorylation of GSK3 and, finally, activation of glycogen synthase. When insulin binds IR-A, a positive-feedback loop is furthermore activated to increase insulin and IR-A expression via the transcription activator p70. IGF-II can also signal via IR-A to activate PI3 kinase and downstream PKB/Akt. In cells non-responsive to insulin, i.e. fetal or tumorigenic cells, the IGF-II activated signal cascade diverges at the point of PKB/Akt activation from insulin stimulation (29, 49). Instead, Akt phosphorylation leads to transcriptional activation of factors promoting cell migration, proliferation, and protection from apoptosis. Alternatively, IGF-II may also lead to phosphorylation of Grb2 via IR-A, which subsequently activates Sos and the downstream mitogen-activated protein kinase (MAPK) cascade. The latter pathway has been suggested to be necessary for expressing genes involved in protection from apoptosis, such as acidic nuclear phosphoprotein 32, as well as genes involved in angiogenesis, such as Mrp/prl and proliferin (29, 201).

Our studies suggest there is increased activation of the downstream MAPK pathway, but not the PI3K pathway, in KSHV-infected endothelial cells. The MAPK pathway is a target of KSHV during *de novo* infection to modulate initial cellular and viral gene expression (169). We can rule out direct KSHV involvement because our analysis of the two IR-activated pathways was performed 4 weeks into the latent phase of the infection. Meanwhile, KSHV activates both MAPK and PI3K pathways immediately after infection. In addition, by inhibiting IR phosphorylation with the small molecule inhibitor HNMPA-(AM₃), we inhibit Erk phosphorylation. PI3K is also activated early in KSHV infection (169), while at the latent stage we did not see PI3K activation. Since

there was no change in Akt phosphorylation in KSHV infected E-DMVEC, activation of the PI3K pathway via IR can be ruled out.

Both insulin and IGF-II are present in the culture media added to E-DMVEC, suggesting that either ligand could be responsible for activating IR. Concomitant with a higher level of IR-A, observations suggesting that the IGF-II binding protein IGFBP-6 inhibits KSHV-mediated DMVEC transformation (Ashlee Moses, unpublished observations) would favor IGF-II as the predominant ligand in this system. Yet, preliminary data suggests that in fact insulin may be responsible for activating the insulin receptor because adding IGF-II to starved cells did not activate MAPK (Appendix IV, Figure 1).

Although we can show a link between IR induction and downstream MAPK activation but not Akt, Akt or MAPK phosphorylation via other tyrosine kinase receptors is also possible. In KSHV-infected spindle cells, at least two other tyrosine kinase receptors, c-Kit (125) and IGF-IR (17), have been implicated in KSHV-mediated tumorigenesis. Many tyrosine kinase receptors overlap in their ability to activate both MAPK and Akt signaling cascades. In the case of the insulin receptor, uninfected endothelial cells do not generally express the IR-A isoform. Consequently the insulin receptor may argue a function when contributing to tumorigenesis in endothelial cells that is normally reserved for fetal development. Here, the IR isoform IR-A responds to ligands in adult differentiated endothelial cells forcing aberrant gene transcription to promote tumor growth. It is likely that other tyrosine kinase receptors function similarly, in cells where they are not normally expressed or overcompensate due to overexpression. While many members of the cytokine receptor superfamily can activate the same

downstream signaling cascades, these receptors may activate separate pathways in KS. In this fashion, each receptor becomes functionally important in activating a specific pathway to drive tumorigenesis, yet individually they are not sufficient to cause tumor growth (discussed later). This hypothesis does not exclude redundancy among signaling pathways.

The IGF-independent function of the IGF-II receptor in KS.

The IGF-IIR is an exception to the list of IGF members deregulated by KSHV because initially the receptor did not pass the stringent test of microarray analysis. In fact, the two different probe sets representing IGF-IIR were only induced in two out of the four KSHV infected samples consistently. Nevertheless, both quantitative RT-PCR and Western blot documented that both gene and protein expression were consistently induced during KSHV infection. The induction was not as dramatic as that of the insulin receptor *in vitro*; however, quantitative RT-PCR of KS tissue later revealed that IGF-IIR expression was induced to the same extent as the IR *in vivo*.

IGF-IIR is not associated with any known downstream signaling cascade because the receptor does not possess any signal transduction capacity. Instead, the IGF-IIR is thought to regulate IGF-II levels by acting as a clearance receptor for IGF-II. Binding of IGF-II inevitably results in internalizing and consequent degradation of the ligand (122, 163). Relevant to IGF-IIR involvement in regulating IGF-II concentrations, studies have shown that IGF-IIR is important for tumor suppression by acting as a growth inhibitor (62, 130). A loss of IGF-IIR function has been documented in a variety of cancers supporting the suggested role of a tumor suppressor (64). It was, therefore, unexpected to

find that IGF-IIR expression was induced in KSHV-infected E-DMVEC. To date there have been no other reports indicating that an overexpression of IGF-IIR facilitates tumorigenesis. The induction of IGF-IIR adds to the trend of other IGF members' apparent IGF-independent functions, which may be more relevant in KSHV-driven tumorigenesis.

The IGF-IIR is also known as a cation-independent mannose 6-phosphate receptor (M6PR). Located mainly in the Golgi, but also present in the plasma membrane, this receptor plays a vital role in endocytosis and intracellular trafficking of mannose 6-phosphate-tagged proteins, such as lysosomal enzymes. Similar to the IGF-IIR acting as a tumor suppressor in regulating growth via IGF-II internalization, a loss of M6PR function has been proposed to lead to the release of cysteine proteases into the extracellular space (107, 205). The release of active proteases can contribute to tumor invasion of surrounding tissues, as well as degradation of basement membrane proteins to allow cells to become metastatic. This has been shown for cathepsin D, an aspartyl protease, whose increase in secretion correlated with a reduction in M6PR expression and subsequently led to increased tumor invasiveness in human breast carcinoma (9, 64, 107).

Our studies suggest that instead of secreted cathepsins assisting in tissue invasion of the tumor, IGF-IIR/M6PR retains CTSB activity by increasing endo-lysosomal targeting of this cysteine protease.

Retaining CTSB requires IGF-IIR/M6PR receptor overexpression.

Cysteine proteases are essential for tumor growth, invasion, migration and metastasis (20, 87, 88, 93, 194). The highly vascular and invasive nature of tumors

requires extensive degradation and remodeling of the extracellular matrix for which cysteine proteases can be responsible. To date, the only assessment of cysteine proteases in KS involved immunohistochemistry of skin biopsies. Thewes et al. performed immunohistochemical analysis on several KS tissue biopsies, but they did not detect any CTSB or cathepsin L (189). Therefore, the *in vivo* relevance of the *in vitro* discoveries implicating CTSB in Kaposi sarcoma still requires confirmation. Based on our data, it could be that CTSB protein expression *in vivo* is below detection limits, and a better approach would be to screen for an increase in activity using activity based probes.

The significance of CTSB has been documented in a variety of human tumors (176, 185, 191, 210). In some instances, the increase in CTSB expression or activity has been suggested as a tumor marker for disease progression (27, 181, 182). The role of cysteine proteases in KS was established by visually assessing whether KSHV-infected E-DMVEC would be able to form spindle cells and foci during constant treatment with the selective inhibitor LHVS. Since the cysteine protease inhibitor LHVS successfully reduced spindle cell and foci formation, the list of candidate cysteine proteases was immediately reduced to cathepsins L, B, and S. The existing microarray data was analyzed for changes in cathepsin L, B, and S gene expression patterns. The arrays showed there was no increase in gene expression by microarray. Concomitant with gene expression patterns, there was no change in protein expression measured by Western blot for cathepsins B or L. Two probe sets representing cathepsin S were induced; however, cathepsin S was induced in KSHV-infected samples as well as IFN and TNF- α -treated samples as previously indicated.

Cathepsin S is involved in processing the associated invariant chain of MHC class II (193). Cathepsin S is interferon- γ inducible (154), and it is most likely that the induction of cathepsin S is an innate immune response to KSHV infection of endothelial cells. As cathepsin S is involved in anti-viral activity, the microarray data predicted this protease is would not be required for KSHV-induced tumorigenesis. Despite increased expression of cathepsin S, similar to cathepsin L siRNA treatment, siRNA targeting of cathepsin S had no effect on inhibition of KSHV-induced tumorigenesis. Instead, siRNA designed against CTSB efficiently reduced CTSB protein expression (Appendix III, Figure 2) and was able to inhibit spindle cell and foci formation.

CTSB has been documented to be essential for lysosomal protein turnover; however, intracellular relocalization and even secretion of CTSB can occur. By changing the localization of CTSB, the protease can become directly involved in degrading the extracellular matrix, if secreted. Alternatively, intracellular relocalization of CTSB could activate other proteolysis pathways required for tumor invasion, such as matrix-metallo proteases (81, 88, 175). Cytosolic CTSB was previously shown to act as an execution protease of programmed cell death in tumor cells upon extrinsic stimuli, particularly by TNF and TNF-related ligands (14, 58, 102). CTSB has also been identified as an inhibitor of p53-dependent gene transcription and associated p53-dependent apoptosis in a genome-wide screen of p53 modulators (78). The pro-apoptotic function of CTSB is thought to involve its release from the lysosomes into the cytosol upon lysosomal breakdown during apoptosis. KSHV-infected E-DMVEC are already insensitive to programmed cell death, and any pro-apoptotic effect of CTSB can be excluded because inhibiting CTSB activity did not increase live cell populations in an Annexin-

V/propidium iodide stain. In addition, staining live cells with the activity-based probe, GB-111 FL, and cell compartment trackers for the endoplasmic reticulum, mitochondria, and lysosomes, identified endosomal/lysosomal compartments as the site of concentrated CTSB activity (Appendix III, Figure 1). This conclusively ruled out that CTSB is not cytosolic, where it could act as a pro-apoptotic factor.

To further characterize the role of CTSB in KS, we employed two versions of the activity-based CTSB inhibitor CA-074, a non-membrane permeable version and CA-074ME, a membrane-permeable methyl ester modified proinhibitor of CA-074. Both inhibitors can successfully inhibit CTSB activity *in vitro*; however, the methyl ester derivative loses specificity because of the membrane-permeable modification. Once CA-074ME crosses the membrane, it becomes less selective for CTSB and has also been shown to inhibit cathepsin L in murine fibroblasts (117). While the promiscuity of CA-074ME raises some concern, the siRNA experiments clearly excluded cathepsin L involvement in KSHV-induced tumorigenesis. Consequently, further discoveries made with these two inhibitors would highly suggest involvement of CTSB in KS rather than cathepsin L.

After treating KSHV-infected E-DMVEC for 14 days with the two inhibitors, only CA-074ME inhibited spindle cell and foci formation. The result added to the argument that intracellular CTSB was required in spindle-cell and foci formation and not secreted CTSB. Continuous treatment with CA-074ME, but not CA-074, also reduced the number of LANA-1 positive cells suggesting that inhibiting CTSB activity may impair KSHV-infected E-DMVEC propagation or stimulate a loss of the viral genome. LANA-1 tethers the viral genome of KSHV to the cellular chromosome and therefore

LANA-1 is a good indicator of KSHV-infected E-DMVEC. Any cytotoxic effect of the CTSB inhibitors could be ruled out with an ATP-cell viability assay and an Annexin-V/propidium iodide stain for apoptosis. It could be that the cathepsin inhibitors are in fact repressing KSHV-induced tumorigenesis, and the culture loses virus-positive cells.

To elucidate the mechanism by which CTSB inhibitors affect KSHV-induced tumorigenesis, proliferation and soft agar assays were employed. The inhibitors did not negate any growth advantage of KSHV-infected E-DMVEC over uninfected E-DMVEC as neither of the CTSB inhibitors had any effect on cell growth pre-confluency. Instead, the methyl ester version of CA-074, CA-074ME, restricted post-confluent growth inhibiting the ability of KSHV-infected E-DMVEC to form foci. This was also determined by the ability of CA-074ME to inhibit growth of KSHV-infected E-DMVEC in soft agar. The results suggest that any advantage in post-confluent growth and loss of contact inhibition is neutralized in the presence of the inhibitors. It could still potentially be that CTSB activity is essential for later stages of tumor development, i.e. contact-independent growth and invasion.

A closer look at the distribution of CTSB activity in KSHV-infected E-DMVEC versus uninfected revealed that the majority of enzyme activity is retained intracellularly in KSHV-infected E-DMVEC. This convincingly ruled out that CTSB is directly involved in degradation of the extracellular matrix. In contrast uninfected E-DMVEC secrete the majority of active CTSB, while very little is retained intracellularly. This was also established visually by comparing live cell staining of uninfected and KSHV-infected E-DMVEC with the activity-based probe, GB-111 FL. There was an increased

number of organized vesicles tightly packed into KSHV-infected E-DMVEC compared to uninfected, where smaller vesicles appeared spread throughout the cell.

The change in active CTSB distribution appears to be the major difference during tumor development as neither gene transcript nor protein expression changed upon KSHV-infection. This would suggest that the viral infection or KSHV-induced tumorigenesis changes processing or trafficking of CTSB. In other tumors, alternative splicing events cause a change in the distribution of CTSB mRNA species (5, 8, 114, 210). When we examined the CTSB mRNA species, we found no difference in KSHV-infected versus uninfected E-DMVEC. Two dominant species of alternatively spliced products were found, missing either exon 2 or exons 2 and 3, while full-length CTSB mRNA was absent. It has been shown that when exon 2 is absent from the CTSB transcript the translational efficiency increased up to 15-fold (5). When the CTSB mRNA lacks both exons 2 and 3, the mRNA lacks the signal peptide and is improperly trafficked (114). In the absence of the full-length transcript, CTSB was still targeted to the endo-lysosomal compartment (Appendix III, Figure 2). Although we found no difference between uninfected and KSHV-infected E-DMVEC, these truncated species may predispose E-DMVEC to become tumorigenic, once a stimuli such as KSHV has been introduced to induce tumorigenesis.

A possible mechanism of endo-lysosomal targeting has been suggested by the previously described upregulation of IGF-IIR/M6PR in KSHV-infected cells (155). This would explain why IGF-IIR/M6PR has no apparent IGF-dependent function in KSHV-driven tumorigenesis because IGF-IIR/M6PR is predominantly required to retain CTSB in endo-lysosomal compartments. Other groups have shown that CTSB interacts

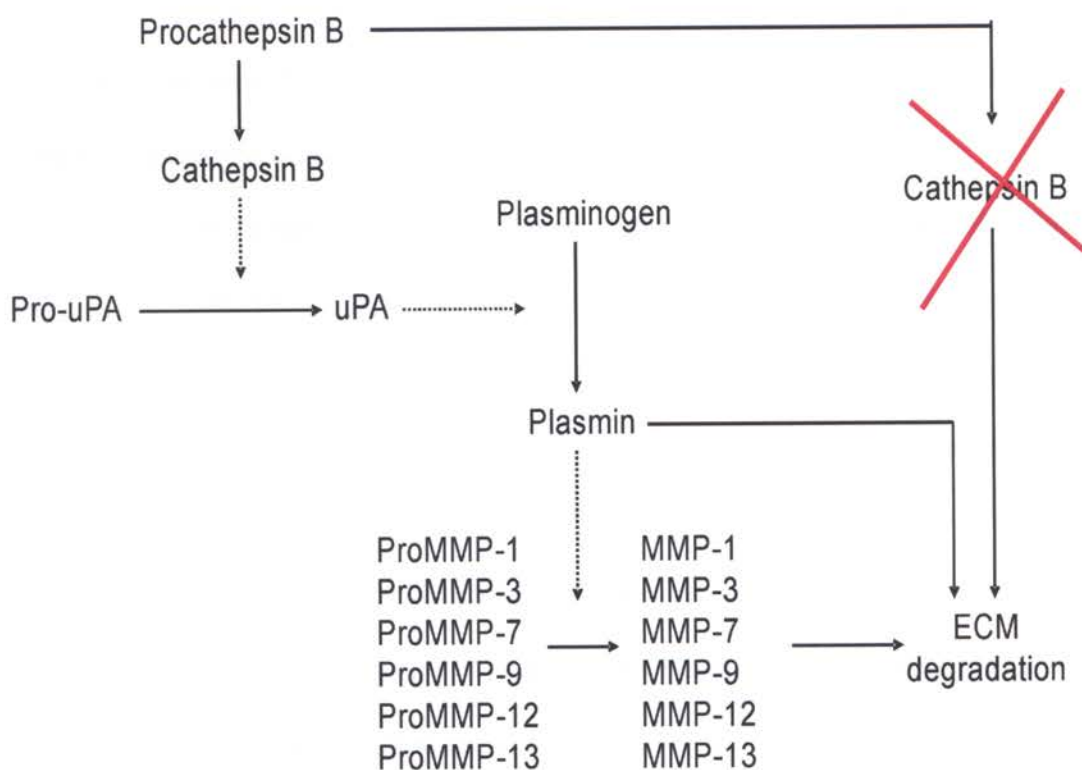
with IGF-IIR/M6PR (158), and in E-DMVEC immunoprecipitation of IGF-IIR/M6PR coprecipitated CTSB relative to IGF-IIR expression levels. Furthermore siRNA treatment of IGF-IIR/M6PR depleted the concentration of active CTSB intracellularly in KSHV-infected E-DMVEC. CTSB activity could be depleted as well by disrupting lysosomal trafficking with NH_4Cl . This suggested that CTSB was concentrated in lysosomal compartments and IGF-IIR/M6PR was responsible for trafficking CTSB to the lysosomes. It has been reported elsewhere that treatment with NH_4Cl increases secretion of CTSB, as the lysosomes are unable to form (60). There was no change in secretion of CTSB after NH_4Cl , while intracellular levels decreased. Instead the levels of secretion remained steady despite the treatment.

Independently, IGF-IIR/M6PR siRNA was also able to inhibit spindle cell and foci formation. It has been reported that IGF-IIR/M6PR has tumor-suppressor functions (64), so reducing the protein expression of IGF-IIR/M6PR could have potentially led to increased spindle cell and foci formation. This was not the case. Aside from the growth-suppressor function in the IGF-dependent system, loss in IGF-IIR/M6PR expression can lead to increased secretion of protease activity and a concomitant increase in tumor invasion (9, 62, 64, 130, 202). Clearly, this apparent contradiction to other studies of IGF-IIR/M6PR requires more attention in order to decipher the actual and potentially as of yet novel involvement of IGF-IIR/M6PR in tumorigenesis.

Taken together, the data shows that CTSB plays an essential role intracellularly during KSHV-mediated tumorigenesis. Based on the functional assays looking at different stages of tumor growth, it appears that CTSB is still involved in tumor invasion. CTSB in KSHV-infected E-DMVEC is taking on a central role in regulating the secretion

of other important proteins, e.g. VEGF, or activating other proteolytic pathways, e.g. matrix-metallo-proteases (MMP), during KSHV-induced tumorigenesis. Other groups have previously documented that intracellular active CTSB can facilitate tumor invasion by acting on such proteins (68, 185). We have observed that there are no changes in weight or ionic charge of cytoplasmic proteins by 2-dimensional electrophoreses of crude cytoplasmic preparations from KSHV-infected E-DMVEC treated with the CTSB inhibitors and compared to untreated samples (personal observation). Consequently, CTSB activity is not involved in changing the intracellular environment.

Instead, in KS MMP-1, -2 and -9 have been shown to be involved in tumor invasion [(22, 41) and unpublished observations by Shane McAllister and Ashlee Moses]. CTSB acts upstream of MMP to regulate their activity, so it is very likely



[taken from Yan et al. (210)]

Figure 5. CTSB contributing to extracellular matrix degradation. Flowchart depicting pathways of how CTSB may facilitate tumor invasion. CTSB may directly be secreted and degrade various components of extracellular matrix e.g. collagen, laminin, and fibronectin. Alternatively, CTSB may regulate matrix-metalloprotease activity by processing upstream stimulators of the MMP proteolytic pathway.

that this is how increased CTSB activity is involved in KS (Figure 5). Active CTSB will activate MMP via urokinase plasminogen activator and plasmin. MMP are then secreted to degrade the extracellular matrix, thereby making CTSB indirectly responsible for tumor invasion. This would explain why inhibiting intracellular CTSB activity will prevent post-confluent foci formation and colony growth in soft agar, which are two mechanisms involved in tumor invasion.

Cysteine proteases are widely expressed and involved in a multitude of molecular functions. An imbalance in protease activity has been described for a wide range of diseases, including rheumatoid arthritis, osteoarthritis, cancer, neurological disorders, osteoporosis, and lysosomal storage diseases (87, 88, 191, 193-195). Not surprisingly, 4 of the 11 characterized human cathepsins have been crystallized by pharmaceutical companies, as their implications in various diseases make them excellent drug targets (193). While the downstream targets of CTSB activity still require further study, CTSB involvement in KS makes it a good target for future anti-cancer therapies.

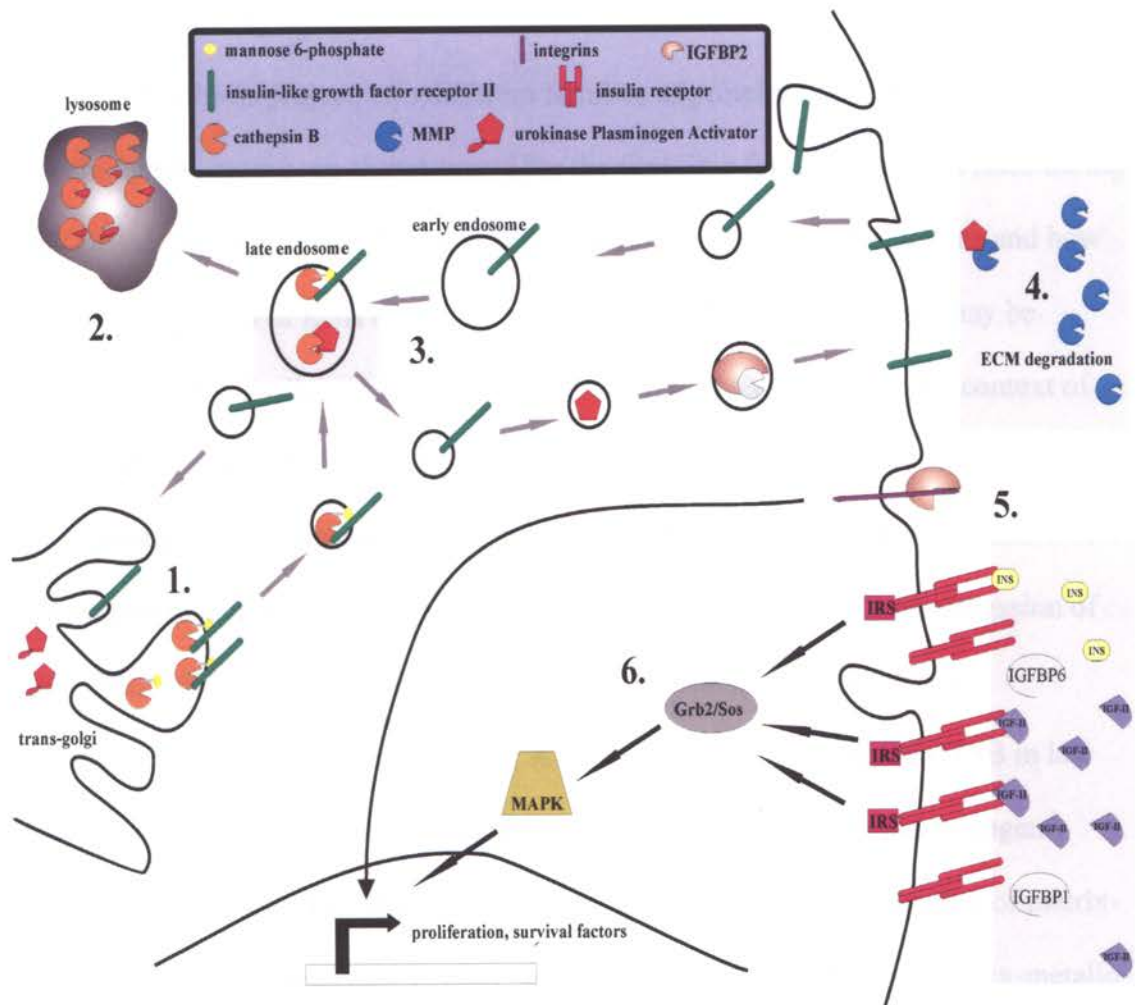


Figure 6. Model of IGF Family and CTSB involvement in KSHV-induced

tumorigenesis. A cartoon summarizing the function of all proteins revealed in this dissertation to progress tumorigenesis in KSHV-infected E-DMVEC. Areas shaded in gray illustrate additional proteins that are well documented in the literature, but are hypothetical in the context of their involvement with these described oncogenes during KSHV-driven tumorigenesis. The numbers highlight events that are essential for tumorigenesis (see text for details).

Summary and Conclusions.

For this thesis project, two different families of proteins, the IGF family and the cathepsin family, have been characterized for the first time for their essential roles during KSHV-driven tumorigenesis. Figure 6 depicts a model of all described events and how they may be involved in KSHV-driven tumorigenesis. While each protein may be necessary but individually not appear to be sufficient to cause cancer, in the context of tumor growth these proteins play essential roles.

Through a serendipitous event the interaction between IGF-IIR/M6PR and CTSB has proven to be indispensable in KSHV-driven tumorigenesis (1.). Overexpression of the IGF-IIR/M6PR leads to an increase in CTSB accumulation within the late endosomal/lysosomal compartments (2.). A high concentration of active CTSB in late endosomal/lysosomal compartments causes more activated urokinase plasminogen activator to be released (3.). This ultimately can cause downstream activation of matrix-metallo-proteases. To resolve a possible relationship between CTSB and matrix-metallo-proteases, siRNA treatment against either protein could be employed with subsequent measurement of matrix-metallo-protease activity. CTSB thus becomes indirectly involved in degrading the extracellular matrix (ECM) for tumor invasion (4.). Alternatively CTSB may be involved in hypoxia/angiogenesis stimulation by regulating the release of VEGF, which can be tested by measuring the release of VEGF from KSHV infected cells with or without CTSB siRNA treatment. Finally, newly established techniques such as isotope labeling strategies (ICAT or iTRAQ), may provide alternative means of discovering still unknown CTSB substrates.

Meanwhile, the processing of IGFBP-2 by cathepsins L, S or B enables the IGF-independent interaction between IGFBP-2 and integrins to stimulate cell growth and survival. Independently, the absence of IGFBP-1 and -6 increases the signaling potential of IGF-II via the insulin receptor. Although the data favor that IGF-II signals through the insulin receptor, some preliminary data suggests this may instead occur via insulin (Appendix IV, Figure 1) (5.). Further study will be required to clarify this discrepancy. What is more, the relevance of either IR isoform will need to be resolved by expressing each isoform individually in retroviral constructs and measuring cellular properties upon constant IR isoform expression. An alternative to increased signaling capacity to activate downstream signaling cascades may be prolonged signaling of IR. For human and bovine papilloma virus, the E5 gene has been documented to amplify the signaling capacity of PDGFR (BPV) or EGFR (HPV) by delaying endosomal acidification, for example (44). Irrespective of the stimulating ligand, the insulin receptor phosphorylates mitogen-activated protein kinases, which leads to transcriptional activation of pro-survival and growth factors. MAPK transcriptional activation may occur through the AP-1 activator complex, which may target the oncogene secreted protein acidic and rich in cysteine glycoprotein (SPARC), SSecks (cell cycle control) or heparin binding-EGF-like growth factor (6.). These potential targets will need to be resolved using reporter construct assays. The activities of IGFBP-2 and IR thus appear to contribute to contact-independent foci formation in KSHV-infected E-DMVEC.

What has not been addressed in these studies is what causes these proteins to deviate from their normal function. Based on the design of the microarray analysis, KSHV proteins should be implicated in causing these events. I would hesitate to make

that prediction. Microarray gene expression profiling using various combinations of adenovirus vectors that contained the latent genes, LANA-1, vFLIP, vCyc, did not show an induction of any of the proteins described here (unpublished observations of microarray analysis done for Ashlee Moses). This approach has some limitations because adenovirus vectors only transiently express the proteins over a matter of days, while events of KSHV-driven tumorigenesis occurred after weeks of infection. Second, adenovirus vectors overexpress the viral protein beyond physiological conditions, which alone may cause a different outcome. Still, the data provided by this experimental approach may provide useful for other genes induced in KSHV-driven tumorigenesis. An alternative technique would be to employ retroviral vectors for consistent and long-term expression of KSHV latency genes; however, this approach similarly may not be very successful at recreating the proper tumor environment. A better method will be to use a KSHV knock-out virus, which has not been successfully established to date. The latency genes can then be studied in the proper context and potential involvement of other as yet unidentified viral genes needed for tumorigenesis may be a result of this approach. Several labs, including the Moses lab, are working on creating a reliable knock-out virus to do such studies.

KSHV latency genes are also less likely to be responsible for deregulating these oncogenes, e.g. the insulin receptor and CTSB, because in many other tumors these cellular oncogenes have been proposed as progression and prognosis markers in later stages of cancer (27, 49, 181, 182). This means that KSHV latency genes may not be directly responsible for inducing these oncogenes during initiation of tumor development. The KSHV latency genes may be the initiator of many changes early after infection that

results in these oncogenes being activated later for tumor growth and progression. This would explain why the insulin receptor is not significantly induced as early as for hours and as late as 4 days post-infection when latency has fully established itself (155).

Tumorigenesis is a complex orchestration of events, and each event requires many different molecules to facilitate a successful execution. Therefore, multiple molecules involved in tumorigenesis that seem to be essential are not always sufficient to cause cancer. The complexity of tumorigenesis is best illustrated by the fact that three different tyrosine kinase receptors, c-Kit, IGF-IR, and IR, with overlapping downstream signal transduction cascades are essential for KSHV-driven tumorigenesis. The distinct function of each receptor may evolve from the receptor being overexpressed in non-traditional tissues during tumor formation. This theory is further supported by the example of neuritin, which is a growth-promoting protein known to normally mediate neurite outgrowth. Raggo et al. have found that neuritin is highly induced in KSHV-infected endothelial cells, which can also cause tumors when neuritin overexpressing cells are implanted into immunodeficient mice (150).

The studies of the IGF system and CTSB in this dissertation by no means identify the one event required to understand tumorigenesis. Although some of the functions for these oncogenes are described here for the first time, they allow us to better appreciate the dynamic mechanisms of KS. The hope is these results will encourage further investigation into these families of proteins in the context of KS and contribute to a new line of anti-cancer therapies, which may also be potentially beneficial to other types of cancer as well.

RERFERENCES

1. **Adams, J.** 2004. The development of proteasome inhibitors as anticancer drugs. *Cancer Cell* **5**:417-21.
2. **Albini, A., I. Paglieri, G. Orengo, S. Carlone, M. G. Aluigi, R. DeMarchi, C. Matteucci, A. Mantovani, F. Carozzi, S. Donini, and R. Benelli.** 1997. The beta-core fragment of human chorionic gonadotrophin inhibits growth of Kaposi's sarcoma-derived cells and a new immortalized Kaposi's sarcoma cell line. *Aids* **11**:713-21.
3. **An, F.-Q., H. M. Folarin, N. Compitello, J. Roth, S. L. Gerson, K. R. McCrae, F. D. Fakhari, D. P. Dittmer, and R. Renne.** 2006. Long-Term-Infected Telomerase-Immortalized Endothelial Cells: a Model for Kaposi's Sarcoma-Associated Herpesvirus Latency In Vitro and In Vivo. *J. Virol.* **80**:4833-4846.
4. **Badinga, L., S. Song, R. C. Simmen, J. B. Clarke, D. R. Clemmons, and F. A. Simmen.** 1999. Complex mediation of uterine endometrial epithelial cell growth by insulin-like growth factor-II (IGF-II) and IGF-binding protein-2. *J Mol Endocrinol* **23**:277-85.
5. **Baici, A., K. Muntener, A. Willimann, and R. Zwicky.** 2006. Regulation of human cathepsin B by alternative mRNA splicing: homeostasis, fatal errors and cell death. *Biol Chem* **387**:1017-21.
6. **Baltensperger, K., R. E. Lewis, C. W. Woon, P. Vissavajhala, A. H. Ross, and M. P. Czech.** 1992. Catalysis of serine and tyrosine autophosphorylation by the human insulin receptor. *Proc Natl Acad Sci U S A* **89**:7885-9.

7. **Baxter, R. C.** 2000. Insulin-like growth factor (IGF)-binding proteins: interactions with IGFs and intrinsic bioactivities. *Am J Physiol Endocrinol Metab* **278**:E967-76.
8. **Berquin, I. M., L. Cao, D. Fong, and B. F. Sloane.** 1995. Identification of two new exons and multiple transcription start points in the 5'-untranslated region of the human cathepsin-B-encoding gene. *Gene* **159**:143-9.
9. **Berthe, M. L., M. Esslimani Sahla, P. Roger, M. Gleizes, G. J. Lemamy, J. P. Brouillet, and H. Rochefort.** 2003. Mannose-6-phosphate/insulin-like growth factor-II receptor expression levels during the progression from normal human mammary tissue to invasive breast carcinomas. *Eur J Cancer* **39**:635-42.
10. **Boshoff, C., and Y. Chang.** 2001. Kaposi's sarcoma-associated herpesvirus: a new DNA tumor virus. *Annu Rev Med* **52**:453-70.
11. **Boshoff, C., T. F. Schulz, M. M. Kennedy, A. K. Graham, C. Fisher, A. Thomas, J. O. McGee, R. A. Weiss, and J. J. O'Leary.** 1995. Kaposi's sarcoma-associated herpesvirus infects endothelial and spindle cells. *Nat Med* **1**:1274-8.
12. **Braulke, T., M. Claussen, P. Saftig, M. Wendland, K. Neifer, B. Schmidt, J. Zapf, K. von Figura, and C. Peters.** 1995. Proteolysis of IGFBPs by cathepsin D in vitro and in cathepsin D-deficient mice. *Prog Growth Factor Res* **6**:265-71.
13. **Bunn, R. C., and J. L. Fowlkes.** 2003. Insulin-like growth factor binding protein proteolysis. *Trends Endocrinol Metab* **14**:176-81.
14. **Bursch, W.** 2001. The autophagosomal-lysosomal compartment in programmed cell death. *Cell Death Differ* **8**:569-81.

15. **Carroll, P. A., E. Brazeau, and M. Lagunoff.** 2004. Kaposi's sarcoma-associated herpesvirus infection of blood endothelial cells induces lymphatic differentiation. *Virology* **328**:7-18.
16. **Casper, C., M. Redman, M. L. Huang, J. Pauk, T. M. Lampinen, S. E. Hawes, C. W. Critchlow, R. A. Morrow, L. Corey, N. Kiviat, and A. Wald.** 2004. HIV infection and human herpesvirus-8 oral shedding among men who have sex with men. *J Acquir Immune Defic Syndr* **35**:233-8.
17. **Catrina, S. B., M. Lewitt, C. Massambu, A. Dricu, J. Grunler, M. Axelson, P. Biberfeld, and K. Brismar.** 2005. Insulin-like growth factor-I receptor activity is essential for Kaposi's sarcoma growth and survival. *Br J Cancer* **92**:1467-74.
18. **Cesarman, E., Y. Chang, P. S. Moore, J. W. Said, and D. M. Knowles.** 1995. Kaposi's sarcoma-associated herpesvirus-like DNA sequences in AIDS-related body-cavity-based lymphomas. *N Engl J Med* **332**:1186-91.
19. **Chang, Y., E. Cesarman, M. S. Pessin, F. Lee, J. Culpepper, D. M. Knowles, and P. S. Moore.** 1994. Identification of herpesvirus-like DNA sequences in AIDS-associated Kaposi's sarcoma. *Science* **266**:1865-9.
20. **Chapman, H. A., R. J. Riese, and G. P. Shi.** 1997. Emerging roles for cysteine proteases in human biology. *Annu Rev Physiol* **59**:63-88.
21. **Chugh, P., H. Matta, S. Schamus, S. Zachariah, A. Kumar, J. A. Richardson, A. L. Smith, and P. M. Chaudhary.** 2005. Constitutive NF-kappaB activation, normal Fas-induced apoptosis, and increased incidence of lymphoma in human herpes virus 8 K13 transgenic mice. *Proc Natl Acad Sci U S A* **102**:12885-90.

22. **Cianfrocca, M., T. P. Cooley, J. Y. Lee, M. A. Rudek, D. T. Scadden, L. Ratner, J. M. Pluda, W. D. Figg, S. E. Krown, and B. J. Dezube.** 2002. Matrix metalloproteinase inhibitor COL-3 in the treatment of AIDS-related Kaposi's sarcoma: a phase I AIDS malignancy consortium study. *J Clin Oncol* **20**:153-9.
23. **Ciufo, D. M., J. S. Cannon, L. J. Poole, F. Y. Wu, P. Murray, R. F. Ambinder, and G. S. Hayward.** 2001. Spindle Cell Conversion by Kaposi's Sarcoma-Associated Herpesvirus: Formation of Colonies and Plaques with Mixed Lytic and Latent Gene Expression in Infected Primary Dermal Microvascular Endothelial Cell Cultures. *J. Virol.* **75**:5614-5626.
24. **Cohen, P., D. M. Peehl, T. A. Stamey, K. F. Wilson, D. R. Clemmons, and R. G. Rosenfeld.** 1993. Elevated levels of insulin-like growth factor-binding protein-2 in the serum of prostate cancer patients. *J Clin Endocrinol Metab* **76**:1031-5.
25. **Cui, H., M. Cruz-Correa, F. M. Giardiello, D. F. Hutcheon, D. R. Kafonek, S. Brandenburg, Y. Wu, X. He, N. R. Powe, and A. P. Feinberg.** 2003. Loss of IGF2 imprinting: a potential marker of colorectal cancer risk. *Science* **299**:1753-5.
26. **Damania, B.** 2004. Oncogenic gamma-herpesviruses: comparison of viral proteins involved in tumorigenesis. *Nat Rev Microbiol* **2**:656-68.
27. **Dengler, R., T. Lah, D. Gabrijelcic, V. Turk, H. Fritz, and B. Emmerich.** 1991. Detection of cathepsin B in tumor cytosol and urine of breast cancer patients. *Biomed Biochim Acta* **50**:555-60.
28. **Denley, A., E. R. Bonython, G. W. Booker, L. J. Cosgrove, B. E. Forbes, C. W. Ward, and J. C. Wallace.** 2004. Structural determinants for high-affinity

- binding of insulin-like growth factor II to insulin receptor (IR)-A, the exon 11 minus isoform of the IR. *Mol Endocrinol* **18**:2502-12.
29. **Denley, A., J. C. Wallace, L. J. Cosgrove, and B. E. Forbes.** 2003. The insulin receptor isoform exon 11- (IR-A) in cancer and other diseases: a review. *Horm Metab Res* **35**:778-85.
 30. **Dennis, P. A., and D. B. Rifkin.** 1991. Cellular activation of latent transforming growth factor beta requires binding to the cation-independent mannose 6-phosphate/insulin-like growth factor type II receptor. *Proc Natl Acad Sci U S A* **88**:580-4.
 31. **Dezube, B. J., R. Sullivan, and H. B. Koon.** 2006. Emerging targets and novel strategies in the treatment of AIDS-related Kaposi's sarcoma: Bidirectional translational science. *J Cell Physiol* **209**:659-62.
 32. **Dittmer, D., C. Stoddart, R. Renne, V. Linnik-Stepps, M. E. Moreno, C. Bare, J. M. McCune, and D. Ganem.** 1999. Experimental transmission of Kaposi's sarcoma-associated herpesvirus (KSHV/HHV-8) to SCID-hu Thy/Liv mice. *J Exp Med* **190**:1857-68.
 33. **Dourmishev, L. A., A. L. Dourmishev, D. Palmeri, R. A. Schwartz, and D. M. Lukac.** 2003. Molecular genetics of Kaposi's sarcoma-associated herpesvirus (human herpesvirus-8) epidemiology and pathogenesis. *Microbiol Mol Biol Rev* **67**:175-212, table of contents.
 34. **Dupin, N., C. Fisher, P. Kellam, S. Ariad, M. Tulliez, N. Franck, E. van Marck, D. Salmon, I. Gorin, J. P. Escande, R. A. Weiss, K. Alitalo, and C. Boshoff.** 1999. Distribution of human herpesvirus-8 latently infected cells in

- Kaposi's sarcoma, multicentric Castleman's disease, and primary effusion lymphoma. *Proc Natl Acad Sci U S A* **96**:4546-51.
35. **Dupin, N., and P. A. Grange.** 2006. Looking for the target cell of Kaposi's sarcoma-associated herpesvirus. *J Invest Dermatol* **126**:545-7.
 36. **Elminger, M. W., M. Bell, B. S. Schuett, M. Langkamp, E. Kutoh, and M. B. Ranke.** 2001. Transactivation of the IGFBP-2 promoter in human tumor cell lines. *Mol Cell Endocrinol* **175**:211-8.
 37. **Elmlinger, M. W., M. H. Deininger, B. S. Schuett, R. Meyermann, F. Duffner, E. H. Grote, and M. B. Ranke.** 2001. In vivo expression of insulin-like growth factor-binding protein-2 in human gliomas increases with the tumor grade. *Endocrinology* **142**:1652-8.
 38. **Ensoli, B., C. Sgadari, G. Barillari, M. C. Sirianni, M. Sturzl, and P. Monini.** 2001. Biology of Kaposi's sarcoma. *European Journal of Cancer* **37**:1251-1269.
 39. **Ensoli, B., and M. Sturzl.** 1998. Kaposi's sarcoma: a result of the interplay among inflammatory cytokines, angiogenic factors and viral agents. *Cytokine & Growth Factor Reviews* **9**:63-83.
 40. **Felbor, U., L. Dreier, R. A. Bryant, H. L. Ploegh, B. R. Olsen, and W. Mothes.** 2000. Secreted cathepsin L generates endostatin from collagen XVIII. *Embo J* **19**:1187-94.
 41. **Fingleton, B., and L. M. Matrisian.** 2001. Matrix metalloproteinases as targets for therapy in Kaposi sarcoma. *Curr Opin Oncol* **13**:368-73.
 42. **Firth, S. M., and R. C. Baxter.** 2002. Cellular actions of the insulin-like growth factor binding proteins. *Endocr Rev* **23**:824-54.

43. **Flamand, L., R. A. Zeman, J. L. Bryant, Y. Lunardi-Iskandar, and R. C. Gallo.** 1996. Absence of human herpesvirus 8 DNA sequences in neoplastic Kaposi's sarcoma cell lines. *J Acquir Immune Defic Syndr Hum Retrovirol* **13**:194-7.
44. **Flint, S. J., Enquist, L.W., Krug, R. M., Racaniello, V.R., Skalka, A.M.** 2000. *Principles of Virology.* American Society for Microbiology Press, Washington DC.
45. **Flore, O., S. Rafii, S. Ely, J. J. O'Leary, E. M. Hyjek, and E. Cesarman.** 1998. Transformation of primary human endothelial cells by Kaposi's sarcoma-associated herpesvirus. *Nature* **394**:588-592.
46. **Flyvbjerg, A., O. Mogensen, B. Mogensen, and O. S. Nielsen.** 1997. Elevated serum insulin-like growth factor-binding protein 2 (IGFBP-2) and decreased IGFBP-3 in epithelial ovarian cancer: correlation with cancer antigen 125 and tumor-associated trypsin inhibitor. *J Clin Endocrinol Metab* **82**:2308-13.
47. **Foreman, K. E., J. Friberg, B. Chandran, H. Katano, T. Sata, M. Mercader, G. J. Nabel, and B. J. Nickoloff.** 2001. Injection of human herpesvirus-8 in human skin engrafted on SCID mice induces Kaposi's sarcoma-like lesions. *J Dermatol Sci* **26**:182-93.
48. **Fottner, C., A. Hoeflich, E. Wolf, and M. M. Weber.** 2004. Role of the insulin-like growth factor system in adrenocortical growth control and carcinogenesis. *Horm Metab Res* **36**:397-405.
49. **Frasca, F., G. Pandini, P. Scalia, L. Sciacca, R. Mineo, A. Costantino, I. D. Goldfine, A. Belfiore, and R. Vigneri.** 1999. Insulin receptor isoform A, a newly

- recognized, high-affinity insulin-like growth factor II receptor in fetal and cancer cells. *Mol Cell Biol* **19**:3278-88.
50. **Frlan, R., and S. Gobec.** 2006. Inhibitors of cathepsin B. *Curr Med Chem* **13**:2309-27.
51. **Fuller, G. N., C. H. Rhee, K. R. Hess, L. S. Caskey, R. Wang, J. M. Bruner, W. K. Yung, and W. Zhang.** 1999. Reactivation of insulin-like growth factor binding protein 2 expression in glioblastoma multiforme: a revelation by parallel gene expression profiling. *Cancer Res* **59**:4228-32.
52. **Gao, S. J., J. H. Deng, and F. C. Zhou.** 2003. Productive lytic replication of a recombinant Kaposi's sarcoma-associated herpesvirus in efficient primary infection of primary human endothelial cells. *J Virol* **77**:9738-49.
53. **Gibson, T. L., and P. Cohen.** 1999. Inflammation-related neutrophil proteases, cathepsin G and elastase, function as insulin-like growth factor binding protein proteases. *Growth Horm IGF Res* **9**:241-53.
54. **Gondi, C. S., S. S. Lakka, N. Yanamandra, W. C. Olivero, D. H. Dinh, M. Gujrati, C. H. Tung, R. Weissleder, and J. S. Rao.** 2004. Adenovirus-Mediated Expression of Antisense Urokinase Plasminogen Activator Receptor and Antisense Cathepsin B Inhibits Tumor Growth, Invasion, and Angiogenesis in Gliomas 10.1158/0008-5472.CAN-04-1243. *Cancer Res* **64**:4069-4077.
55. **Grundhoff, A., and D. Ganem.** 2004. Inefficient establishment of KSHV latency suggests an additional role for continued lytic replication in Kaposi sarcoma pathogenesis. *J Clin Invest* **113**:124-36.

56. **Guasparri, I., S. A. Keller, and E. Cesarman.** 2004. KSHV vFLIP is essential for the survival of infected lymphoma cells. *J Exp Med* **199**:993-1003.
57. **Guerra, F. K., A. M. Eijan, L. Puricelli, D. F. Alonso, E. Bal de Kier Joffe, A. R. Kornblihtt, E. H. Charreau, and P. V. Elizalde.** 1996. Varying patterns of expression of insulin-like growth factors I and II and their receptors in murine mammary adenocarcinomas of different metastasizing ability. *Int J Cancer* **65**:812-20.
58. **Guicciardi, M. E., J. Deussing, H. Miyoshi, S. F. Bronk, P. A. Svingen, C. Peters, S. H. Kaufmann, and G. J. Gores.** 2000. Cathepsin B contributes to TNF-alpha-mediated hepatocyte apoptosis by promoting mitochondrial release of cytochrome c. *J Clin Invest* **106**:1127-37.
59. **Hailey, J., E. Maxwell, K. Koukouras, W. R. Bishop, J. A. Pachter, and Y. Wang.** 2002. Neutralizing Anti-Insulin-like Growth Factor Receptor 1 Antibodies Inhibit Receptor Function and Induce Receptor Degradation in Tumor Cells. *Mol Cancer Ther* **1**:1349-1353.
60. **Hanewinkel, H., J. Glossl, and H. Kresse.** 1987. Biosynthesis of cathepsin B in cultured normal and I-cell fibroblasts. *J Biol Chem* **262**:12351-5.
61. **Haque, M., V. Wang, D. A. Davis, Z. M. Zheng, and R. Yarchoan.** 2006. Genetic organization and hypoxic activation of the Kaposi's sarcoma-associated herpesvirus ORF34-37 gene cluster. *J Virol* **80**:7037-51.
62. **Hawkes, C., and S. Kar.** 2004. The insulin-like growth factor-II/mannose-6-phosphate receptor: structure, distribution and function in the central nervous system. *Brain Res Brain Res Rev* **44**:117-40.

63. **Hayward, G. S.** 2003. Initiation of angiogenic Kaposi's sarcoma lesions. *Cancer Cell* **3**:1-3.
64. **Hebert, E.** 2006. Mannose-6-phosphate/insulin-like growth factor II receptor expression and tumor development. *Biosci Rep* **26**:7-17.
65. **Hengge, U. R., T. Ruzicka, S. K. Tyring, M. Stuschke, M. Roggendorf, R. A. Schwartz, and S. Seeber.** 2002. Update on Kaposi's sarcoma and other HHV8 associated diseases. Part 1: epidemiology, environmental predispositions, clinical manifestations, and therapy. *Lancet Infect Dis* **2**:281-92.
66. **Hengge, U. R., T. Ruzicka, S. K. Tyring, M. Stuschke, M. Roggendorf, R. A. Schwartz, and S. Seeber.** 2002. Update on Kaposi's sarcoma and other HHV8 associated diseases. Part 2: pathogenesis, Castleman's disease, and pleural effusion lymphoma. *Lancet Infect Dis* **2**:344-52.
67. **Herndier, B. G., A. Werner, P. Arnstein, N. W. Abbey, F. Demartis, R. L. Cohen, M. A. Shuman, and J. A. Levy.** 1994. Characterization of a human Kaposi's sarcoma cell line that induces angiogenic tumors in animals. *Aids* **8**:575-81.
68. **Hill, P. A., D. J. Buttle, S. J. Jones, A. Boyde, M. Murata, J. J. Reynolds, and M. C. Meikle.** 1994. Inhibition of bone resorption by selective inactivators of cysteine proteinases. *J Cell Biochem* **56**:118-30.
69. **Ho, P. J., and R. C. Baxter.** 1997. Insulin-like growth factor-binding protein-2 in patients with prostate carcinoma and benign prostatic hyperplasia. *Clin Endocrinol (Oxf)* **46**:333-42.

70. **Hoeflich, A., O. Fettscher, H. Lahm, W. F. Blum, H. J. Kolb, D. Engelhardt, E. Wolf, and M. M. Weber.** 2000. Overexpression of insulin-like growth factor-binding protein-2 results in increased tumorigenic potential in Y-1 adrenocortical tumor cells. *Cancer Res* **60**:834-8.
71. **Hoeflich, A., R. Reisinger, H. Lahm, W. Kiess, W. F. Blum, H. J. Kolb, M. M. Weber, and E. Wolf.** 2001. Insulin-like growth factor-binding protein 2 in tumorigenesis: protector or promoter? *Cancer Res* **61**:8601-10.
72. **Hoeflich, A., R. Reisinger, B. S. Schuett, M. W. Elmlinger, V. C. Russo, G. A. Vargas, P. M. Jehle, H. Lahm, I. Renner-Muller, and E. Wolf.** 2004. Peri/nuclear localization of intact insulin-like growth factor binding protein-2 and a distinct carboxyl-terminal IGFBP-2 fragment in vivo. *Biochem Biophys Res Commun* **324**:705-10.
73. **Hoeflich, A., R. Reisinger, G. A. Vargas, M. W. Elmlinger, B. Schuett, P. M. Jehle, I. Renner-Muller, H. Lahm, V. C. Russo, and E. Wolf.** 2002. Mutation of the RGD sequence does not affect plasma membrane association and growth inhibitory effects of elevated IGFBP-2 in vivo. *FEBS Lett* **523**:63-7.
74. **Hoflich, A., H. Lahm, W. Blum, H. Kolb, and E. Wolf.** 1998. Insulin-like growth factor-binding protein-2 inhibits proliferation of human embryonic kidney fibroblasts and of IGF-responsive colon carcinoma cell lines. *FEBS Lett* **434**:329-34.
75. **Holly, J. M., and J. A. Wass.** 1989. Insulin-like growth factors; autocrine, paracrine or endocrine? New perspectives of the somatomedin hypothesis in the light of recent developments. *J Endocrinol* **122**:611-8.

76. **Hong, Y. K., K. Foreman, J. W. Shin, S. Hirakawa, C. L. Curry, D. R. Sage, T. Libermann, B. J. Dezube, J. D. Fingerth, and M. Detmar.** 2004. Lymphatic reprogramming of blood vascular endothelium by Kaposi sarcoma-associated herpesvirus. *Nat Genet* **36**:683-5.
77. **Hribal, M. L., L. Perego, S. Lovari, F. Andreozzi, R. Menghini, C. Perego, G. Finzi, L. Usellini, C. Placidi, C. Capella, V. Guzzi, D. Lauro, F. Bertuzzi, A. Davalli, G. Pozza, A. Pontiroli, M. Federici, R. Lauro, A. Brunetti, F. Folli, and G. Sesti.** 2003. Chronic hyperglycemia impairs insulin secretion by affecting insulin receptor expression, splicing, and signaling in RIN beta cell line and human islets of Langerhans. *Faseb J* **17**:1340-2.
78. **Huang, Q., A. Raya, P. DeJesus, S. H. Chao, K. C. Quon, J. S. Caldwell, S. K. Chanda, J. C. Izpisua-Belmonte, and P. G. Schultz.** 2004. Identification of p53 regulators by genome-wide functional analysis. *Proc Natl Acad Sci U S A* **101**:3456-61.
79. **Huet, G., R. M. Flipo, C. Colin, A. Janin, B. Hemon, M. Collyn-d'Hooghe, R. Lafyatis, B. Duquesnoy, and P. Degand.** 1993. Stimulation of the secretion of latent cysteine proteinase activity by tumor necrosis factor alpha and interleukin-1. *Arthritis Rheum* **36**:772-80.
80. **Hwa, V., Y. Oh, and R. G. Rosenfeld.** 1999. The insulin-like growth factor-binding protein (IGFBP) superfamily. *Endocr Rev* **20**:761-87.
81. **Im, E., A. Venkatakrishnan, and A. Kazlauskas.** 2005. Cathepsin B regulates the intrinsic angiogenic threshold of endothelial cells. *Mol Biol Cell* **16**:3488-500.

82. **Janeway, C. A., Travers, P., Walport, M., Capra, J.D.** 1999. Immunobiology: The Immune System in Health and Disease, 4th Edision ed. Elsevier Science Ltd/Garland Publishing, New York.
83. **Jarviluoma, A., and P. M. Ojala.** 2006. Cell signaling pathways engaged by KSHV. *Biochim Biophys Acta* **1766**:140-58.
84. **Jenner, R. G., and C. Boshoff.** 2002. The molecular pathology of Kaposi's sarcoma-associated herpesvirus. *Biochim Biophys Acta* **1602**:1-22.
85. **Jones, J. I., and D. R. Clemmons.** 1995. Insulin-like growth factors and their binding proteins: biological actions. *Endocr Rev* **16**:3-34.
86. **Jones, J. I., A. Gockerman, W. H. Busby, Jr., G. Wright, and D. R. Clemmons.** 1993. Insulin-like growth factor binding protein 1 stimulates cell migration and binds to the alpha 5 beta 1 integrin by means of its Arg-Gly-Asp sequence. *Proc Natl Acad Sci U S A* **90**:10553-7.
87. **Joyce, J. A., A. Baruch, K. Chehade, N. Meyer-Morse, E. Giraud, F. Y. Tsai, D. C. Greenbaum, J. H. Hager, M. Bogyo, and D. Hanahan.** 2004. Cathepsin cysteine proteases are effectors of invasive growth and angiogenesis during multistage tumorigenesis. *Cancer Cell* **5**:443-53.
88. **Joyce, J. A., and D. Hanahan.** 2004. Multiple roles for cysteine cathepsins in cancer. *Cell Cycle* **3**:1516-619.
89. **Kalli, K. R., O. I. Falowo, L. K. Bale, M. A. Zschunke, P. C. Roche, and C. A. Conover.** 2002. Functional insulin receptors on human epithelial ovarian carcinoma cells: implications for IGF-II mitogenic signaling. *Endocrinology* **143**:3259-67.

90. **Kanety, H., Y. Madjar, Y. Dagan, J. Levi, M. Z. Papa, C. Pariente, B. Goldwasser, and A. Karasik.** 1993. Serum insulin-like growth factor-binding protein-2 (IGFBP-2) is increased and IGFBP-3 is decreased in patients with prostate cancer: correlation with serum prostate-specific antigen. *J Clin Endocrinol Metab* **77**:229-33.
91. **Kiunga, G. A., J. Raju, N. Sabljic, G. Bajaj, C. K. Good, and R. P. Bird.** 2004. Elevated insulin receptor protein expression in experimentally induced colonic tumors. *Cancer Lett* **211**:145-53.
92. **Kiyama, S., K. Morrison, T. Zellweger, M. Akbari, M. Cox, D. Yu, H. Miyake, and M. E. Gleave.** 2003. Castration-induced increases in insulin-like growth factor-binding protein 2 promotes proliferation of androgen-independent human prostate LNCaP tumors. *Cancer Res* **63**:3575-84.
93. **Koblinski, J. E., M. Ahram, and B. F. Sloane.** 2000. Unraveling the role of proteases in cancer. *Clin Chim Acta* **291**:113-35.
94. **Koon, H. B., G. Bublely, L. Pantanowitz, D. Masiello, J. Proper, W. Weeden, S. Tahan, and B. Dezube.** 2003. Presented at the American Society of Clinical Oncology.
95. **Krishnan, H. H., P. P. Naranatt, M. S. Smith, L. Zeng, C. Bloomer, and B. Chandran.** 2004. Concurrent expression of latent and a limited number of lytic genes with immune modulation and antiapoptotic function by Kaposi's sarcoma-associated herpesvirus early during infection of primary endothelial and fibroblast cells and subsequent decline of lytic gene expression. *J Virol* **78**:3601-20.

96. **Krueger, S., C. Haeckel, F. Buehling, and A. Roessner.** 1999. Inhibitory Effects of Antisense Cathepsin B cDNA Transfection on Invasion and Motility in a Human Osteosarcoma Cell Line. *Cancer Res* **59**:6010-6014.
97. **Lagunoff, M., J. Bechtel, E. Venetsanakos, A.-M. Roy, N. Abbey, B. Herndier, M. McMahon, and D. Ganem.** 2002. De Novo Infection and Serial Transmission of Kaposi's Sarcoma-Associated Herpesvirus in Cultured Endothelial Cells. *J. Virol.* **76**:2440-2448.
98. **Lakka, S. S., C. S. Gondi, and J. S. Rao.** 2005. Proteases and glioma angiogenesis. *Brain Pathol* **15**:327-41.
99. **Lakka, S. S., C. S. Gondi, N. Yanamandra, W. C. Olivero, D. H. Dinh, M. Gujrati, and J. S. Rao.** 2004. Inhibition of cathepsin B and MMP-9 gene expression in glioblastoma cell line via RNA interference reduces tumor cell invasion, tumor growth and angiogenesis. *Oncogene* **23**:4681-9.
100. **Lan, K., D. A. Koppers, S. C. Verma, and E. S. Robertson.** 2004. Kaposi's sarcoma-associated herpesvirus-encoded latency-associated nuclear antigen inhibits lytic replication by targeting Rta: a potential mechanism for virus-mediated control of latency. *J Virol* **78**:6585-94.
101. **Leibiger, B., I. B. Leibiger, T. Moede, S. Kemper, R. N. Kulkarni, C. R. Kahn, L. M. de Vargas, and P. O. Berggren.** 2001. Selective insulin signaling through A and B insulin receptors regulates transcription of insulin and glucokinase genes in pancreatic beta cells. *Mol Cell* **7**:559-70.
102. **Leist, M., and M. Jaattela.** 2001. Triggering of apoptosis by cathepsins. *Cell Death Differ* **8**:324-6.

103. **LeRoith, D., R. Baserga, L. Helman, and C. T. Roberts, Jr.** 1995. Insulin-like growth factors and cancer. *Ann Intern Med* **122**:54-9.
104. **LeRoith, D., and C. T. Roberts, Jr.** 2003. The insulin-like growth factor system and cancer. *Cancer Lett* **195**:127-37.
105. **Li, J. H., and J. S. Pober.** 2005. The cathepsin B death pathway contributes to TNF plus IFN-gamma-mediated human endothelial injury. *J Immunol* **175**:1858-66.
106. **Livak, K. J., and T. D. Schmittgen.** 2001. Analysis of relative gene expression data using real-time quantitative PCR and the 2(-Delta Delta C(T)) Method. *Methods* **25**:402-8.
107. **Lorenzo, K., P. Ton, J. L. Clark, S. Coulibaly, and L. Mach.** 2000. Invasive properties of murine squamous carcinoma cells: secretion of matrix-degrading cathepsins is attributable to a deficiency in the mannose 6-phosphate/insulin-like growth factor II receptor. *Cancer Res* **60**:4070-6.
108. **Lunardi-Iskandar, Y., P. Gill, V. H. Lam, R. A. Zeman, F. Michaels, D. L. Mann, M. S. Reitz, Jr., M. Kaplan, Z. N. Berneman, D. Carter, and et al.** 1995. Isolation and characterization of an immortal neoplastic cell line (KS Y-1) from AIDS-associated Kaposi's sarcoma. *J Natl Cancer Inst* **87**:974-81.
109. **Matter, H., and M. Schudok.** 2004. Recent advances in the design of matrix metalloprotease inhibitors. *Curr Opin Drug Discov Devel* **7**:513-35.
110. **Mbulaiteye, S. M., D. M. Parkin, and C. S. Rabkin.** 2003. Epidemiology of AIDS-related malignancies an international perspective. *Hematol Oncol Clin North Am* **17**:673-96, v.

111. **McAllister, S. C., S. G. Hansen, R. A. Ruhl, C. M. Raggo, V. R. DeFilippis, D. Greenspan, K. Fruh, and A. V. Moses.** 2004. Kaposi sarcoma-associated herpesvirus (KSHV) induces heme oxygenase-1 expression and activity in KSHV-infected endothelial cells. *Blood* **103**:3465-3473.
112. **McAllister, S. C., Moses, A. V. (ed.).** 2007. *Endothelial Cell- and Lymphocyte-Based In Vitro Systems for Understanding KSHV Biology.* Springer Verlag, Heidelberg.
113. **McCormick, C., and D. Ganem.** 2005. The kaposin B protein of KSHV activates the p38/MK2 pathway and stabilizes cytokine mRNAs. *Science* **307**:739-41.
114. **Mehtani, S., Q. Gong, J. Panella, S. Subbiah, D. M. Peffley, and A. Frankfater.** 1998. In vivo expression of an alternatively spliced human tumor message that encodes a truncated form of cathepsin B. Subcellular distribution of the truncated enzyme in COS cells. *J Biol Chem* **273**:13236-44.
115. **Menouny, M., M. Binoux, and S. Babajko.** 1998. IGFBP-2 expression in a human cell line is associated with increased IGFBP-3 proteolysis, decreased IGFBP-1 expression and increased tumorigenicity. *Int J Cancer* **77**:874-9.
116. **Mohanam, S., S. L. Jasti, S. R. Kondraganti, N. Chandrasekar, S. S. Lakka, Y. Kin, G. N. Fuller, A. W. Yung, A. P. Kyritsis, D. H. Dinh, W. C. Olivero, M. Gujrati, F. Ali-Osman, and J. S. Rao.** 2001. Down-regulation of cathepsin B expression impairs the invasive and tumorigenic potential of human glioblastoma cells. *Oncogene* **20**:3665-73.

117. **Montaser, M., G. Lalmanach, and L. Mach.** 2002. CA-074, but not its methyl ester CA-074Me, is a selective inhibitor of cathepsin B within living cells. *Biol Chem* **383**:1305-8.
118. **Montella, M., D. Serraino, A. Crispo, G. Rezza, S. Carbone, and M. Tamburini.** 2000. Is volcanic soil a cofactor for classic Kaposi's sarcoma? *Eur J Epidemiol* **16**:1185-6.
119. **Moore, P. S.** 2003. Transplanting cancer: donor-cell transmission of Kaposi sarcoma. *Nat Med* **9**:506-8.
120. **Moore, P. S., and Y. Chang.** 1998. Antiviral activity of tumor-suppressor pathways: clues from molecular piracy by KSHV. *Trends Genet* **14**:144-50.
121. **Moore, P. S., and Y. Chang.** 2003. Kaposi's sarcoma-associated herpesvirus immunoevasion and tumorigenesis: two sides of the same coin? *Annu Rev Microbiol* **57**:609-39.
122. **Moschos, S. J., and C. S. Mantzoros.** 2002. The role of the IGF system in cancer: from basic to clinical studies and clinical applications. *Oncology* **63**:317-32.
123. **Moses, A. V., K. N. Fish, R. Ruhl, P. P. Smith, J. G. Strussenberg, L. Zhu, B. Chandran, and J. A. Nelson.** 1999. Long-term infection and transformation of dermal microvascular endothelial cells by human herpesvirus 8. *J Virol* **73**:6892-902.
124. **Moses, A. V., M. A. Jarvis, C. Raggo, Y. C. Bell, R. Ruhl, B. G. Luukkonen, D. J. Griffith, C. L. Wait, B. J. Druker, M. C. Heinrich, J. A. Nelson, and K.**

- Fruh.** 2002. A functional genomics approach to Kaposi's sarcoma. *Ann N Y Acad Sci* **975**:180-91.
125. **Moses, A. V., M. A. Jarvis, C. Raggo, Y. C. Bell, R. Ruhl, B. G. Luukkonen, D. J. Griffith, C. L. Wait, B. J. Druker, M. C. Heinrich, J. A. Nelson, and K. Fruh.** 2002. Kaposi's sarcoma-associated herpesvirus-induced upregulation of the c-kit proto-oncogene, as identified by gene expression profiling, is essential for the transformation of endothelial cells. *J Virol* **76**:8383-99.
126. **Muller, H. L., Y. Oh, T. Lehrnbecher, W. F. Blum, and R. G. Rosenfeld.** 1994. Insulin-like growth factor-binding protein-2 concentrations in cerebrospinal fluid and serum of children with malignant solid tumors or acute leukemia. *J Clin Endocrinol Metab* **79**:428-34.
127. **Naranatt, P. P., H. H. Krishnan, S. R. Svojanovsky, C. Bloomer, S. Mathur, and B. Chandran.** 2004. Host gene induction and transcriptional reprogramming in Kaposi's sarcoma-associated herpesvirus (KSHV/HHV-8)-infected endothelial, fibroblast, and B cells: insights into modulation events early during infection. *Cancer Res* **64**:72-84.
128. **Nitert, M. D., S. I. Chisalita, K. Olsson, K. E. Bornfeldt, and H. J. Arnqvist.** 2005. IGF-I/insulin hybrid receptors in human endothelial cells. *Mol Cell Endocrinol* **229**:31-7.
129. **O'Connor, R.** 2003. Regulation of IGF-I receptor signaling in tumor cells. *Horm Metab Res* **35**:771-7.
130. **O'Gorman, D. B., J. Weiss, A. Hettiaratchi, S. M. Firth, and C. D. Scott.** 2002. Insulin-like growth factor-II/mannose 6-phosphate receptor overexpression

- reduces growth of choriocarcinoma cells in vitro and in vivo. *Endocrinology* **143**:4287-94.
131. **Oh, Y., H. L. Muller, G. Lamson, and R. G. Rosenfeld.** 1993. Insulin-like growth factor (IGF)-independent action of IGF-binding protein-3 in Hs578T human breast cancer cells. Cell surface binding and growth inhibition. *J Biol Chem* **268**:14964-71.
132. **Orem, J., M. W. Otieno, and S. C. Remick.** 2004. AIDS-associated cancer in developing nations. *Curr Opin Oncol* **16**:468-76.
133. **Ottensmeyer, F. P., D. R. Beniac, R. Z. Luo, and C. C. Yip.** 2000. Mechanism of transmembrane signaling: insulin binding and the insulin receptor. *Biochemistry* **39**:12103-12.
134. **Palmer, J. T., D. Rasnick, J. L. Klaus, and D. Bromme.** 1995. Vinyl sulfones as mechanism-based cysteine protease inhibitors. *J Med Chem* **38**:3193-6.
135. **Pandini, G., E. Medico, E. Conte, L. Sciacca, R. Vigneri, and A. Belfiore.** 2003. Differential gene expression induced by insulin and insulin-like growth factor-II through the insulin receptor isoform A. *J Biol Chem* **278**:42178-89.
136. **Pantanowitz, L., and B. J. Dezube.** 2004. Advances in the pathobiology and treatment of Kaposi sarcoma. *Curr Opin Oncol* **16**:443-9.
137. **Parkin, D. M.** 2006. The global health burden of infection-associated cancers in the year 2002. *Int J Cancer* **118**:3030-44.
138. **Parravicini, C., B. Chandran, M. Corbellino, E. Berti, M. Paulli, P. S. Moore, and Y. Chang.** 2000. Differential viral protein expression in Kaposi's sarcoma-

- associated herpesvirus-infected diseases: Kaposi's sarcoma, primary effusion lymphoma, and multicentric Castleman's disease. *Am J Pathol* **156**:743-9.
139. **Parsons, C. H., L. A. Adang, J. Overdevest, C. M. O'Connor, J. R. Taylor, Jr., D. Camerini, and D. H. Kedes.** 2006. KSHV targets multiple leukocyte lineages during long-term productive infection in NOD/SCID mice. *J Clin Invest* **116**:1963-73.
140. **Pellet, C., D. Kerob, A. Dupuy, M. V. Carmagnat, S. Mourah, M. P. Podgorniak, C. Toledano, P. Morel, O. Verola, C. Dosquet, Y. Hamel, F. Calvo, C. Rabian, and C. Lebbe.** 2006. Kaposi's sarcoma-associated herpesvirus viremia is associated with the progression of classic and endemic Kaposi's sarcoma. *J Invest Dermatol* **126**:621-7.
141. **Pereira, J. J., T. Meyer, S. E. Docherty, H. H. Reid, J. Marshall, E. W. Thompson, J. Rossjohn, and J. T. Price.** 2004. Bimolecular interaction of insulin-like growth factor (IGF) binding protein-2 with alphavbeta3 negatively modulates IGF-I-mediated migration and tumor growth. *Cancer Res* **64**:977-84.
142. **Perks, C. M., P. V. Newcomb, M. R. Norman, and J. M. Holly.** 1999. Effect of insulin-like growth factor binding protein-1 on integrin signalling and the induction of apoptosis in human breast cancer cells. *J Mol Endocrinol* **22**:141-50.
143. **Philchenkov, A., M. Zavelevich, T. J. Krocak, and M. Los.** 2004. Caspases and cancer: mechanisms of inactivation and new treatment modalities. *Exp Oncol* **26**:82-97.
144. **Picchio, G. R., R. E. Sabbe, R. J. Gulizia, M. McGrath, B. G. Herndier, and D. E. Mosier.** 1997. The KSHV/HHV8-infected BCBL-1 lymphoma line causes

- tumors in SCID mice but fails to transmit virus to a human peripheral blood mononuclear cell graft. *Virology* **238**:22-9.
145. **Podgrabinska, S., P. Braun, P. Velasco, B. Kloos, M. S. Pepper, and M. Skobe.** 2002. Molecular characterization of lymphatic endothelial cells. *Proc Natl Acad Sci U S A* **99**:16069-74.
146. **Pollak, M. N., E. S. Schernhammer, and S. E. Hankinson.** 2004. Insulin-like growth factors and neoplasia. *Nat Rev Cancer* **4**:505-18.
147. **Poole, L. J., Y. Yu, P. S. Kim, Q. Z. Zheng, J. Pevsner, and G. S. Hayward.** 2002. Altered patterns of cellular gene expression in dermal microvascular endothelial cells infected with Kaposi's sarcoma-associated herpesvirus. *J Virol* **76**:3395-420.
148. **Popescu, N. C., D. B. Zimonjic, S. Leventon-Kriss, J. L. Bryant, Y. Lunardi-Iskandar, and R. C. Gallo.** 1996. Deletion and translocation involving chromosome 3 (p14) in two tumorigenic Kaposi's sarcoma cell lines. *J Natl Cancer Inst* **88**:450-5.
149. **Rabkin, C. S.** 2001. AIDS and cancer in the era of highly active antiretroviral therapy (HAART). *Eur J Cancer* **37**:1316-9.
150. **Raggio, C., R. Ruhl, S. McAllister, H. Koon, B. J. Dezube, K. Fruh, and A. V. Moses.** 2005. Novel Cellular Genes Essential for Transformation of Endothelial Cells by Kaposi's Sarcoma-Associated Herpesvirus. *Cancer Res* **65**:5084-5095.
151. **Rajah, R., B. Valentinis, and P. Cohen.** 1997. Insulin-like growth factor (IGF)-binding protein-3 induces apoptosis and mediates the effects of transforming

- growth factor-beta1 on programmed cell death through a p53- and IGF-independent mechanism. *J Biol Chem* **272**:12181-8.
152. **Rajaram, S., D. J. Baylink, and S. Mohan.** 1997. Insulin-like growth factor-binding proteins in serum and other biological fluids: regulation and functions. *Endocr Rev* **18**:801-31.
153. **Reiss, K., and K. Khalili.** 2003. Viruses and cancer: lessons from the human polyomavirus, JCV. *Oncogene* **22**:6517-23.
154. **Riese, R. J., P. R. Wolf, D. Bromme, L. R. Natkin, J. A. Villadangos, H. L. Ploegh, and H. A. Chapman.** 1996. Essential role for cathepsin S in MHC class II-associated invariant chain processing and peptide loading. *Immunity* **4**:357-66.
155. **Rose, P. P., J. M. Carroll, P. A. Carroll, V. R. Defilippis, M. Lagunoff, A. V. Moses, C. T. Roberts, Jr., and K. Fruh.** 2006. The insulin receptor is essential for virus-induced tumorigenesis of Kaposi's sarcoma. *Oncogene*.
156. **Rose, T. M., J. T. Ryan, E. R. Schultz, B. W. Raden, and C. C. Tsai.** 2003. Analysis of 4.3 kilobases of divergent locus B of macaque retroperitoneal fibromatosis-associated herpesvirus reveals a close similarity in gene sequence and genome organization to Kaposi's sarcoma-associated herpesvirus. *J Virol* **77**:5084-97.
157. **Rose, T. M., K. B. Strand, E. R. Schultz, G. Schaefer, G. W. Rankin, Jr., M. E. Thouless, C. C. Tsai, and M. L. Bosch.** 1997. Identification of two homologs of the Kaposi's sarcoma-associated herpesvirus (human herpesvirus 8) in retroperitoneal fibromatosis of different macaque species. *J Virol* **71**:4138-44.

158. **Roshy, S., B. F. Sloane, and K. Moin.** 2003. Pericellular cathepsin B and malignant progression. *Cancer Metastasis Rev* **22**:271-86.
159. **Sadler, R., L. Wu, B. Forghani, R. Renne, W. Zhong, B. Herndier, and D. Ganem.** 1999. A complex translational program generates multiple novel proteins from the latently expressed kaposin (K12) locus of Kaposi's sarcoma-associated herpesvirus. *J Virol* **73**:5722-30.
160. **Saharinen, P., T. Tammela, M. J. Karkkainen, and K. Alitalo.** 2004. Lymphatic vasculature: development, molecular regulation and role in tumor metastasis and inflammation. *Trends Immunol* **25**:387-95.
161. **Sallinen, S. L., P. K. Sallinen, H. K. Haapasalo, H. J. Helin, P. T. Helen, P. Schraml, O. P. Kallioniemi, and J. Kononen.** 2000. Identification of differentially expressed genes in human gliomas by DNA microarray and tissue chip techniques. *Cancer Res* **60**:6617-22.
162. **Saperstein, R., P. P. Vicario, H. V. Strout, E. Brady, E. E. Slater, W. J. Greenlee, D. L. Ondeyka, A. A. Patchett, and D. G. Hangauer.** 1989. Design of a selective insulin receptor tyrosine kinase inhibitor and its effect on glucose uptake and metabolism in intact cells. *Biochemistry* **28**:5694-701.
163. **Scharf, J. G., and T. Braulke.** 2003. The role of the IGF axis in hepatocarcinogenesis. *Horm Metab Res* **35**:685-93.
164. **Schutt, B. S., M. Langkamp, U. Rauschnabel, M. B. Ranke, and M. W. Elmlinger.** 2004. Integrin-mediated action of insulin-like growth factor binding protein-2 in tumor cells. *J Mol Endocrinol* **32**:859-68.

165. **Schwartz, R. A., Van Voorhees, A., Wells, M. J., Mowad, C. M., Gelfand, J. M., Elston, D. M.** . 2006. Kaposi Sarcoma. *In* R. A. Schwartz (ed.). Emedicine from WebMD.
166. **Sciacca, L., A. Costantino, G. Pandini, R. Mineo, F. Frasca, P. Scalia, P. Sbraccia, I. D. Goldfine, R. Vigneri, and A. Belfiore.** 1999. Insulin receptor activation by IGF-II in breast cancers: evidence for a new autocrine/paracrine mechanism. *Oncogene* **18**:2471-9.
167. **Sciacca, L., R. Mineo, G. Pandini, A. Murabito, R. Vigneri, and A. Belfiore.** 2002. In IGF-I receptor-deficient leiomyosarcoma cells autocrine IGF-II induces cell invasion and protection from apoptosis via the insulin receptor isoform A. *Oncogene* **21**:8240-50.
168. **Searles, R. P., E. P. Bergquam, M. K. Axthelm, and S. W. Wong.** 1999. Sequence and genomic analysis of a Rhesus macaque rhadinovirus with similarity to Kaposi's sarcoma-associated herpesvirus/human herpesvirus 8. *J Virol* **73**:3040-53.
169. **Sharma-Walia, N., H. H. Krishnan, P. P. Naranatt, L. Zeng, M. S. Smith, and B. Chandran.** 2005. ERK1/2 and MEK1/2 Induced by Kaposi's Sarcoma-Associated Herpesvirus (Human Herpesvirus 8) Early during Infection of Target Cells Are Essential for Expression of Viral Genes and for Establishment of Infection. *J. Virol.* **79**:10308-10329.
170. **Shay, J. W.** 2005. Meeting report: the role of telomeres and telomerase in cancer. *Cancer Res* **65**:3513-7.

171. **Shay, J. W., and W. E. Wright.** 2005. Senescence and immortalization: role of telomeres and telomerase. *Carcinogenesis* **26**:867-74.
172. **Sieber, O., K. Heinemann, and I. Tomlinson.** 2005. Genomic stability and tumorigenesis. *Semin Cancer Biol* **15**:61-6.
173. **Siegel, B., S. Levinton-Kriss, A. Schiffer, J. Sayar, I. Engelberg, A. Vonsover, Y. Ramon, and E. Rubinstein.** 1990. Kaposi's sarcoma in immunosuppression. Possibly the result of a dual viral infection. *Cancer* **65**:492-8.
174. **Sissolak, G., and P. Mayaud.** 2005. AIDS-related Kaposi's sarcoma: epidemiological, diagnostic, treatment and control aspects in sub-Saharan Africa. *Trop Med Int Health* **10**:981-92.
175. **Sloane, B., K. Moin, M. Sameni, L. Tait, J. Rozhin, and G. Ziegler.** 1994. Membrane association of cathepsin B can be induced by transfection of human breast epithelial cells with c-Ha-ras oncogene. *J Cell Sci* **107**:373-384.
176. **Sloane, B. F., S. Yan, I. Podgorski, B. E. Linebaugh, M. L. Cher, J. Mai, D. Cavallo-Medved, M. Sameni, J. Dosesco, and K. Moin.** 2005. Cathepsin B and tumor proteolysis: contribution of the tumor microenvironment. *Seminars in Cancer Biology* **15**:149-157.
177. **Slootweg, M. C., C. Ohlsson, J. P. Salles, C. P. de Vries, and J. C. Netelenbos.** 1995. Insulin-like growth factor binding proteins-2 and -3 stimulate growth hormone receptor binding and mitogenesis in rat osteosarcoma cells. *Endocrinology* **136**:4210-7.
178. **Staskus, K. A., W. Zhong, K. Gebhard, B. Herndier, H. Wang, R. Renne, J. Beneke, J. Pudney, D. J. Anderson, D. Ganem, and A. T. Haase.** 1997.

- Kaposi's sarcoma-associated herpesvirus gene expression in endothelial (spindle) tumor cells. *J Virol* **71**:715-9.
179. **Staudt, M. R., Dittmer, D.P.** 2007. The Rta/Orf50 Transactivator Proteins of the Gamma-Herpesviridae, p. 71-100. *In* C. Boshoff, Weiss, R.A. (ed.), *Kaposi Sarcoma Herpesvirus: New Perspectives*. Springer Verlag, Heidelberg.
180. **Stewart, C. E., and P. Rotwein.** 1996. Growth, differentiation, and survival: multiple physiological functions for insulin-like growth factors. *Physiol Rev* **76**:1005-26.
181. **Strojnik, T., J. Kos, B. Zidanik, R. Golouh, and T. Lah.** 1999. Cathepsin B immunohistochemical staining in tumor and endothelial cells is a new prognostic factor for survival in patients with brain tumors. *Clin Cancer Res* **5**:559-67.
182. **Sukoh, N., S. Abe, S. Ogura, H. Isobe, H. Takekawa, K. Inoue, and Y. Kawakami.** 1994. Immunohistochemical study of cathepsin B. Prognostic significance in human lung cancer. *Cancer* **74**:46-51.
183. **Sun, Q., H. Matta, G. Lu, and P. M. Chaudhary.** 2006. Induction of IL-8 expression by human herpesvirus 8 encoded vFLIP K13 via NF-kappaB activation. *Oncogene* **25**:2717-26.
184. **Surmacz, E.** 2003. Growth factor receptors as therapeutic targets: strategies to inhibit the insulin-like growth factor I receptor. *Oncogene* **22**:6589-97.
185. **Szpaderska, A. M., and A. Frankfater.** 2001. An intracellular form of cathepsin B contributes to invasiveness in cancer. *Cancer Res* **61**:3493-500.

186. **Tang, D. G., and C. J. Conti.** 2004. Endothelial cell development, vasculogenesis, angiogenesis, and tumor neovascularization: an update. *Semin Thromb Hemost* **30**:109-17.
187. **Tappero, J. W., M. A. Conant, S. F. Wolfe, and T. G. Berger.** 1993. Kaposi's sarcoma. Epidemiology, pathogenesis, histology, clinical spectrum, staging criteria and therapy. *J Am Acad Dermatol* **28**:371-95.
188. **Templeton, A. C.** 1981. Kaposi's sarcoma. *Pathol Annu* **16**:315-36.
189. **Thewes, M., R. Engst, M. Jurgens, and S. Borelli.** 1997. Immunohistochemical analysis of procathepsin L and cathepsin B in cutaneous Kaposi's sarcoma. *Int J Dermatol* **36**:100-3.
190. **Thurmond, R. L., S. Sun, L. Karlsson, and J. P. Edwards.** 2005. Cathepsin S inhibitors as novel immunomodulators. *Curr Opin Investig Drugs* **6**:473-82.
191. **Turk, B., D. Turk, and V. Turk.** 2000. Lysosomal cysteine proteases: more than scavengers. *Biochim Biophys Acta* **1477**:98-111.
192. **Turk, B., V. Turk, and D. Turk.** 1997. Structural and functional aspects of papain-like cysteine proteinases and their protein inhibitors. *Biol Chem* **378**:141-50.
193. **Turk, D., and G. Guncar.** 2003. Lysosomal cysteine proteases (cathepsins): promising drug targets. *Acta Crystallogr D Biol Crystallogr* **59**:203-13.
194. **Turk, V., J. Kos, and B. Turk.** 2004. Cysteine cathepsins (proteases)--on the main stage of cancer? *Cancer Cell* **5**:409-10.
195. **Turk, V., B. Turk, and D. Turk.** 2001. Lysosomal cysteine proteases: facts and opportunities. *Embo J* **20**:4629-33.

196. **Valentinis, B., A. Bhala, T. DeAngelis, R. Baserga, and P. Cohen.** 1995. The human insulin-like growth factor (IGF) binding protein-3 inhibits the growth of fibroblasts with a targeted disruption of the IGF-I receptor gene. *Mol Endocrinol* **9**:361-7.
197. **Vella, V., G. Pandini, L. Sciacca, R. Mineo, R. Vigneri, V. Pezzino, and A. Belfiore.** 2002. A novel autocrine loop involving IGF-II and the insulin receptor isoform-A stimulates growth of thyroid cancer. *J Clin Endocrinol Metab* **87**:245-54.
198. **Venetsanakos, E., A. Mirza, C. Fanton, S. R. Romanov, T. Tlsty, and M. McMahon.** 2002. Induction of tubulogenesis in telomerase-immortalized human microvascular endothelial cells by glioblastoma cells. *Exp Cell Res* **273**:21-33.
199. **Verma, S. C., Lan, K., and Robertson, E. .** 2007. Structure and Function of Latency-Associated Nuclear Antigen, p. 101-136. *In* C. Boshoff, Weiss, R.A. (ed.), *Kaposi Sarcoma Herpesvirus: New Perspectives*, 1st ed. Springer Verlag, Heidelberg.
200. **Verma, S. C., and E. S. Robertson.** 2003. Molecular biology and pathogenesis of Kaposi sarcoma-associated herpesvirus. *FEMS Microbiol Lett* **222**:155-63.
201. **Virkamaki, A., K. Ueki, and C. R. Kahn.** 1999. Protein–protein interaction in insulin signaling and the molecular mechanisms of insulin resistance. *J. Clin. Invest.* **103**:931-943.
202. **von Figura, K.** 1991. Molecular recognition and targeting of lysosomal proteins. *Curr Opin Cell Biol* **3**:642-6.

203. **Walker, G. E., H.-S. Kim, Y.-F. Yang, and Y. Oh.** 2003. IGF-Independent Effects of the IGFBP Superfamily, p. 1-22. *In* D. L. Roith, W. Zumkeller, and R. Baxter (ed.), *Insulin-Like Growth Factors*.
204. **Wang, H. W., M. W. Trotter, D. Lagos, D. Bourboulia, S. Henderson, T. Makinen, S. Elliman, A. M. Flanagan, K. Alitalo, and C. Boshoff.** 2004. Kaposi sarcoma herpesvirus-induced cellular reprogramming contributes to the lymphatic endothelial gene expression in Kaposi sarcoma. *Nat Genet* **36**:687-93.
205. **Wang, Z. Q., M. R. Fung, D. P. Barlow, and E. F. Wagner.** 1994. Regulation of embryonic growth and lysosomal targeting by the imprinted *Igf2/Mpr* gene. *Nature* **372**:464-7.
206. **Weich, H. A., S. Z. Salahuddin, P. Gill, S. Nakamura, R. C. Gallo, and J. Folkmann.** 1991. AIDS-associated Kaposi's sarcoma-derived cells in long-term culture express and synthesize smooth muscle alpha-actin. *Am J Pathol* **139**:1251-8.
207. **Woelfle, J., D. J. Chia, M. B. Massart-Schlesinger, P. Moyano, and P. Rotwein.** 2005. Molecular physiology, pathology, and regulation of the growth hormone/insulin-like growth factor-I system. *Pediatr Nephrol* **20**:295-302.
208. **Wong, S. W., E. P. Bergquam, R. M. Swanson, F. W. Lee, S. M. Shiigi, N. A. Avery, J. W. Fanton, and M. K. Axthelm.** 1999. Induction of B cell hyperplasia in simian immunodeficiency virus-infected rhesus macaques with the simian homologue of Kaposi's sarcoma-associated herpesvirus. *J Exp Med* **190**:827-40.

209. **Wood, T. L., L. E. Rogler, M. E. Czick, A. G. Schuller, and J. E. Pintar.** 2000. Selective alterations in organ sizes in mice with a targeted disruption of the insulin-like growth factor binding protein-2 gene. *Mol Endocrinol* **14**:1472-82.
210. **Yan, S., and B. F. Sloane.** 2003. Molecular regulation of human cathepsin B: implication in pathologies. *Biol Chem* **384**:845-54.
211. **Yanamandra, N., K. V. Gumidyala, K. G. Waldron, M. Gujrati, W. C. Olivero, D. H. Dinh, J. S. Rao, and S. Mohanam.** 2004. Blockade of cathepsin B expression in human glioblastoma cells is associated with suppression of angiogenesis. *Oncogene* **23**:2224-30.
212. **Ye, F. C., F. C. Zhou, S. M. Yoo, J. P. Xie, P. J. Browning, and S. J. Gao.** 2004. Disruption of Kaposi's sarcoma-associated herpesvirus latent nuclear antigen leads to abortive episome persistence. *J Virol* **78**:11121-9.
213. **Ziegler, J. L., T. Simonart, and R. Snoeck.** 2001. Kaposi's sarcoma, oncogenic viruses, and iron. *J Clin Virol* **20**:127-30.
214. **Zwad, O., B. Kubler, W. Roth, J. G. Scharf, P. Saftig, C. Peters, and T. Braulke.** 2002. Decreased intracellular degradation of insulin-like growth factor binding protein-3 in cathepsin L-deficient fibroblasts. *FEBS Lett* **510**:211-5.

**Appendix I. Modulation of Gene Expression after treatment with IFN, TNF- α or
infected with KSHV.**

Modulation of Gene Expression after treatment with IFN, TNF- α or infected with KSHV. cDNA synthesis, hybridization to HG_U133A (Affymetrix) and signal intensity normalization were performed at the OHSU microarray core facility. Gene Chip data was analyzed with Arrayassist (Stratagene). Comparisons were made between passage-matched KSHV infected E-DMVEC, IFN or TNF- α treated E-DMVEC harvested at times 6, 12, and 24 hours after treatment and mock infected E-DMVEC. To define the baseline from which changes in gene expression data was determined in KSHV-infected, IFN or TNF- α treated samples, a virtual chip comprising all mock infected control samples was created. A master data table consisting of expression values extracted from all CEL files was created with the Probe Logarithmic Error Intensity Estimate (PLIER) method. Significant changes with a p-value of $p=0.01$ was determined by ANOVA with variance stabilization and no p-value correction. All genes listed in the table were changed by two-fold or higher on a \log_2 scale.

Table 1. Genes Downregulated in all three treatments

Probe Set ID	Gene Name	Gene Symbol
205301_s_at	8-oxoguanine DNA glycosylase	OGG1
214535_s_at	a disintegrin-like and metalloprotease with thrombospondin type 1 motif	ADAMTS2
213768_s_at	achaete-scute complex-like 1 (Drosophila)	ASCL1
205891_at	adenosine A2b receptor	ADORA2B
219308_s_at	adenylate kinase 5	AK5
206385_s_at	ankyrin 3, node of Ranvier (ankyrin G)	ANK3
206029_at	ankyrin repeat domain 1 (cardiac muscle)	ANKRD1
220093_at	anthrax toxin receptor 1	ANTXR1
206714_at	arachidonate 15-lipoxygenase, second type	ALOX15B
204288_s_at	Arg/Abl-interacting protein ArgBP2	ARGBP2
217516_x_at	armadillo repeat gene deletes in velocardiofacial syndrome	ARVCF
207522_s_at,213036_x_at	ATPase, Ca ⁺⁺ transporting, ubiquitous	ATP2A3
209641_s_at	ATP-binding cassette, sub-family C (CFTR/MRP), member 3	ABCC3
203196_at	ATP-binding cassette, sub-family C (CFTR/MRP), member 4	ABCC4
204129_at	B-cell CLL/lymphoma 9	BCL9
206746_at	beaded filament structural protein 1, filensin	BFSP1
201262_s_at	biglycan	BGN
204167_at	biotinidase	BTD
213578_at,204832_s_at	bone morphogenetic protein receptor, type IA	BMPRIA
218456_at	C1q domain containing 1	C1QDC1
213108_at	calcium/calmodulin-dependent protein kinase (CaM kinase) II alpha	CAMK2A
203535_at	calgranulin B	S100A9
207317_s_at	calsequestrin 2 (cardiac muscle)	CASQ2
213436_at	cannabinoid receptor 1 (brain)	CNR1
214049_x_at	CD7 antigen (p41)	CD7
214381_at	CDNA clone MGC:87642 IMAGE:5265802, complete cds	n/a
209687_at,203666_at	chemokine (C-X-C motif) ligand 12 (stromal cell-derived factor 1)	CXCL12
211174_s_at	cholecystokinin A receptor	CCKAR
210123_s_at	cholinergic receptor, nicotinic, alpha polypeptide 7	CHRFAM7A
208791_at,208792_s_at	clusterin	CLU
40687_at,204904_at	connexin 37	GJA4
208590_x_at	connexin 46	GJA3
206843_at	crystallin, beta A4	CRYBA4
47553_at	deafness, autosomal recessive 31	DFNB31
205492_s_at	dihydropyrimidinase-like 4	DPYSL4
218218_at	DIP13 beta	DIP13B
203810_at,203811_s_at	DnaJ (Hsp40) homolog, subfamily B, member 4	DNAJB4
204014_at,204015_s_at	dual specificity phosphatase 4	DUSP4
204797_s_at	echinoderm microtubule associated protein like 1	EML1
213877_x_at	elongin B	TCEB2
203249_at	enhancer of zeste homolog 1 (Drosophila)	EZH1
201579_at	FAT tumor suppressor homolog 1 (Drosophila)	FAT
204421_s_at	fibroblast growth factor 2 (basic)	FGF2
204452_s_at	frizzled homolog 1 (Drosophila)	FZD1
210220_at	frizzled homolog 2 (Drosophila)	FZD2

210560_at	gastrulation brain homeo box 2	GBX2
214040_s_at	gelsolin	GSN
207355_at	glutamate transporter	SLC1A7
205280_at	glycine receptor, beta	GLRB
209304_x_at	growth arrest and DNA-damage-inducible, beta	GADD45B
212206_s_at	H2A histone family, member V	H2AFV
208493_at	homeo box A11	HOXA11
209558_s_at	huntingtin interacting protein-1-related	HIP1R
220258_s_at	hypothetical protein FLJ10385	FLJ10385
218546_at	hypothetical protein FLJ14146	FLJ14146
220309_at	hypothetical protein FLJ20619	FLJ20619
213643_s_at	inositol polyphosphate-5-phosphatase, 75kDa	INPP5B
204686_at	insulin receptor substrate 1	IRS1
204989_s_at, 204990_s_at	integrin, beta 4	ITGB4
209297_at	intersectin 1 (SH3 domain protein)	ITSN1
201650_at	keratin 19	KRT19
202291_s_at	matrix Gla protein	MGP
210983_s_at	MCM7 minichromosome maintenance deficient 7 (S. cerevisiae)	MCM7
209858_x_at	metallophosphoesterase 1	MPPE1
210482_x_at	mitogen-activated protein kinase kinase 5	MAP2K5
206599_at	monocarboxylic acid transporters	SLC16A5
210113_s_at	NACHT, leucine rich repeat and PYD containing 1	NALP1
209159_s_at	NDRG family member 4	NDRG4
213479_at	neuronal pentraxin II	NPTX2
205920_at	neurotransmitter transporter, taurine	SLC6A6
205581_s_at	nitric oxide synthase 3 (endothelial cell)	NOS3
209261_s_at	nuclear receptor subfamily 2, group F, member 6	NR2F6
212183_at	nudix-type motif 4	NUDT4
218736_s_at	palmdelphin	PALMD
208518_s_at	period homolog 2 (Drosophila)	PER2
221529_s_at	plasmalemma vesicle associated protein	PLVAP
215807_s_at	plexin B1	PLXNB1
222238_s_at	polymerase (DNA directed), mu	POLM
201701_s_at	progesterone receptor membrane component 2	PGRMC2
206998_x_at	proline-rich protein BstNI subfamily 2	PRB2
204896_s_at	prostaglandin E receptor 4	PTGER4
212879_x_at	protein inhibitor of activated STAT, 4	PIAS4
209049_s_at	protein kinase C binding protein 1	PRKCBP1
213093_at	protein kinase C, alpha	PRKCA
219562_at	RAB26, member RAS oncogene family	RAB26
215506_s_at	ras homolog gene family, member I	ARHI
216184_s_at	regulating synaptic membrane exocytosis 1	RIMS1
212444_at	retinoic acid induced 3	RAI3
203186_s_at	S100 calcium binding protein A4	S100A4
207763_at	S100 calcium binding protein A5	S100A5
213435_at	SATB family member 2	SATB2
219689_at	semaphorin sem2	LOC56920
214722_at	similar to NOTCH2 protein	N2N

207069_s_at	SMAD, mothers against DPP homolog 6 (Drosophila)	SMAD6
208458_at	sodium channel, nonvoltage-gated 1, delta	SCNN1D
209736_at	SRY-box 13	SOX13
219993_at	SRY-box 17	SOX17
205131_x_at	stem cell growth factor	SCGF
212158_at	syndecan 2	SDC2
205104_at	syntaphilin	SNPH
212701_at	talin 2	TLN2
91703_at	tangerin	DKFZp762C186
215855_s_at	TATA element modulatory factor 1	TMF1
219682_s_at	T-box 3	TBX3
213135_at	T-cell lymphoma invasion and metastasis 1	TIAM1
205286_at	transcription factor AP-2 gamma	TFAP2C
40837_at	transducin-like enhancer of split 2 (E(sp1) homolog, Drosophila)	TLE2
211841_s_at	tumor necrosis factor receptor superfamily, member 25	TNFRSF25
205694_at	tyrosinase-related protein 1	TYRP1
210121_at	UDP-Gal:betaGlcNAc beta 1,3-galactosyltransferase, polypeptide 2	B3GALT2
207035_at	zinc transporter	SLC30A3

Table 2. Genes Induced in All Three Conditions

Probe Set ID	Gene Name	Gene Symbol
202672_s_at	activating transcription factor 3	ATF3
204908_s_at	B-cell CLL/lymphoma 3	BCL3
204821_at	butyrophilin, subfamily 3, member A3	BTN3A3
209970_x_at, 211366_x_at, 211368_s_at	caspase 1	CASP1
202902_s_at	cathepsin S	CTSS
209774_x_at	chemokine (C-X-C motif) ligand 2	CXCL2
217967_s_at	chromosome 1 open reading frame 24	C1orf24
210785_s_at	chromosome 1 open reading frame 38	C1orf38
212067_s_at	complement component 1, r subcomponent	C1R
204224_s_at	GTP cyclohydrolase 1 (dopa-responsive dystonia)	GCH1
202269_x_at, 202270_at	guanylate binding protein 1	GBP1
214290_s_at	histone 2, H2aa	HIST2H2AA
210514_x_at, 211529_x_at, 211530_x_at	HLA-G histocompatibility antigen, class I, G	HLA-G
219209_at	interferon induced with helicase C domain 1	IFIH1
204747_at	interferon-induced protein with tetratricopeptide repeats 3	IFIT3
205992_s_at	interleukin 15	IL15
206148_at	interleukin 3 receptor, alpha (low affinity)	IL3RA
205207_at	interleukin 6 (interferon, beta 2)	IL6
201473_at	jun B proto-oncogene	JUNB
203236_s_at	lectin, galactoside-binding, soluble, 9 (galectin 9)	LGALS9
201212_at	legumain	LGMN
205569_at	lysosomal-associated membrane protein 3	LAMP3
208729_x_at, 209140_x_at	major histocompatibility complex, class I, B	HLA-B
211799_x_at, 211911_x_at	major histocompatibility complex, class I, C	HLA-C
221875_x_at, 204806_x_at	major histocompatibility complex, class I, F	HLA-F
205932_s_at	msh homeo box homolog 1 (Drosophila)	MSX1
209040_s_at	proteasome (prosome, macropain) subunit, beta type, 8	PSMB8
204279_at	proteasome (prosome, macropain) subunit, beta type, 9	PSMB9
213716_s_at	secreted and transmembrane 1	SECTM1
219593_at	solute carrier family 15, member 3	SLC15A3
212110_at	solute carrier family 39 (zinc transporter), member 14	SLC39A14
210592_s_at	spermidine/spermine N1-acetyltransferase	SAT
221477_s_at, 215223_s_at, 216841_s_at	superoxide dismutase 2, mitochondrial	SOD2
206271_at	toll-like receptor 3	TLR3
202307_s_at	transporter 1, ATP-binding cassette, sub-family B (MDR/TAP)	TAP1
203567_s_at	tripartite motif-containing 38	TRIM38
205153_s_at	tumor necrosis factor receptor superfamily, member 5	TNFRSF5
205890_s_at	ubiquitin D	UBD
201649_at	ubiquitin-conjugating enzyme E2L 6	UBE2L6

Table 3. KSHV Downmodulated Genes

Probe Set ID	Gene Name	Gene Symbol
213108_at	CaM kinase II alpha	CAMK2A
204904_at, 40687_at	connexin 37	GJA4
208590_x_at	connexin 46	GJA3
202003_s_at	acetyl-Coenzyme A acyltransferase 2	ACAA2
201951_at, 201952_at	activated leukocyte cell adhesion molecule	ALCAM
201792_at	AE binding protein 1	AEBP1
202888_s_at	alanyl (membrane) aminopeptidase	ANPEP
205083_at	aldehyde oxidase 1	AOX1
201272_at	aldo-keto reductase family 1, member B1 (aldose reductase)	AKR1B1
209369_at	annexin A3	ANXA3
203074_at	annexin A8	ANXA8
201242_s_at, 201243_s_at	ATPase, Na ⁺ /K ⁺ transporting, beta 1 polypeptide	ATP1B1
202685_s_at, 202686_s_at	AXL receptor tyrosine kinase	AXL
221530_s_at	basic helix-loop-helix domain containing, class B, 3	BHLHB3
205715_at	bone marrow stromal cell antigen 1	BST1
211518_s_at	bone morphogenetic protein 4	BMP4
206176_at	bone morphogenetic protein 6	BMP6
202391_at	brain abundant, membrane attached signal protein 1	BASP1
218332_at	brain expressed, X-linked 1	BEX1
217728_at	calcyclin	S100A6
201850_at	capping protein gelsolin-like	CAPG
219500_at	cardiotrophin-like cytokine	CLC
204489_s_at, 204490_s_at, 209835_x_at, 210916_s_at, 212014_x_at, 212063_at	CD44 antigen	CD44
202870_s_at	CDC20 cell division cycle 20 homolog (<i>S. cerevisiae</i>)	CDC20
204693_at	CDC42 effector protein 1	CDC42EP1
214721_x_at	CDC42 effector protein 4	CDC42EP4
221436_s_at	cell division cycle associated 3	CDCA3
221520_s_at	cell division cycle associated 8	CDCA8
210821_x_at	centromere protein A, 17kDa	CENPA
219529_at	chloride intracellular channel 3	CLIC3
212992_at	chromosome 14 open reading frame 78	C14orf78
218541_s_at	chromosome 8 open reading frame 4	C8orf4
205076_s_at	cisplatin resistance associated	CRA
202790_at	claudin 7	CLDN7
206429_at, 213506_at	coagulation factor II receptor-like 1	F2RL1
211343_s_at	collagen, type XIII, alpha 1	COL13A1
207442_at	colony stimulating factor 3 (granulocyte)	CSF3
209101_at	connective tissue growth factor	CTGF
210182_at	cortistatin	CORT
209283_at	crystallin, alpha B	CRYAB
220180_at	CTCL tumor antigen se57-1	SE57-1
202157_s_at	CUG triplet repeat, RNA binding protein 2	CUGBP2
208712_at	cyclin D1 (PRAD1: parathyroid adenomatosis 1)	CCND1
200621_at	cysteine and glycine-rich protein 1	CSRPI
205081_at	cysteine-rich protein 1 (intestinal)	CRIP1
219837_s_at	cytokine-like protein C17	C17
214724_at	DIX domain containing 1	DIXDC1
212886_at	DKFZP434C171 protein	DKFZP434C171
204135_at	downregulated in ovarian cancer 1	DOC1
218424_s_at	dudulin 2	TSAP6

215116_s_at	dynamain 1	DNM1
201341_at	ectodermal-neural cortex (with BTB-like domain)	ENC1
221732_at	ectonucleoside triphosphate diphosphohydrolase 8	ENTPD8
217992_s_at	EF hand domain containing 2	EFHD2
208112_x_at,209038_s_at,222221_x_at	EH-domain containing 1	EHD1
218995_s_at	endothelin 1	EDN1
209589_s_at,211165_x_at	EphB2	EPHB2
201983_s_at,201984_s_at,211607_x_at	epidermal growth factor receptor	EGFR
202609_at	epidermal growth factor receptor pathway substrate 8	EPS8
203729_at	epithelial membrane protein 3	EMP3
220161_s_at	erythrocyte membrane protein band 4.1 like 4B	EPB41L4B
203720_s_at	complementation group 1	ERCC1
209365_s_at	extracellular matrix protein 1	ECM1
202305_s_at	fasciculation and elongation protein zeta 2 (zygin II)	FEZ2
212464_s_at,211719_x_at	fibronectin 1	FN1
213746_s_at,200859_x_at	filamin A, alpha (actin binding protein 280)	FLNA
208613_s_at,208614_s_at	filamin B, beta (actin binding protein 278)	FLNB
207876_s_at	filamin C, gamma (actin binding protein 280)	FLNC
206857_s_at	FK506 binding protein 1B, 12.6 kDa	FKBP1B
40850_at	FK506 binding protein 8, 38kDa	FKBP8
203592_s_at	follistatin-like 3 (secreted glycoprotein)	FSTL3
218980_at	formin homology 2 domain containing 3	FHOD3
204420_at	FOS-like antigen 1	FOSL1
214505_s_at	four and a half LIM domains 1	FHL1
203988_s_at	fucosyltransferase 8	FUT8
209631_s_at	G protein-coupled receptor 37	GPR37
206582_s_at,212070_at	G protein-coupled receptor 56	GPR56
218913_s_at	GEM interacting protein	GMIP
211125_x_at	glutamate receptor, ionotropic, N-methyl D-aspartate 1	GRIN1
207235_s_at	glutamate receptor, metabotropic 5	GRM5
218468_s_at,218469_at	gremlin 1 homolog, cysteine knot superfamily (Xenopus laevis)	GREM1
206204_at	growth factor receptor-bound protein 14	GRB14
202072_at	heterogeneous nuclear ribonucleoprotein L	HNRPL
206074_s_at,210457_x_at	high mobility group AT-hook 1	HMGA1
211597_s_at	homeodomain-only protein	HOP
205523_at,205524_s_at	hyaluronan and proteoglycan link protein 1	HAPLN1
221525_at	hypothetical protein DKFZp76112123	DKFZp76112123
58780_s_at	hypothetical protein FLJ10357	FLJ10357
220486_x_at	hypothetical protein FLJ22679	FLJ22679
210511_s_at	inhibin, beta A	INHBA
202661_at,202662_s_at	inositol 1,4,5-triphosphate receptor, type 2	ITPR2
201188_s_at	inositol 1,4,5-triphosphate receptor, type 3	ITPR3
205302_at	insulin-like growth factor binding protein 1	IGFBP1
203851_at	insulin-like growth factor binding protein 6	IGFBP6
202746_at,202747_s_at	integral membrane protein 2A	ITM2A
206766_at	integrin, alpha 10	ITGA10
201474_s_at	integrin, alpha 3 (antigen CD49C, alpha 3 subunit of VLA-3 receptor)	ITGA3
209016_s_at	keratin 7	KRT7
214954_at	KIAA0527 protein	KIAA0527
213444_at	KIAA0543 protein	KIAA0543
220911_s_at	KIAA1305	KIAA1305
221843_s_at	KIAA1609 protein	KIAA1609
203411_s_at,212089_at	lamin A/C	LMNA

210150_s_at	laminin, alpha 5	LAMA5
209270_at	laminin, beta 3	LAMB3
204682_at	latent transforming growth factor beta binding protein 2	LTBP2
209179_s_at, 211037_s_at	leukocyte receptor cluster (LRC) member 4	LENG4
220765_s_at	LIM and senescent cell antigen-like domains 2	LIMS2
219181_at	lipase, endothelial	LIPG
219058_x_at	lipocalin 7	LCN7
200784_s_at	low density lipoprotein-related protein 1 (alpha-2-macroglobulin receptor)	LRP1
37408_at, 209280_at	mannose receptor, C type 2	MRC2
204575_s_at	matrix metalloproteinase 19	MMP19
201069_at	matrix metalloproteinase 2	MMP2
218211_s_at	melanophilin	MLPH
203434_s_at	membrane metallo-endopeptidase	MME
205330_at	meningioma (disrupted in balanced translocation) 1	MN1
214972_at	meningioma expressed antigen 5 (hyaluronidase)	MGEA5
216336_x_at	metallothionein 1A	MT1A
212859_x_at	metallothionein 1E	MT1E
213629_x_at	metallothionein 1F	MT1F
217165_x_at	metallothionein 1F	MT1F
204745_x_at	metallothionein 1G	MT1G
206461_x_at	metallothionein 1H	MT1H
208581_x_at	metallothionein 1X	MT1X
212185_x_at	metallothionein 2A	MT2A
202788_at	mitogen-activated protein kinase-activated protein kinase 3	MAPKAPK3
201058_s_at	myosin, light polypeptide 9, regulatory	MYL9
202555_s_at	myosin, light polypeptide kinase	MYLK
203961_at, 203962_s_at	nebulette	NEBL
218376_s_at	NEDD9 interacting protein with calponin homology and LIM domains	NICAL
202627_s_at, 202628_s_at	nexin, plasminogen activator inhibitor type 1	SERPINE1
212190_at	nexin, plasminogen activator inhibitor type 1, member 2	SERPINE2
201591_s_at	nischarin	NISCH
210756_s_at	Notch homolog 2 (Drosophila)	NOTCH2
219557_s_at	nuclear receptor interacting protein 3	NRIP3
218199_s_at	nucleolar protein family 6 (RNA-associated)	NOL6
204766_s_at	nudix-type motif 1	NUDT1
219855_at	nudix-type motif 11	NUDT11
33814_at	p21(CDKN1A)-activated kinase 4	PAK4
209598_at	paraneoplastic antigen MA2	PNMA2
203369_x_at, 203370_s_at, 214266_s_at	PDZ and LIM domain 7 (enigma)	PDLIM7
204604_at	PFTAIRE protein kinase 1	PFTK1
213384_x_at	phospholipase C, beta 3	PLCB3
201481_s_at	phosphorylase, glycogen	PYGB
203554_x_at	pituitary tumor-transforming 1	PTTG1
205479_s_at, 211668_s_at	plasminogen activator, urokinase	PLAU
218644_at	pleckstrin 2	PLEK2
222238_s_at	polymerase mu	POLM
204401_at	small conductance calcium-activated channel, subfamily N, member 4	KCNN4
221584_s_at	large conductance calcium-activated channel, subfamily M, alpha member 1	KCNMA1
207650_x_at	prostaglandin E receptor 1	PTGER1
204284_at	protein phosphatase 1, regulatory (inhibitor) subunit 3C	PPP1R3C

200635 s at, 200637 s at	protein tyrosine phosphatase, receptor type, F	PTPRF
210448 s at	purinergic receptor P2X, ligand-gated ion channel, 5	P2RX5
213524 s at	putative lymphocyte G0/G1 switch gene	G0S2
201482 at	quiescin Q6	QSCN6
205924 at, 205925 s at	RAB3B, member RAS oncogene family	RAB3B
212724 at	ras homolog gene family, member E	ARHE
219045 at	ras homolog gene family, member F (in filopodia)	RHOF
221789 x at	ras homolog gene family, member T2	RHOT2
205805 s at	receptor tyrosine kinase-like orphan receptor 1	ROR1
216184 s at	regulating synaptic membrane exocytosis 1	RIMS1
204337 at, 204338 s at, 204339 s at	regulator of G-protein signalling 4	RGS4
212647 at	related RAS viral (r-ras) oncogene homolog	RRAS
206625 at	retinal degeneration, slow	RDS
201288 at	Rho GDP dissociation inhibitor (GDI) beta	ARHGDI2
201785 at	ribonuclease, RNase A family, 1	RNASE1
219550 at	roundabout, axon guidance receptor, homolog 3 (Drosophila)	ROBO3
204268 at	S100 calcium binding protein A2	S100A2
206027 at	S100 calcium binding protein A3	S100A3
220330 s at	SAM domain, SH3 domain and nuclear localisation signals, 1	SAMSN1
219416 at	scavenger receptor class A, member 3	SCARA3
203789 s at	semaphorin 3C	SEMA3C
204614 at	serine (or cysteine) proteinase inhibitor, clade B (ovalbumin), member 2	SERPIN2
206421 s at	serine (or cysteine) proteinase inhibitor, clade B (ovalbumin), member 7	SERPIN7
201739 at	serum/glucocorticoid regulated kinase	SGK
205743 at	SH3 and cysteine rich domain	STAC
205542 at	six transmembrane epithelial antigen of the prostate	STEAP
209897 s at	slit homolog 2 (Drosophila)	SLIT2
205596 s at	SMAD specific E3 ubiquitin protein ligase 2	SMURF2
201801 s at, 201802 at	nucleoside transporters	SLC29A1
202111 at	solute carrier family 4, anion exchanger, member 2	SLC4A2
203615 x at, 215299 x at	sulfotransferase family, cytosolic, 1A, phenol-preferring, member 1	SULT1A1
211385 x at	sulfotransferase family, cytosolic, 1A, phenol-preferring, member 2	SULT1A2
209607 x at, 210580 x at	sulfotransferase family, cytosolic, 1A, phenol-preferring, member 3	SULT1A3
210612 s at	synaptojanin 2	SYNJ2
222173 s at	TBC1 domain family, member 2	TBC1D2
205016 at	transforming growth factor, alpha	TGFA
201506 at	transforming growth factor, beta-induced, 68kDa	TGFBI
210986 s at	tropomyosin 1 (alpha)	TPM1
218368 s at	tumor necrosis factor receptor superfamily, member 12A	TNFRSF12A
218856 at	tumor necrosis factor receptor superfamily, member 21	TNFRSF21
208998 at	uncoupling protein 2 (mitochondrial, proton carrier)	UCP2
208622 s at	villin 2 (ezrin)	VIL2
214226 at	vitamin K epoxide reductase complex, subunit 1	VKORC1
213906 at	v-myb myeloblastosis viral oncogene homolog (avian)-like 1	MYBL1
205497 at	zinc finger protein 175	ZNF175
203585 at	zinc finger protein 185 (LIM domain)	ZNF185
215706 x at, 200808 s at	zyxin	ZYX

Table 4. KSHV Induced Genes

Probe Set ID	Gene Name	Gene Symbol
217757_at	alpha-2-macroglobulin	A2M
210082_at	ATP-binding cassette, sub-family A (ABC1), member 4	ABCA4
219935_at	a disintegrin-like and metalloprotease (repolysin type) with thrombospondin type 1 motif	ADAMT5
219558_at	ATPase family homolog up-regulated in senescence cells	AFURS1
205572_at, 211148_s_at	angiopoietin 2	ANGPT2
219514_at	angiopoietin-like 2	ANGPTL2
204671_s_at	ankyrin repeat domain 6	ANKRD6
201613_s_at	adaptor-related protein complex 1, gamma 2 subunit	APIG2
201525_at	apolipoprotein D	APOD
219842_at	ADP-ribosylation factor related protein 2	ARFRP2
219168_s_at	Rho GTPase activating protein 8	ARHGAP8
218857_s_at	asparaginase like 1	ASRGL1
203231_s_at	ataxin 1	ATXN1
205289_at, 205290_s_at	bone morphogenetic protein 2	BMP2
202877_s_at	complement component 1, q subcomponent, receptor 1	C1QR1
204364_s_at	chromosome 2 open reading frame 23	C2orf23
207698_at	chromosome 6 open reading frame 123	C6orf123
220285_at	chromosome 9 open reading frame 77	C9orf77
209301_at	carbonic anhydrase II	CA2
206208_at	carbonic anhydrase IV	CA4
219572_at	Ca ²⁺ -dependent activator protein for secretion 2	CADPS2
210815_s_at	calcitonin receptor-like	CALCRL
213268_at	calmodulin binding transcription activator 1	CAMTA1
204606_at	chemokine (C-C motif) ligand 21	CCL21
201743_at	CD14 antigen	CD14
209582_s_at, 209583_s_at	CD200 antigen	CD200
212864_at	CDP-diacylglycerol synthase (phosphatidate cytidylyltransferase) 2	CDS2
213006_at	CCAAT/enhancer binding protein (C/EBP), delta	CEBPD
206210_s_at	cholesteryl ester transfer protein, plasma	CETP
215388_s_at	complement factor H-related 1	CFHL1
219049_at	chondroitin beta1,4 N-acetylgalactosaminyltransferase	ChGn
206756_at	carbohydrate (N-acetylglucosamine 6-O) sulfotransferase 7	CHST7
204482_at	claudin 5 (transmembrane protein deleted in velocardiofacial syndrome)	CLDN5
206682_at	C-type (calcium dependent, carbohydrate-recognition domain) lectin, superfamily member 14 (macrophage-derived)	CLECSF14
213415_at	chloride intracellular channel 2	CLIC2
205518_s_at, 210571_s_at	cytidine monophosphate-N-acetylneuraminic acid hydroxylase (CMP-N-acetylneuraminic acid hydroxylase)	CMAH
203477_at	collagen, type XV, alpha 1	COL15A1
208096_s_at	collagen, type XXI, alpha 1	COL21A1
205624_at	carboxypeptidase A3 (mast cell)	CPA3
208146_s_at	carboxypeptidase, vitellogenic-like	CPVL
207630_s_at, 209967_s_at, 214508_x_at	cAMP responsive element modulator	CREM
207030_s_at	cysteine and glycine-rich protein 2	CSRP2

219652_s_at	chromosome X open reading frame 36	CXorf36
202437_s_at	cytochrome P450, family 1, subfamily B, polypeptide 1	CYP1B1
219825_at	cytochrome P450, family 26, subfamily B, polypeptide 1	CYP26B1
220331_at	cytochrome P450, family 46, subfamily A, polypeptide 1	CYP46A1
218858_at	DEP domain containing 6	DEPDC6
221031_s_at	hypothetical protein DKFZp434F0318	DKFZP434F0318
219872_at	hypothetical protein DKFZp434L142	DKFZp434L142
218976_at	DnaJ (Hsp40) homolog, subfamily C, member 12	DNAJC12
215238_s_at	dedicator of cytokinesis 9	DOCK9
201430_s_at	dihydropyrimidinase-like 3	DPYSL3
208370_s_at	Down syndrome critical region gene 1	DSCR1
203498_at	Down syndrome critical region gene 1-like 1	DSCR1L1
204271_s_at, 204273_at, 206701_x_at	endothelin receptor type B	EDNRB
219232_s_at	egl nine homolog 3 (<i>C. elegans</i>)	EGLN3
218935_at	EH-domain containing 3	EHD3
213779_at	EMI domain containing 1	EMID1
209392_at, 210839_s_at	ectonucleotide pyrophosphatase/phosphodiesterase 2 (autotaxin)	ENPP2
205756_s_at	coagulation factor VIII, procoagulant component (hemophilia A)	F8
219383_at	hypothetical protein FLJ14213	FLJ14213
206786_at	hypothetical protein FLJ14957	FLJ14957
218454_at	hypothetical protein FLJ22662	FLJ22662
215910_s_at	fibronectin type III domain containing 3	FNDC3
205860_x_at, 215363_x_at	folate hydrolase (prostate-specific membrane antigen) 1	FOLH1
217897_at	FXFD domain containing ion transport regulator 6	FXFD6
206082_at	HLA complex P5	HCP5
212641_at	human immunodeficiency virus type 1 enhancer binding protein 2	HIVBP2
214438_at	H2.0-like homeo box 1 (<i>Drosophila</i>)	HLX1
203665_at	heme oxygenase (decycling) 1	HMOX1
205604_at	homeo box D9	HOXD9
203854_at	I factor (complement)	IF
202718_at	insulin-like growth factor binding protein 2, 36kDa	IGFBP2
202948_at	interleukin 1 receptor, type I	IL1R1
205945_at	interleukin 6 receptor	IL6R
205258_at	inhibin, beta B (activin AB beta polypeptide)	INHBB
213792_s_at	insulin receptor	INSR
214660_at	integrin, alpha 1	ITGA1
206009_at	integrin, alpha 9	ITGA9
203723_at	inositol 1,4,5-trisphosphate 3-kinase B	ITPKB
203710_at, 211323_s_at	inositol 1,4,5-triphosphate receptor, type 1	ITPR1
210119_at	potassium inwardly-rectifying channel, subfamily J, member 15	KCNJ15
206765_at	potassium inwardly-rectifying channel, subfamily J, member 2	KCNJ2
212806_at	KIAA0367	KIAA0367
213155_at	KIAA0523 protein	KIAA0523
213157_s_at	KIAA0523 protein	KIAA0523
204301_at	KIAA0711 gene product	KIAA0711
212504_at	KIAA0934	KIAA0934

203940_s_at	KIAA1036	KIAA1036
212325_at, 212327_at, 212328_at	KIAA1102 protein	KIAA1102
204411_at	kinesin family member 21B	KIF21B
205051_s_at	v-kit Hardy-Zuckerman 4 feline sarcoma viral oncogene homolog	KIT
210990_s_at	laminin, alpha 4	LAMA4
219884_at	LIM homeobox 6	LHX6
200704_at, 200706_s_at	lipopolysaccharide-induced TNF factor	LITAF
43427_at	hypothetical protein LOC283445	LOC283445
214719_at	hypothetical protein LOC283537	LOC283537
209679_s_at	hypothetical protein from clone 643	LOC57228
221447_s_at	glycosyltransferase	LOC83468
204298_s_at, 213640_s_at, 215446_s_at	lysyl oxidase	LOX
35974_at	lymphoid-restricted membrane protein	LRMP
206363_at, 209348_s_at	v-maf musculoaponeurotic fibrosarcoma oncogene homolog (avian)	MAF
214180_at, 218918_at	mannosidase, alpha, class 1C, member 1	MAN1C1
202350_s_at	matrilin 2	MATN2
205017_s_at	muscleblind-like 2 (Drosophila)	MBNL2
220122_at	multiple C2-domains with two transmembrane regions 1	MCTP1
205442_at	microfibrillar-associated protein 3-like	MFAP3L
204501_at, 214321_at	nephroblastoma overexpressed gene	NOV
204648_at, 32625_at	natriuretic peptide receptor A/guanylate cyclase A (atrionatriuretic peptide receptor A)	NPR1
208337_s_at, 208343_s_at, 210174_at	nuclear receptor subfamily 5, group A, member 2	NR5A2
211844_s_at	neuropilin 2	NRP2
219708_at	5',3'-nucleotidase, mitochondrial	NT5M
213131_at	olfactomedin 1	OLFM1
207455_at	purinergic receptor P2Y, G-protein coupled, 1	P2RY1
219656_at	protocadherin 12	PCDH12
207414_s_at	proprotein convertase subtilisin/kexin type 6	PCSK6
219304_s_at	platelet derived growth factor D	PDGFD
219132_at	pellino homolog 2 (Drosophila)	PELI2
212239_at	phosphoinositide-3-kinase, regulatory subunit, polypeptide 1 (p85 alpha)	PIK3R1
214735_at	phosphoinositide-binding protein PIP3-E	PIP3-E
206942_s_at	pro-melanin-concentrating hormone	PMCH
209147_s_at	phosphatidic acid phosphatase type 2A	PPAP2A
214374_s_at	PTPRF interacting protein, binding protein 1 (liprin beta 1)	PPF1BP1
202178_at	protein kinase C, zeta	PRKCZ
211303_x_at	prostate-specific membrane antigen-like protein	PSMAL/GCP III
206631_at	prostaglandin E receptor 2 (subtype EP2), 53kDa	PTGER2
206574_s_at	protein tyrosine phosphatase type IVA, member 3	PTP4A3
203329_at	protein tyrosine phosphatase, receptor type, M	PTPRM
205645_at	RALBP1 associated Eps domain containing 2	REPS2
218723_s_at	response gene to complement 32	RGC32
209324_s_at	regulator of G-protein signalling 16	RGS16

209325_s_at		
220334_at	regulator of G-protein signalling 17	RGS17
210479_s_at	RAR-related orphan receptor A	RORA
220232_at	stearoyl-CoA desaturase 4	SCD4
210432_s_at	sodium channel, voltage-gated, type III, alpha	SCN3A
204722_at, 204723_at	sodium channel, voltage-gated, type III, beta	SCN3B
205464_at	sodium channel, nonvoltage-gated 1, beta (Liddle syndrome)	SCNN1B
201427_s_at	selenoprotein P, plasma, 1	SEPP1
205933_at	SET binding protein 1	SETBP1
204688_at	sarcoglycan, epsilon	SGCE
205768_s_at, 205769_at	solute carrier family 27 (fatty acid transporter), member 2	SLC27A2
222217_s_at	solute carrier family 27 (fatty acid transporter), member 3	SLC27A3
222088_s_at	solute carrier family 2 (facilitated glucose transporter), member 14	SLC2A14
202497_x_at, 202498_s_at, 202499_s_at	solute carrier family 2 (facilitated glucose transporter), member 3	SLC2A3
218404_at	sorting nexin 10	SNX10
206359_at	suppressor of cytokine signaling 3	SOCS3
200795_at	SPARC-like 1 (mast9, hevin)	SPARCL1
209875_s_at	secreted phosphoprotein 1 (osteopontin, bone sialoprotein 1, early T-lymphocyte activation 1)	SPP1
212558_at	sprouty homolog 1, antagonist of FGF signaling (Drosophila)	SPRY1
220114_s_at	stabilin 2	STAB2
204597_x_at	stanniocalcin 1	STC1
205551_at	synaptic vesicle glycoprotein 2B	SV2B
207332_s_at	transferrin receptor (p90, CD71)	TFRC
204731_at	transforming growth factor, beta receptor III (betaglycan, 300kDa)	TGFBR3
201147_s_at, 201148_s_at, 201149_s_at, 201150_s_at	tissue inhibitor of metalloproteinase 3 (Sorsby fundus dystrophy, pseudoinflammatory)	TIMP3
218113_at	transmembrane protein 2	TMEM2
211828_s_at	TRAF2 and NCK interacting kinase	TNIK
203421_at, 214667_s_at	tumor protein p53 inducible protein 11	TP53I11
202341_s_at	tripartite motif-containing 2	TRIM2
210512_s_at	vascular endothelial growth factor	VEGF
209822_s_at	very low density lipoprotein receptor	VLDLR
219059_s_at, 220037_s_at	extracellular link domain containing 1	XLKD1

Appendix II. IGFBP-2 is essential for KSHV-mediated tumorigenesis.

Figure 1. IGFBP-2 Antisense Molecules inhibit Spindle cell and Foci formation. A 20-mer PMO-AS targeting the start codon region of IGFBP-2 as well as non-related PMO-AS oligomers were obtained from Gene-Tools (Philomath, OR). For delivery, PMO-AS molecules are converted to a paired duplex together with a partially complementary cDNA oligonucleotide in the weakly basic delivery reagent ethoxylated polyethylenimine (EPEI). KSHV-infected DMVEC grown to 80% confluence in 35-mm Primaria culture dishes were treated with 1.25 nM of the PMO-EPEI complex for 4 hrs, followed by normal culture conditions. Control DMVEC cultures were loaded with an irrelevant PMO. For siRNA treatment, a siRNA 21-mer targeted to the IGFBP-2 transcript was transfected into DMVEC at 30% confluency using an oligofectamine protocol (Invitrogen). Controls were treated with oligofectamine alone, or treated with a Cy3-tagged control siRNA. Reduction of IGFBP-2-RNA levels in KSHV-infected DMVEC by siRNA to IGFBP-2 was confirmed by qPCR (data not included). Cell monolayers were cultured post-confluence for up to a week to allow the formation of multilayered foci of transformed cells. Control DMVEC grew in disorganized foci characteristic of KSHV-transformation, while those treated with the IGFBP-2-siRNA or PMO maintained a contact-inhibited monolayer. PMO-AS experiments were performed by Ashlee Moses.

Figure 1. IGFBP-2 Antisense Molecules inhibit Spindle cell and Foci formation.

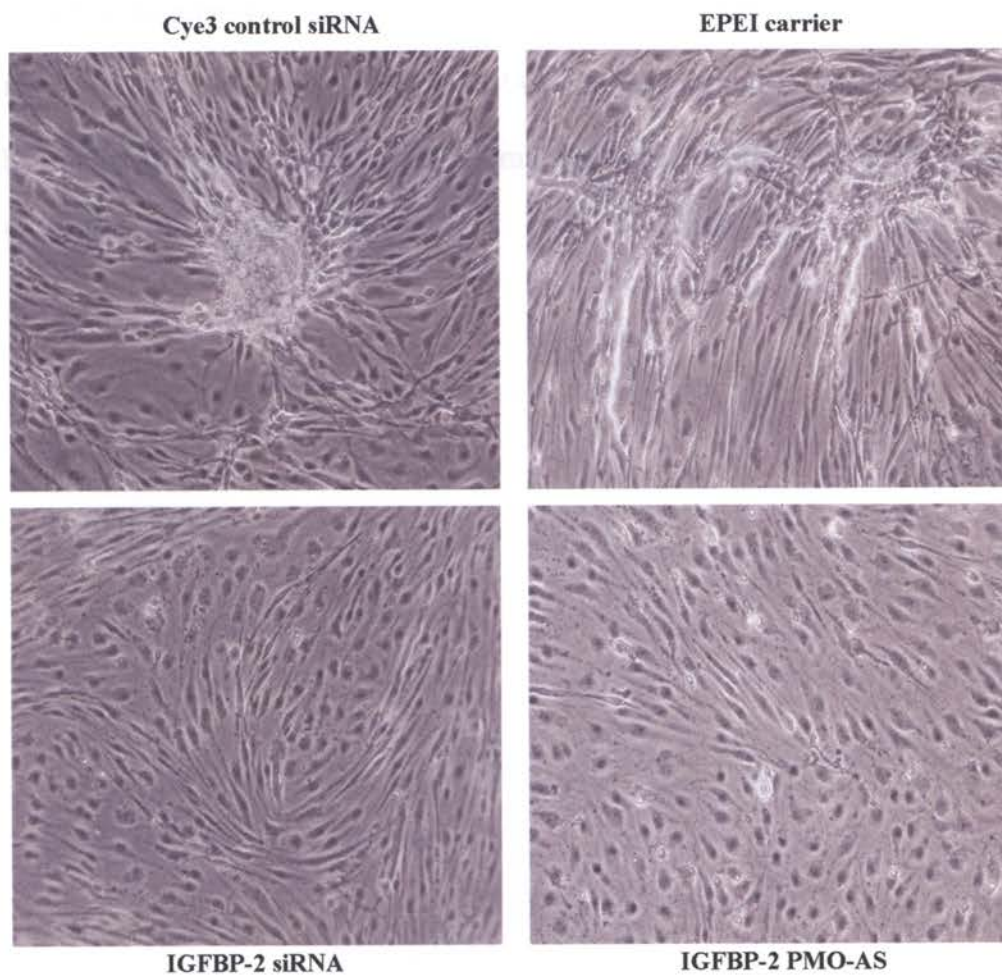
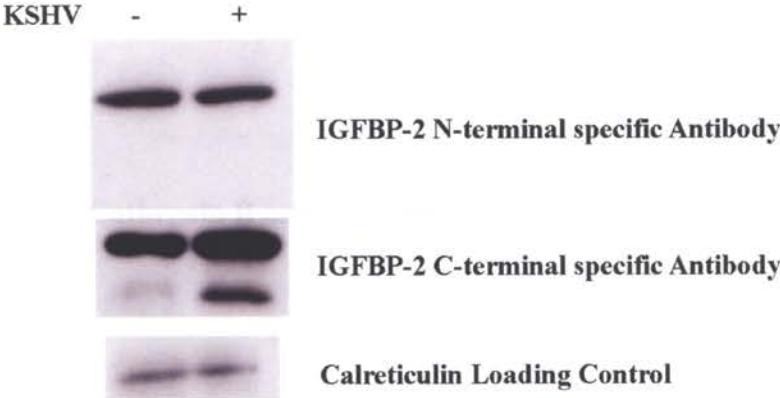


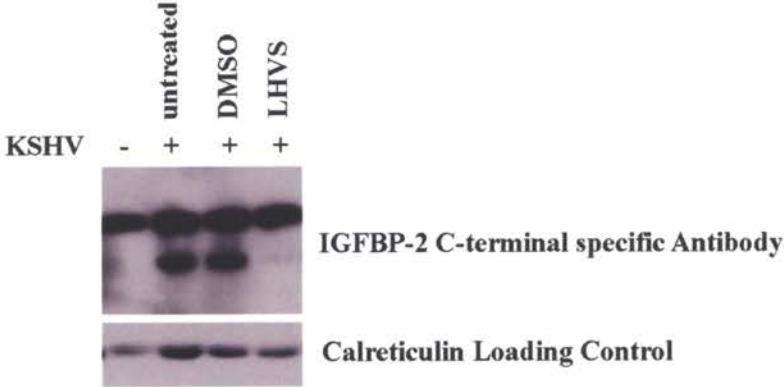
Figure 2. IGFBP-2 is processed by KSHV-induced cathepsins. (A) Western blot comparing IGFBP-2 protein expression in uninfected and KSHV-infected E-DMVEC. Antibodies raised against the IGFBP-2 C-terminus (M-18, Santa Cruz) or N-terminus-specific antisera (H-75, Santa Cruz). A calreticulin-specific antiserum (Stressgen) served as loading control. (B) IGFBP-2 processing was examined in the presence of 25 μ M of the cathepsins S, L and B-specific inhibitor N-morpholinurea-leucine-homophenylalanine-vinylsulfone-phenyl (LHVS). After three days of treatment with LHVS or DMSO, cells were lysed in RIPA buffer and samples analyzed by immunoblot. The smaller-MW product was absent from KSHV-infected DMVEC in the presence of LHVS.

Figure 2. IGFBP-2 is processed by KSHV-induced cathepsins.

A.



B.



Appendix III. Cathepsin B and L are localized to endo-lysosomal compartments.

Figure 1. Cathepsin B siRNA efficiently removes cathepsin B protein, while cathepsin L siRNA does not affect cathepsin B protein expression. KSHV-infected E-DMVEC were treated with siRNA for one week. Cells were washed twice with 1X PBS, fixed in 3.7% formaldehyde for 20 minutes at room temperature. Cells were washed twice again with 1X PBS and permeabilized with 0.1% Triton X-100 for 5 minutes. Subsequently cells were washed three times in 2% PBA (BSA in PBS). To assay CTSB siRNA knockdown, a polyclonal FITC-conjugated anti-cathepsin B antibody (cat#1910-8204, Biogenesis, Kingston, NH) was used at 1:100 for 2 hours at 37°C. Cells were washed again in 1X PBS, and images were analyzed with a Nikon Inverted Fluorescence microscope.

Figure 1. Cathepsin B siRNA efficiently removes cathepsin B protein, while cathepsin L siRNA does not affect cathepsin B protein expression.

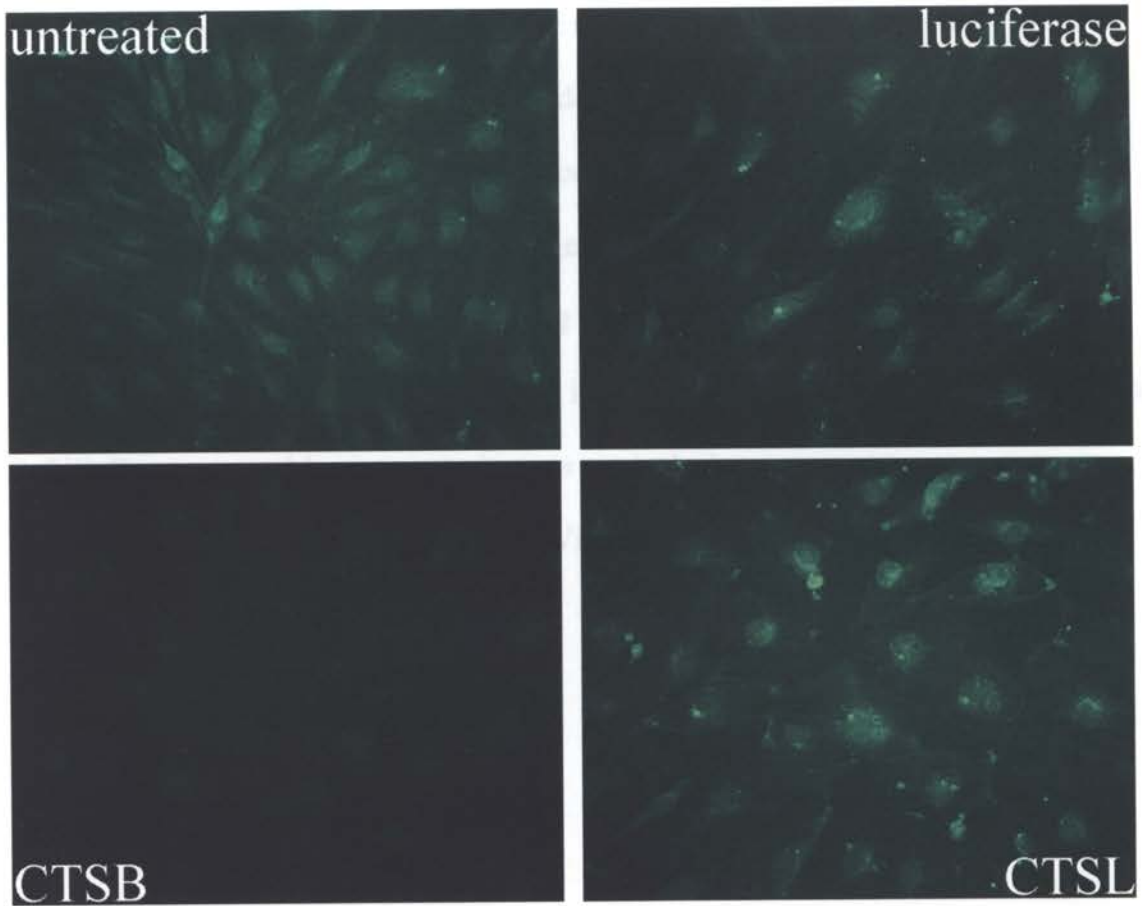
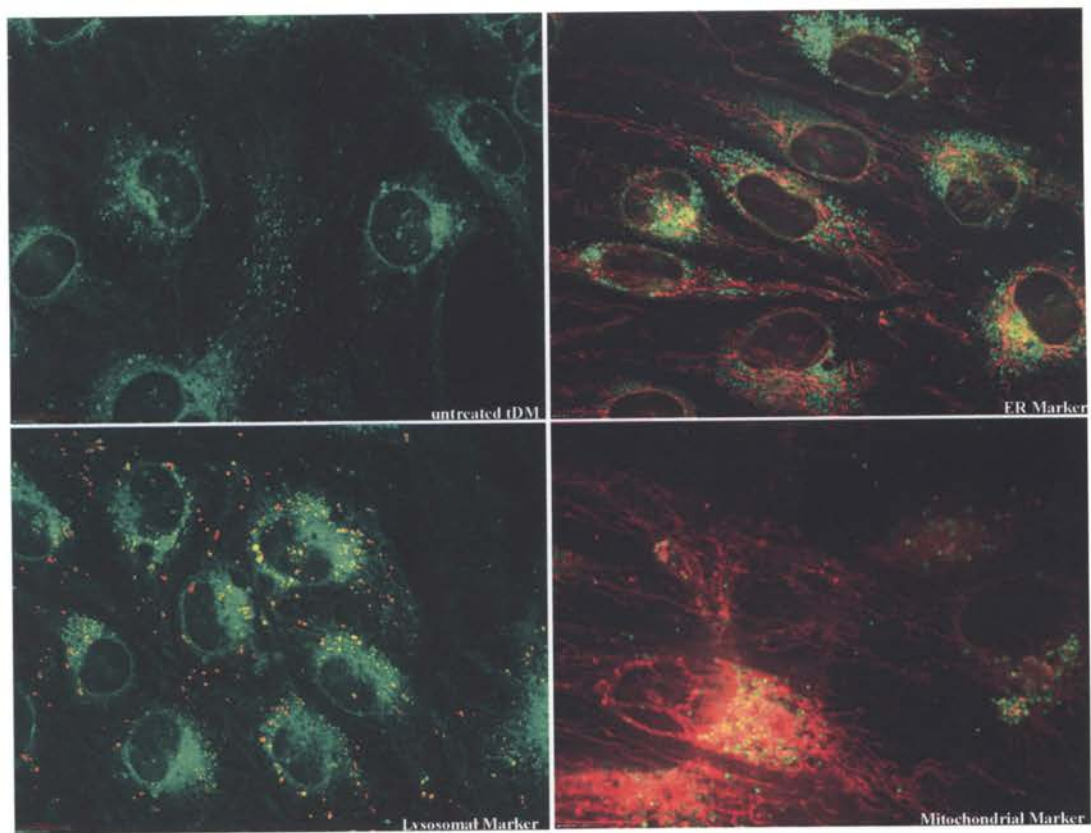


Figure 2. Cathepsin B spliced variant still localize to endo-lysosomal compartments.

For live-staining, uninfected E-DMVEC were seeded at confluency on Lab-Tek II 1.5 Borosilicate chambered coverglass slides (cat# 155382, Electron Microscopy Sciences, Hatfield, PA). The next day cells were being probed with GB111-FL (1 μ M) for 2 hours and various cellular compartment trackers: ER-tracker Red [cat# E34250, Invitrogen], MitoTracker deep red [cat# M-22426, Invitrogen], and LysoTracker [cat# PA-3015, Cambrex]. Images were acquired by Aurelie Snyder of the OHSU-MMI Research Core Facility (<http://www.ohsu.edu/research/core>) with the Applied Precision Deltavision RT™ image restoration system. This includes the API chassis with precision motorized XYZ stage, an Olympus IX-71 inverted fluorescent microscope with standard filter sets, mercury illumination with API light homogenizer, a Nikon CoolSnap Camera and DeltaVision software. Deconvolution using the iterative constrained algorithm of Sedat and Agard and additional image processing is performed on a Linux OS platform with the SoftWoRx program. More scope tech specs can be had at:

http://www.api.com/pdfs/lifescience/DeltaVision_RT_specs.pdf.

Figure 2. Cathepsin B spliced variant still localize to endo-lysosomal compartments.



Appendix IV. Preliminary data on ligands signaling via IR

Figure 1. IR signaling suggests insulin activates mitogen-activated protein kinases.

KSHV infected and uninfected E-DMVEC washed three times in 1X PBS were starved in serum/growth factor-free 199 media (Cellgro, Mediatech Inc.) for 4 hours before the media was replaced with fresh 199 media. After overnight incubation, the 199 media was removed and 199 media, complete media or 199 media supplemented with IGF-II (10ng/ml) or insulin (10ng/ml) were added for the indicated times. Cells were washed three times with cold 1X PBS and lysed in NP-40 buffer [1% NP-40, 150 mM NaCl, 10% glycerol, 20 mM Tris-HCl (pH 8.0), 1 mM EDTA (pH 8.0), 0.2% SDS], containing protease inhibitors (Roche Diagnostics; Indianapolis, IN), 1 mM NaVO₄, and 1 mg/ml pepstatin. Lysates were normalized by Bradford assay and resolved on a 10% acrylamide gel. Samples were first probed with the antibody phospho-Erk (#9101). Afterwards the blots were stripped and reprobed with total Erk (#9102). Both antibodies were obtained from Cell Signaling Technologies (Danvers, MA). * indicates samples treated with the insulin receptor inhibitor HNMPA-(AM₃).

Figure 1. IR signaling suggests insulin activates mitogen-activated protein kinases.

